第９回 鋼構造技術継承講演会

「経験豊富な先人に学ぶ次世代への継承技術」

配布資料

令和３年１２月１６日

土木学会 鋼構造委員会

土木学会鋼構造委員会
技術継承講演会
令和3年12月16日14：05－15：25

鋼橋の疲労設計と維持管理に対する研究

東京都市大学
三木千壽

略歴

1970年3月	**東京工業大学卒業**
1972年3月	同　修士課程修了
1972年9月	同博士課程退学
1972年10月	**東京工業大学助手**
1979年5月	工学博士
1979年8月	**東京大学専任講師**
1980年7月	同助教授
1982年5月-9月	**米国Lehigh大学博士研究員**Research Associate
1984年6月-1985年3月	同客員研究員
1982年10月	**東京工業大学助教授（東大1984年まで併任）**
1990年7月	東京工業大学教授
2003年4月	工学部長
2005年10月	副学長
2012年3月	定年により退職　名誉教授
2012年4月	**東京都市大学総合研究所教授**
2013年4月	副学長
2015年1月	**学長　現在に至る**

同僚の皆さんと博士（48名）のテーマ
（課程博士28名、論文博士20名）

特任教授：市川篤司
助手：佐々木利視、森猛、舘石和雄、穴見健吾、佐々木栄一、田辺篤史、鈴木啓伍、関屋英彦

疲労強度評価（亀裂発生と進展、破壊力学応用）　10
疲労強度改善（構造改善、止端処理、溶接材料）　6
変位と局部応力　(3D変位、変位誘起疲労、実応力比）3
鋼材開発（BHPS, 非磁性鋼、橋梁への適用）3
耐震強度評価（Low cycle fatigue）4
耐震補強（合成化、リブ補強、ダンパー）3
腐食（測定、座屈、疲労）2
メンテナンス計画（データベース、点検ソフト）3
鋼床版（局部応力評価、構造改善、補修補強）3
合成構造（パイプトラス橋、合成構造化）2
橋梁振動（減衰係数評価、衝撃係数）2
モニタリング（BWIM、ネットワーク、MEMS応用）3
非破壊検査（超音波探傷、画像化、フェーズドアレイ）3

東工大　学生、助手

指導教官は**西村俊夫**先生
50トンの疲労試験機を使っての研究
対象は問わない
　高力ボルト摩擦接合、軸力及び表面処理の影響

非常勤講師の**奥村敏恵**先生（東大教授）
疲労の研究はこれから重要となる　自分もIllinois U．留学時代にやった
東大でもやろうと考えている　でもやってくれない
損傷事例を学ぶと良い　先生が集められていた沢山の資料をいただく

建築学科の藤本盛久教授
低サイクル疲労の試験方法のJIS 化をやりたいので手伝わないか
　研究費は用意した　LAB-5の購入
飯田國廣先生（東大船舶教授、疲労研究の第1人者）をご紹介いただく

土木学会誌の記事

当時は学会誌に論文的な記事が登載されていました

学位論文の第1章です


引張応力に起因する鋼構架の変状

西村俊夫

三木千壽

1. はじめに

2. 若干の変状例

Hasselt Bridge Mar. 14, 1938, 全溶接フィレンデール
拘束度の高い突合せ溶接部（現場溶接）に残されていた溶接割れからの脆性破壊ーー＞
溶接の品質管理　奥村先生からいただいた資料です

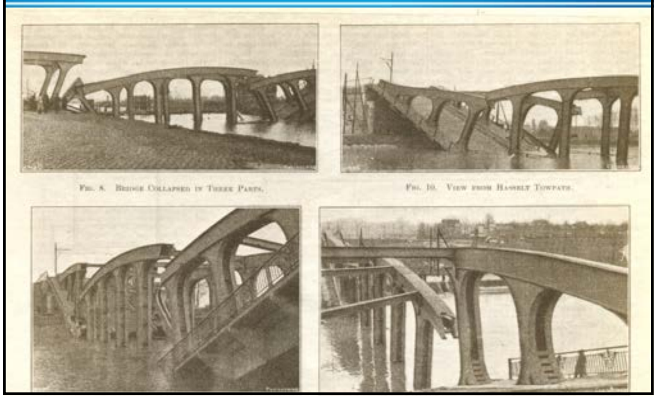
FIG. 8. BRIDGE COLLAPSED IN THREE PARTS.
FIG. 10. VIEW FROM HASSELT TOWPATH.

東工大助手時代 本四疲労との出会い

本州四国連絡橋公団が富士市の建設機械化研究所に
400トンの疲労試験機を設置
　高強度鋼材の溶接部や鋼橋のディテールの疲労

トラス格点部モデルの疲労試験で、理解できない結果が続出した
　その一つが
　試験部（格点部）からは疲労が発生せず、下弦材角継ぎ手から破壊
　これが真実ならトラスの設計ができなくなる
　設計部長の**田島二郎**博士から、一緒に研究しないかとのお誘い

　　溶接欠陥、溶接残留応力、寸法効果、鋼材強度依存性など
　　まさに溶接構造の疲労研究の最先端に引きずり込まれた

学位論文：実橋での損傷事例の分析＋低サイクル疲労＋角継ぎ手の疲労

東大講師・准教授として

東大では新しい分野の研究をするように
　　疲労はダメ（東工大某教授からの指示）

奥村先生、西野先生から、疲労の研究を続けるようにとの指導
奥村先生が設置したアムスラー型疲労試験機（堀川先生が使用）

飯田國廣先生からの、疲労研究への強いお誘い
　　溶接構造の疲労研究についての指導者
　　溶接学会、造船学会での活動

土木学会年次講演会では独立した「疲労」のセッションはなし。
最終日の最後に「疲労・継ぎ手」あるいは「溶接・疲労」の
セッションが実態

溶接構造の疲労研究とIIW

飯田先生の教え
疲労現象は疲労亀裂の**発生、進展、破壊**に分けて考えること
　　発生：局部的なひずみ
　　進展：Paris 則, $da/dN=C(\Delta K)^m$
　　破壊：Kc

疲労を説明するのは**応力**ではなく**ひずみ**（塑性ひずみと弾性ひずみ）

International Institute of Welding(IIW)での活動1982-2012

研究発表及び基準類制定等につながる委員会活動
XIIIが疲労の委員会
疲労の研究者がほぼそろった場となる。
　　S. Maddox, P. Hargensen, P. Hobbacher, G. Marquis,……
年次大会と中間会議、年2回顔を合わせて議論することになる

Steve Maddox と私
IIW Com.XIII, Chairman and Vice Chairman

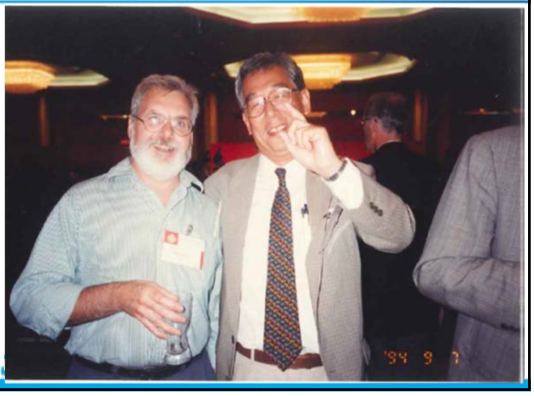

ひずみ制御低サイクル疲労試験

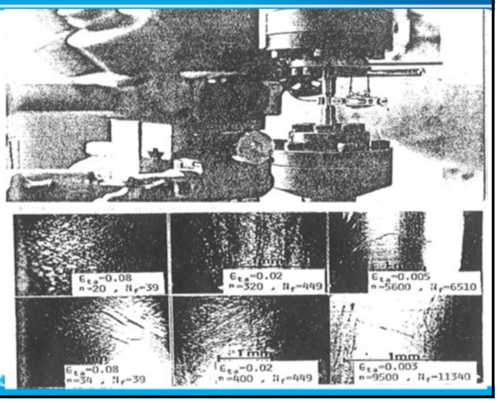

本州四国連絡橋瀬戸大橋（道路鉄道併用）

本四大型疲労試験

HT80、SM 58 溶接継ぎ手部の疲労強度
　縦方向継ぎ手、リブ十字、ガセットなど

構造モデルの疲労
　トラス格点、吊橋ハンガー取り付け部、
　斜張橋ケーブルアンカー部、

トラスの格点部の疲労試験をやっている
しかし、それとは関係ない
弦材角継ぎ手から疲労亀裂が発生する
調べてほしい
田島先生、奥川さん

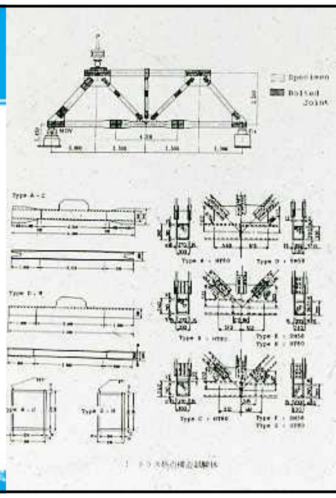

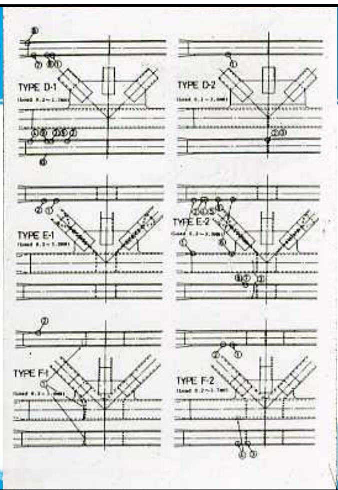

トラス弦材角継ぎ手の研究

縦ビード溶接
荷重非伝達の継ぎ手

ブローホールの影響
残留応力の影響
いずれも影響は小さいとされていた

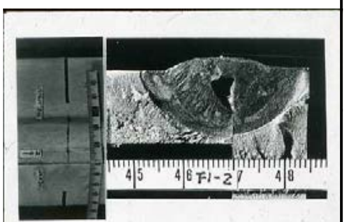

小型ブローホール内在継ぎ手の疲労試験
多くのブローホールから疲労亀裂が発生

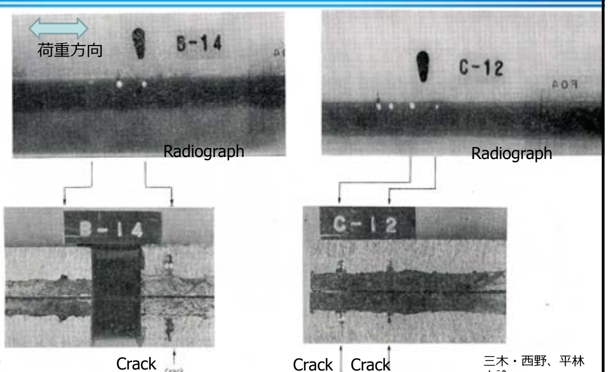

三木・西野、平林
土論1982

残留応力の影響

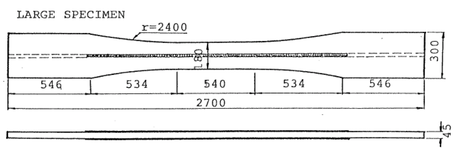

小型試験片は大型試験体
の溶接部を切り出したもの

大型試験体にはフルの
残留応力が存在
小型試験片では
残留応力は解放されている

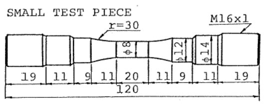

残留応力の測定からの思い付き

ビーチマーク試験の効果

疲労亀裂の発生と進展を観察したい

応力状態が変わると破面にビーチマークが残る

それでは意図的にビーチマークを残そう

試験時間が倍増することから嫌われた

多くのことがビーチマークから明確になった
- 疲労亀裂の発生と進展寿命の分離
- 亀裂の進展挙動
- 亀裂の進展速度

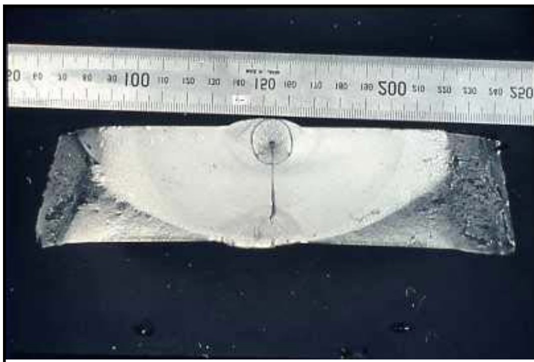

34回の荷重の半減操作」（ステップ）
32個のビーチマークが残されていた
疲労寿命のほとんどが亀裂進展寿命
これは驚き。破壊力学が使える

ビーチマークから求まる疲労亀裂進展速度とΔK

ビーチマークの間は同じ繰り返し数
ビーチマークの間隔から進展速度がわかる

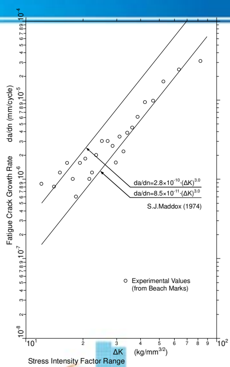

疲労亀裂の起点は大きさ0.7㎜程度のブローホールの壁

き裂発生点（ビーチマークの原点）にはステップ上の痕跡

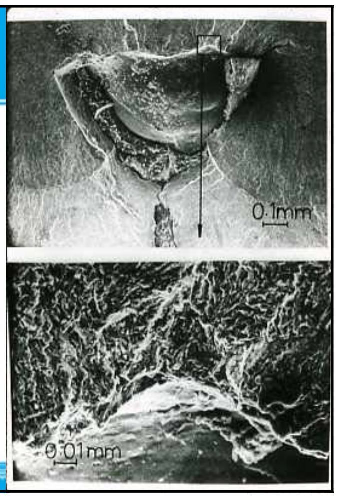

残留応力の影響

疲労強度の差が残留応力

大型試験体、小型試験片とも縦ビード溶接ルートの微小なブローホールから疲労亀裂が発生

寿命のほとんどが亀裂進展に使われる

破壊力学適用で寿命推定が可能
Paris則：$da/dN=C(\Delta K)_m$

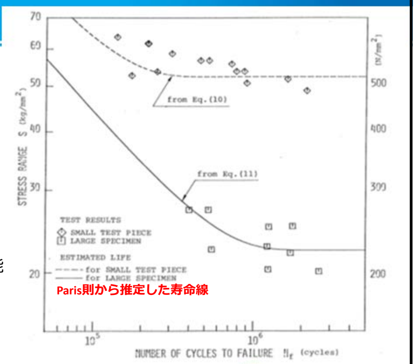

三木・田島、土論1982

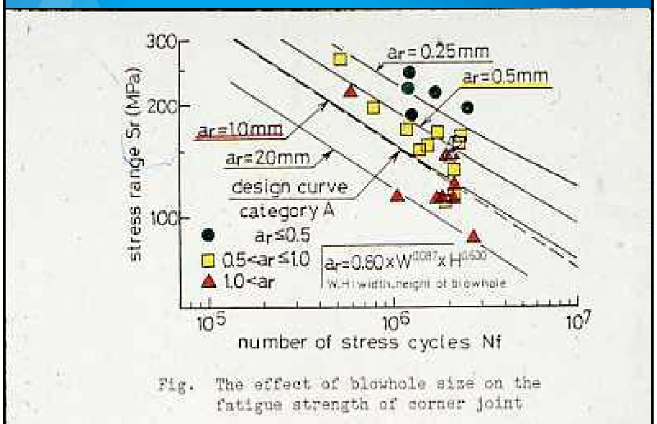

Fig. The effect of blowhole size on the fatigue strength of corner joint

部材の疲労に対する厳しさと溶接要求品質とのリンク

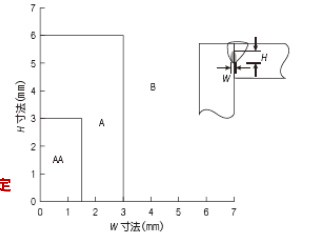

	S_r/S_a	受入れ限界欠陥の寸法	UT の検査率
最も厳しい：AA	$0.7<S_r/S_a$	$W\leq1.5$, $H\leq3.0$	全体
厳しい：A	$0.5\leq S_r/S_a\leq0.7$	$W\leq3.0$, $H\leq6.0$	全体
普通：B	$S_r/S_a<0.5$	〃	20%

角溶接部に対する疲労の厳しさとそれに対応した受入れ限界欠陥

S_r：活荷重に対する応力
S_a：死荷重と活荷重に対する応力
S_r/S_a が 0.7 より大きい（全応力のうち活荷重応力の割合が 70%と高い）場合は AA 部材と分類され，その梁の受入れ限界欠陥は $W\leq1.5$mm, $H\leq3.0$mm となる

図-8.9 トラス試験体に発生した疲労亀裂の分布

角継ぎ手部のルート部に発生する
ブローホールを対象として
疲労許容応力度と受け入れ限界欠陥の規定
世界初のFitness for Purpose design と評価

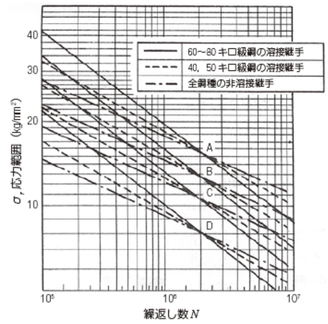

	鋼種	等級分類	m	Constant
溶接継手	40・50キロ級	A	4	1.10×10^{11}
		B		5.20×10^{10}
		C		2.43×10^{10}
		D		8.19×10^{9}
	60～80キロ級	A	3	7.16×10^{9}
		B		4.10×10^{9}
		C		2.31×10^{9}
		D		1.02×10^{9}
非溶接継手	全鋼種	A	5	1.68×10^{12}
		B		6.61×10^{11}
		C		2.55×10^{11}
		D		6.55×10^{10}

$(\sigma_r)^m\cdot N=\text{Constant}$　σ_r : kg/mm²

疲労許容応力度をS-N表示
強度逆依存
Nは1000万回：100年間での新幹線列車と総貨物列車通過トン数から決定

東京都市大学

本四疲労の設計基準類への反映

本四疲労設計指針　S-N線ベースの疲労設計
材料非依存、逆依存

鉄道橋の疲労設計　本四疲労の反映
S-N線ベース
継ぎ手等級の見直し

鋼構造協会疲労設計指針の全面改定

道路橋示方書への疲労設計の導入

ASSHTO　Spec.、IIW疲労設計指針 にも影響

本四疲労は1990年ころまで。様々な構造要素の疲労性能の改善に貢献。
疲労試験設備は今の現役として働いている。

溶接構造の疲労研究の成果
機械部品（機械加工品）とは全く異なる世界

Lehighの研究,TWIを中心としたヨーロッパの研究, 本四の研究
(Fisher)　(Maddox)
ほぼ同じ時期に同じような結果、

・鋼材強度非依存、逆依存：Lehigh,　本四
・溶接残留応力の効果：疲労強度に支配的な影響、応力比非依存
・溶接欠陥の影響：ブローホールのような丸い形状でも強く影響
　面状欠陥は亀裂と同じような効果
・NcとNp：Ncは極めて小さい。m＝3、ただし、疲労限界は存在する
・寸法効果と板厚効果：
・変動応力：打ち切り限界、長寿命域でのm

破壊力学の役割：きわめて有効なコンセプト
　ただし、説明できることとできないことがある

Lehigh大学

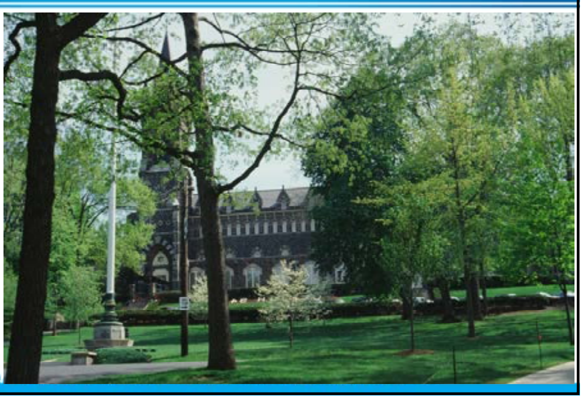

Lehigh University, Fritz Engineering Laboratory

日本人PhDは約20名（土木、建築、造船、など。鋼構造研究の中心）
西野文雄先生、福本先生、藤田譲先生、川合忠彦先生、・・・
柱や桁の耐荷力研究、疲労は少数派

Lehigh での研究
J.W. Fisher 教授との出会い

1982年　最初に担当したProject：Light Pole の柱と横梁の接合部の疲労、
英語が通じない。Work orderが書けない。
Beach Mark Testによりき裂の発生と進展とを分離して示した。
Prof. Fisherとは週1回1時間の面談時間
朝の疲労試験巡回時7:30 とCoffee time10：30での雑談的打ち合わせ

橋の疲労損傷の調査と応力測定に同行。徹底した現場主義を学ぶ。

1984年　文部省在外研究員
余裕のある研究生活
沢山の現場を経験

1980年代
照明柱の疲労が問題となった
原因は風による振動
横梁と柱のconnection,
Base-pklate Connection

California州道路局からの委託

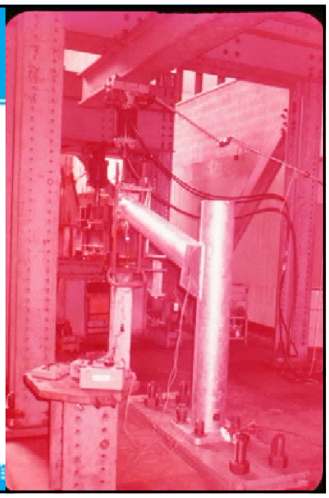

Engineering Structures
Volume 5, Issue 2, April 1983, Pages 90-96

Fatigue strength of steel pipe-base plate connections ☆

John W. Chiher, Chtosshi Miki, Roger G. Slutter, Dennis R. Mertz, William Frank

Show more

Outline | Share　Cite

https://doi.org/10.1016/0141-0296(83)90022-6　　Get rights and content

Abstract

The comparative fatigue resistance of two types of steel light poles is investigated, both experimentally and analytically. The fatigue tests were performed on test specimens designed and proportioned by the California Department of Transportation. The constant amplitude fatigue behaviour wa was obtained at several levels of stress range. Exposed fatigue crack surfaces were studied theascertain the nature of the crack initiation and propagation. Theoretical fatigue life estimates were also made using an existing fracture mechanics model, thought to simulate the geometric condition represented by the welded pipe-base plate connection. The fatigue resistance of the two series of specimens was much lower than originally anticipated. The fatigue resistance was found to be comparable to either category E or E', depending on the weld contact angle.

Previous　　Next

当時はAmerica in Ruinsの真っただ中
Fisher 教授は疲労損傷橋梁の調査の中心

道路1982-11、三木

写真—2　重量制限された橋1)（ペンシルベニア州）

Cable breaks close Brooklyn Bridge walkway

Associated Press

Newsman checks walkway holes after two cables broke.

1981　August

Williamsburg Bridge Open on December 19, 1903 (110 years)


A Bridge Dilemma: Patch It or Scrap It
The condition of the Williamsburg raises concern.

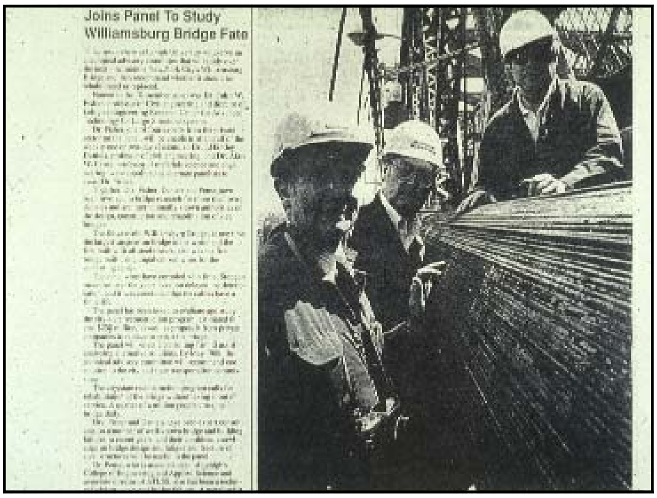
Joins Panel To Study Williamsburg Bridge Fate


Mianus Bridge（米国）
1983.6.28
伸縮装置からの漏水により，ゲルバー部の吊材のピンが腐食，疲労で破断し，落橋した
コネチカット州の技術者が少なく，十分な点検を行えなかったことも原因と言われている
3名死亡
39


疲労き裂とそれを起点とした脆性破壊
40

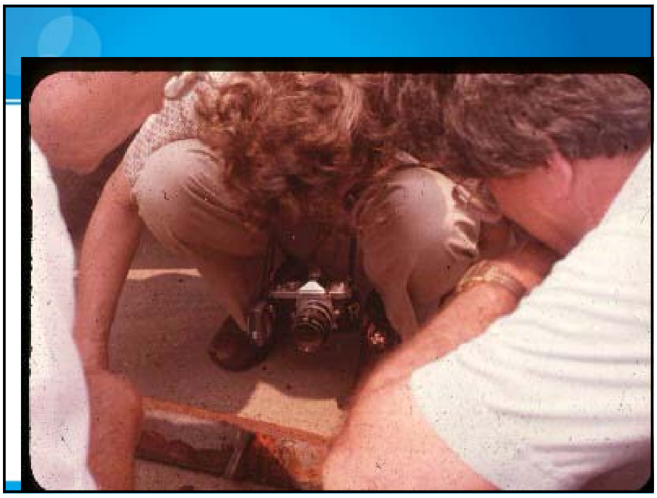


Prof. J.W.Fisherとの継続的関係、
夏休みはLehigh、その後もしばしば滞在
I-35W over the Mississippi River
ミネアポリス,USA、Aug.1, 2007. 6:00p.m.
8/03 12:39 SSMX public ScreenHunter
Open:1967
8 lanes
140000-
200000/day

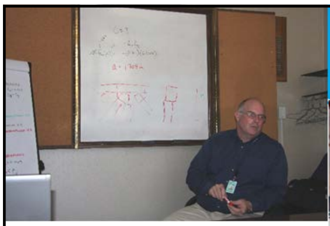

At Turner Fairbank Lab. FHWA
Dr. W. Wright

At Lehigh University,
with Prof. J. W .Fisher

At Univ. of Minnesota
With Prof. T. Galambos and Dr. T. Okazaki
←

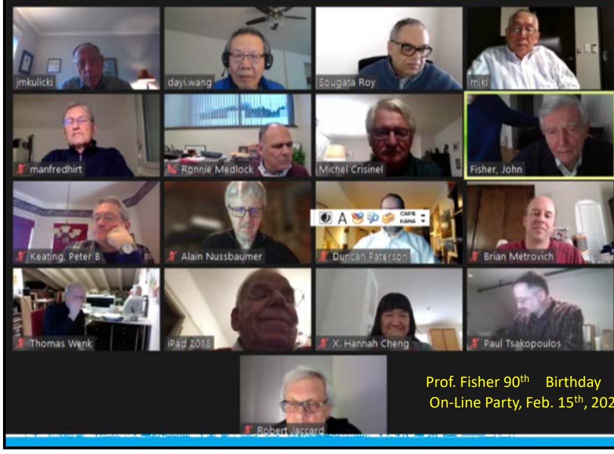

Prof. Fisher 90th Birthday
On-Line Party, Feb. 15th, 2021

鉄道橋の疲労対策

西村俊夫教授、田島二郎教授、阿部英彦教授の流れ
（国鉄構造物設計事務所）

在来線（JR）
- 当初より疲労設計
- 適切なメンテナンス
- 列車重量のコントロール
- 高経年、100年に近づきつつある

東海道新幹線
- 初めての溶接構造
- 疲労設計（70年を想定）－列車本数の増加、
- 当時の疲労設計と現在の疲労設計の差
- 開通後10年くらいから疲労亀裂が見つかり始める。
  - 2次的な応力や振動を原因とする疲労
  - 構造物設計事務所と一緒に原因究明と補修補強
- ＊疲労設計対象外の個所での損傷、2次応力疲労、振動疲労
- ＊予防保全としてのTIG適用　1990－
- ＊疲労許容応力度の見直しに伴う健全度評価
- ＊大規模修繕プログラム、100年を目指す

15-5

初期の補強対策
補剛リブの取り付け　20－30万円/箇所

TIG dressing　30000円/箇所

東海道新幹線橋梁約30000か所に適用。現在までほぼ問題なし。

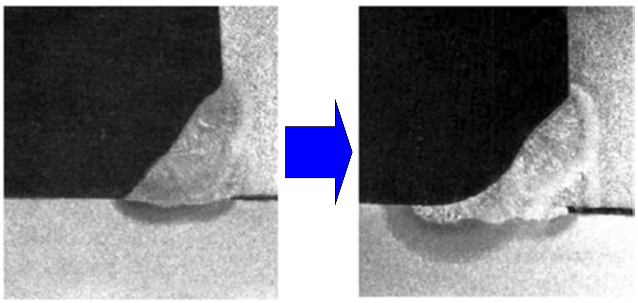

IIW XIII-1815-00

設計疲労許容応力度の見直し

本四疲労による新しい知見の反映

（本四の疲労設計は鉄道橋との併用部材のみ）

- 200万回は疲労限界ではない
- 応力比異存はなし　　応力範囲
- 多くの継ぎ手で非安全
- 鋼材依存性なし

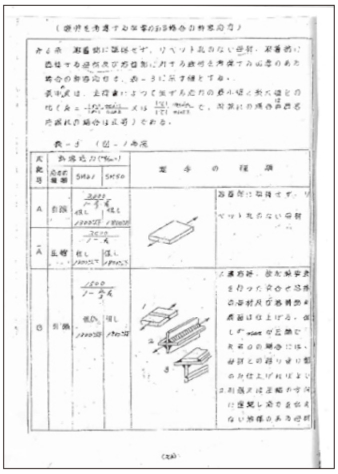

東海道新幹線の設計に用いられた「溶接鋼鉄道橋設計示方書案」(昭和35年7月).
わが国初の溶接構造の疲労設計規定.

鉄道橋設計標準。1960年と現在

Joint Type	Sleeper pad	
Code	Class	Fatigue strength at 2 million cycles (MPa)
Old code '60	D	120
Current code '92	F	65

Joint Type	Out-plane gusset (t=20mm)	
Code	Class	Fatigue strength at 2 million cycles (MPa)
Old code '60	D	100
Current code '92	F	65

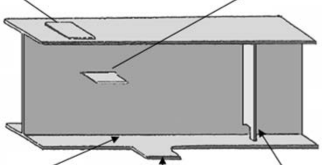

Joint Type	Longitudinal welding	
Code	Class	Fatigue strength at 2 million cycles (MPa)
Old code '60	B	150
Current code '92	C	125

Joint Type	Cruciform weld	
Code	Class	Fatigue strength at 2 million cycles (MPa)
Old code '60	D	100
Current code '92	E	80

Joint Type	In-plane gusset (t=20mm)	
Code	Class	Fatigue strength at 2 million cycles (MPa)
Old code '60	C	126
Current code '92	F	65

疲労強度改善の例：面外ガセット止端部の切削加工（応力集中を下げる）

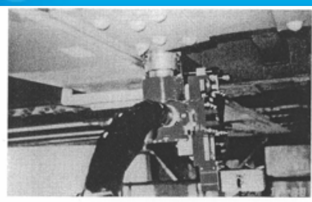

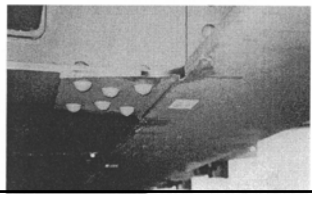

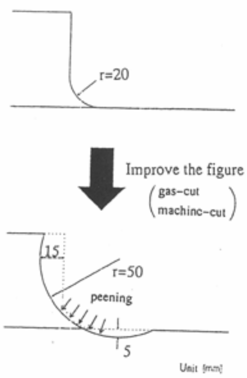

実橋で実現可能な切り欠き加工と応力集中

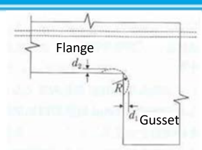

(a) Cut out of gusset end corner

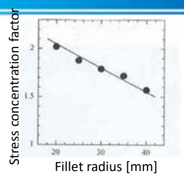

(b) Stress concentration and radius of fillet end R

Modification of the shape of flange gusset end to reduce stress concentration

設計ではR＝20㎜
実施工では実現できていなかったことが問題

機械加工が必須

三木・杉本他、土論1998

Fatigue Strength Improvement
-Grinding-

Flange Gusset Specimen

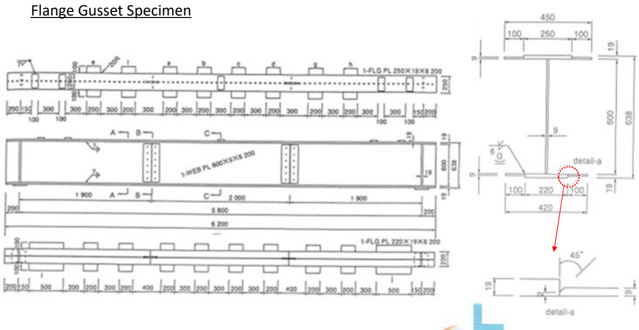

Fatigue Strength Improvement

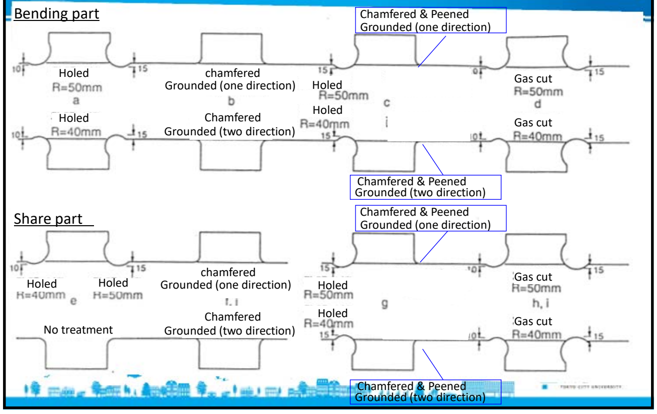

Fatigue Test Result

Upper Flange

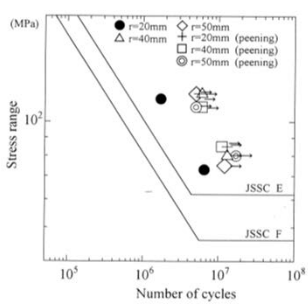

Lower Flange

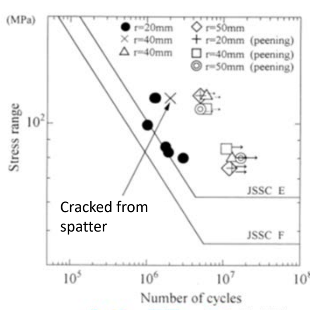

“100年”新幹線へ

東京ー新大阪間（計515・4キロ）のうち、
鉄橋233カ所（計22キロ）
トンネル66カ所（計68キロ）、
高架橋（計98キロ）など
計約240キロで、
工期は平成34年度末までの10年間、
費用は計7300億円を見込む。
橋の架け替えなど大がかりな工事をせず、
補強などの改修だけで強度を保つ、
運行やダイヤへの影響は避けられる見込み。

疲労強度の改善
舟形対策工法（変位の拘束）

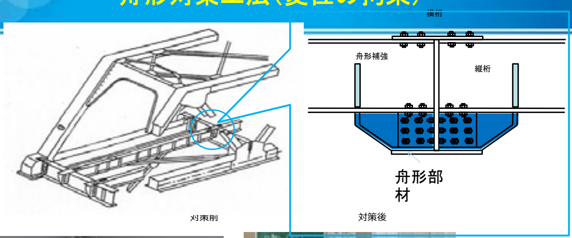

疲労改善：ソールプレート取り付け部の構造改善

ソールプレートのサイズアップ、

溶接ー>高力ボルトによる取り付け、

端補剛材の数と板厚のアップ

道路橋の疲労損傷と疲労設計

1980：
・ランガータイプのアーチ橋垂直補剛材取り付け部：風による疲労
・東名高速道路の対傾構取り付け垂直補剛材
現場では困った、困った。本社では疲労亀裂なんて発生するはずがない。
1885：
・垂直補剛材上端部の亀裂、一般化
・ソールプレート取り付け部の疲労
・様々な疲労亀裂、下フランジの板継ぎ溶接にも発生。
土木学会に疲労に関する小委員会設置

1990：道路協会に疲労損傷調査のWG 設置、1995年までの事例のとりまとめ
道路橋示方書に疲労設計導入の準備
2000：首都高速道路疲労対策室設置；鋼製橋脚隅角部の疲労問題
全国に波及、対策
2002：橋梁委員会で、疲労設計を示方書へ入れること時期尚早、見送りー＞別冊の指針
2012：部分的に導入、2017：全面的に導入、
設計で想定する寿命100年もここで導入（提案は2002年）

実橋の疲労損傷の原因調査と対策は研究ネタの宝庫

61 東京都市大学

損傷の原因調査、補修補強対策などから派生した研究

疲労破壊のモードの構造的同定
Load Induced Fatigue（1次応力に起因する疲労）
Displacement or Distortion Induced Fatigue（変位誘起疲労）

・自動車荷重の実態把握
・Weigh in Motion
・3次元的な変位の把握
・応力測定法
・実応力比
・

・疲労亀裂検知非破壊検査
・疲労亀裂の寸法測定非破壊検査
・疲労亀裂発生伝播のセンシング/モニタリング

・疲労強度改善法：TIG, Peening, UIT,
・構造改善法

62 東京都市大学

管理事務所。見慣れない亀裂が見つかった、どうしよう。ー＞東工大へ 本社技術部。わが社の道路橋に疲労など発生するはずはない。

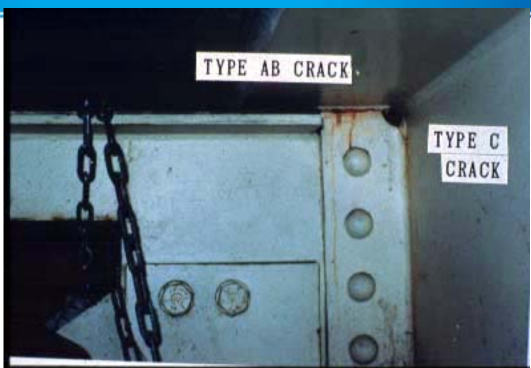

東京都市大学

トラス、主構上弦材と横トラスとの接合部

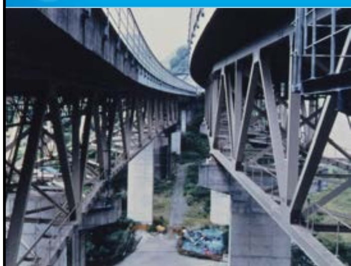


設計では単純支持
フランジ間をつなげたディテールの橋もあり
そのディテールでは亀裂の発生はなし

64 東京都市大学

桁端切り欠き部の疲労

小さいR：形状からくる応力集中
製作管理：フランジ・ウエブの溶接、ギャップ管理、溶接変形

支承部ソールプレート取り付け溶接前縁の亀裂

曲げ応力（公称応力）はゼロ
支承機能のロス（スライディング、回転）
溶接変形

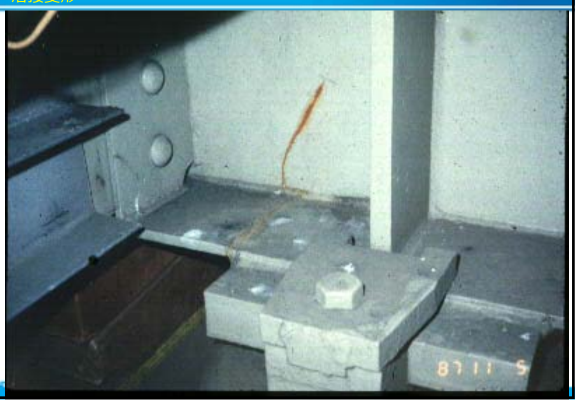

下フランジ板継溶接部の破断

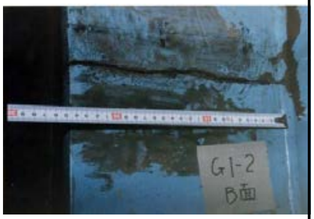

首都高速道路鋼製橋脚隅角部の疲労対策

2001－2005年、
組織（疲労対策室）を作り対応
2000基の橋脚のうちの700基に何らかの異常
300基については補強対策。

→ 他機関の橋脚も同様
設計と製作の問題

設計では完全溶け込み溶接：

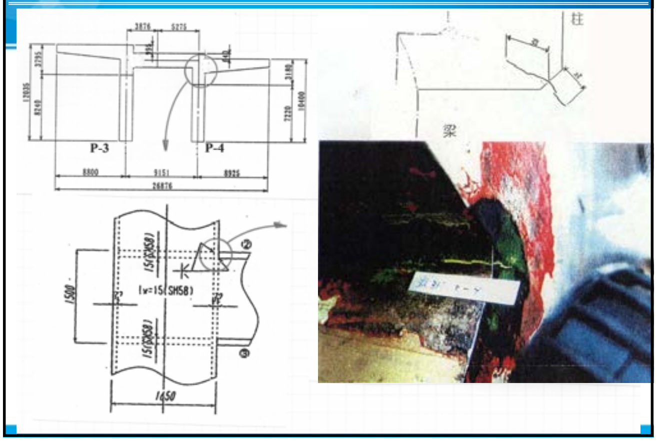

溶接部の疲労強度改善研究

満足な結果が出ていない、
やり残し感。

橋梁への適用性を**実大モデル**で確認
残留応力、実働応力の評価
改善効果、経済性など

低温相変態溶接棒：日本発
Peening処理：昔からある技術、最近はUIT等
過去、TIG, Grinding,軟質溶接棒などの研究
実橋ではルート亀裂が多い。これは難しい。

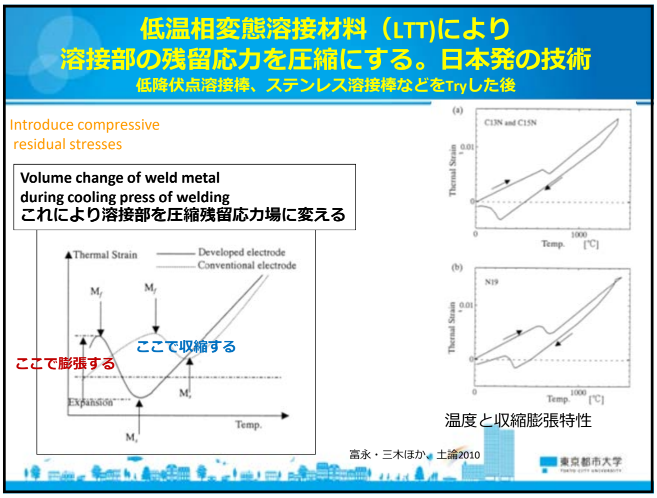
低温相変態溶接材料（LTT)により
溶接部の残留応力を圧縮にする。日本発の技術
低降伏点溶接棒、ステンレス溶接棒などをTryした後
Introduce compressive
residual stresses
Volume change of weld metal
during cooling press of welding
これにより溶接部を圧縮残留応力場に変える
Thermal Strain
Developed electrode
Conventional electrode
ここで収縮する
ここで膨張する
Expansion
Temp.
温度と収縮膨張特性
富永・三木ほか、土論2010
東京都市大学

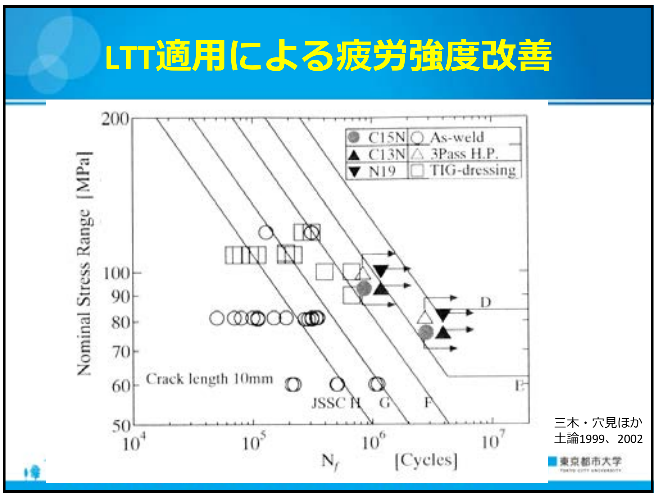
LTT適用による疲労強度改善
Nominal Stress Range [MPa]
C15N As-weld
C13N 3Pass H.P.
N19 TIG-dressing
Crack length 10mm
JSSC H G F E D
Nf [Cycles]
三木・穴見ほか
土論1999、2002
東京都市大学

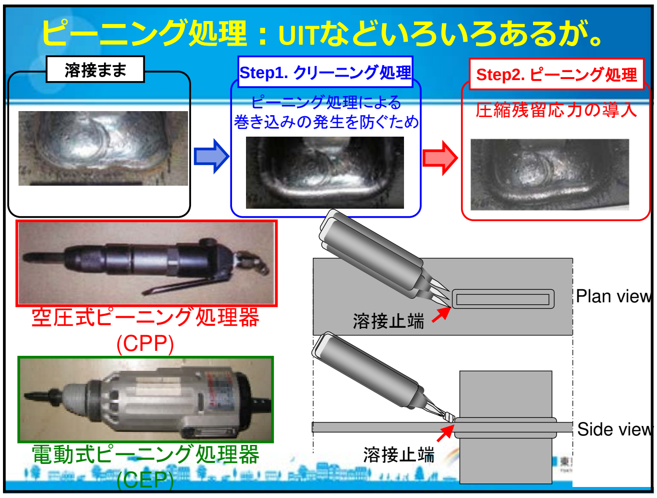
ピーニング処理：UITなどいろいろあるが。
溶接まま
Step1. クリーニング処理
ピーニング処理による
巻き込みの発生を防ぐため
Step2. ピーニング処理
圧縮残留応力の導入
空圧式ピーニング処理器
(CPP)
電動式ピーニング処理器
(CEP)
Plan view
溶接止端
Side view
溶接止端

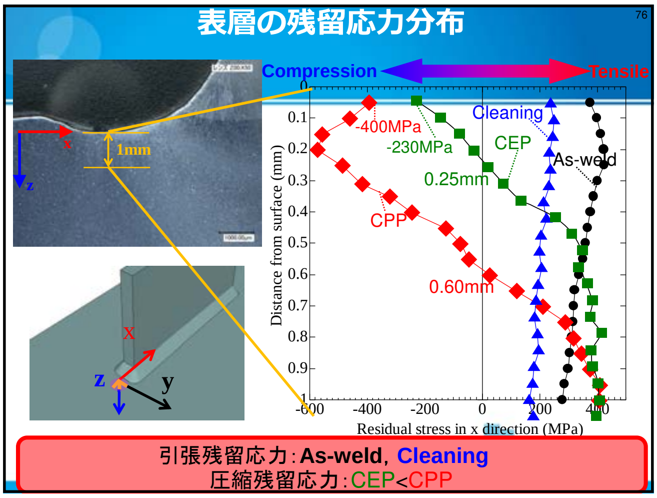
表層の残留応力分布
Compression
Tensile
1mm
-400MPa
-230MPa
Cleaning
CEP
As-weld
0.25mm
CPP
0.60mm
Distance from surface (mm)
Residual stress in x direction (MPa)
引張残留応力：As-weld, Cleaning
圧縮残留応力：CEP<CPP

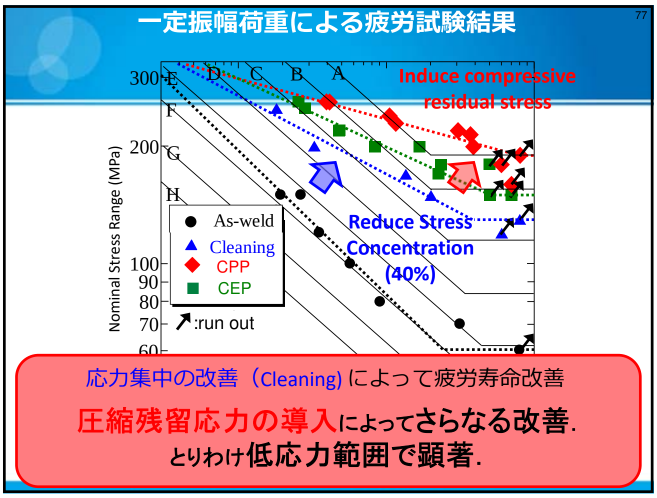
一定振幅荷重による疲労試験結果
Induce compressive
residual stress
Reduce Stress
Concentration
(40%)
Nominal Stress Range (MPa)
As-weld
Cleaning
CPP
CEP
:run out
応力集中の改善（Cleaning）によって疲労寿命改善
圧縮残留応力の導入によってさらなる改善.
とりわけ低応力範囲で顕著.

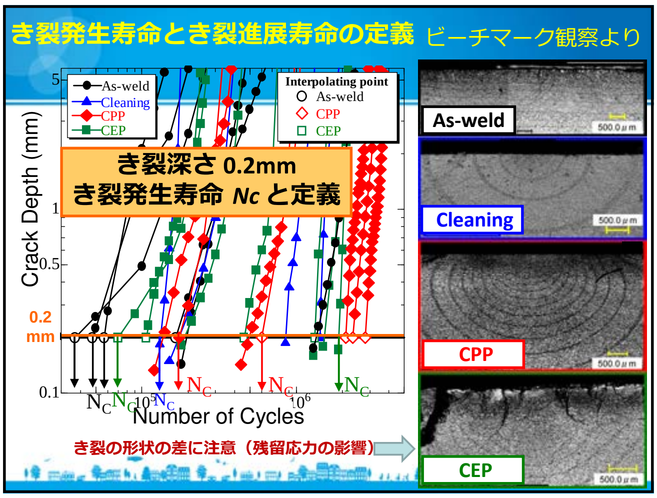
き裂発生寿命とき裂進展寿命の定義 ビーチマーク観察より
As-weld
Cleaning
CPP
CEP
Interpolating point
き裂深さ 0.2mm
き裂発生寿命 Nc と定義
Crack Depth (mm)
0.2 mm
Number of Cycles
き裂の形状の差に注意（残留応力の影響）
As-weld
Cleaning
CPP
CEP

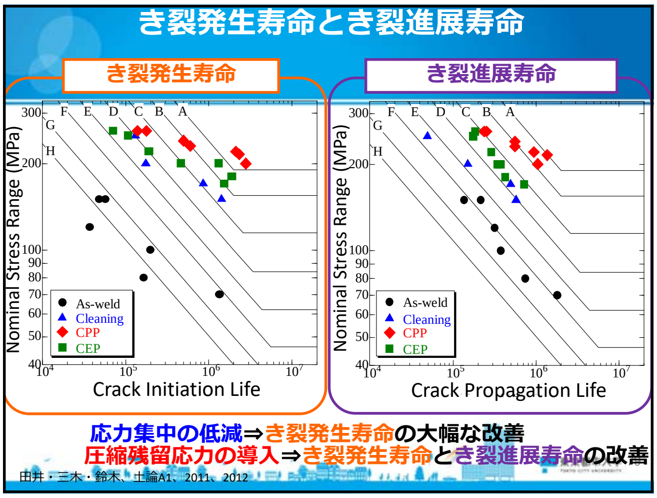
き裂発生寿命とき裂進展寿命
き裂発生寿命
き裂進展寿命
Nominal Stress Range (MPa)
Crack Initiation Life
Crack Propagation Life
As-weld
Cleaning
CPP
CEP
応力集中の低減⇒き裂発生寿命の大幅な改善
圧縮残留応力の導入⇒き裂発生寿命とき裂進展寿命の改善
田井・三木・鈴木、土論A1、2011、2012

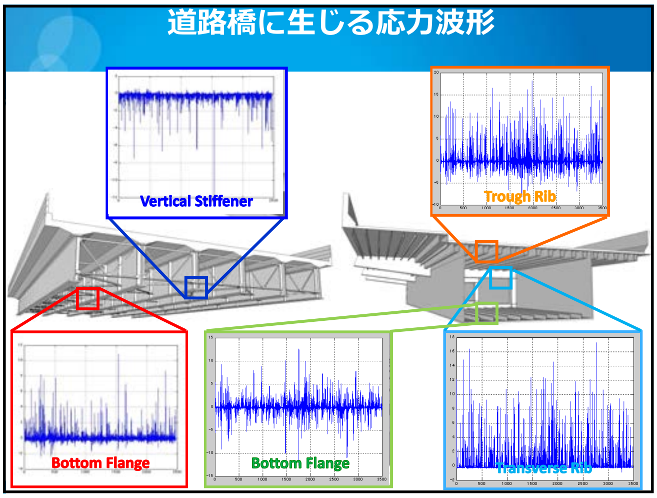
道路橋に生じる応力波形
Vertical Stiffener
Trough Rib
Bottom Flange
Bottom Flange
Transverse Rib

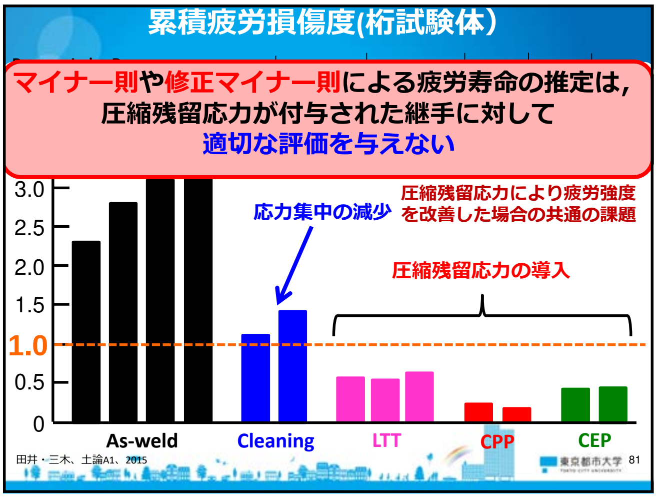
累積疲労損傷度(桁試験体)
マイナー則や修正マイナー則による疲労寿命の推定は,
圧縮残留応力が付与された継手に対して
適切な評価を与えない
応力集中の減少
圧縮残留応力により疲労強度を改善した場合の共通の課題
圧縮残留応力の導入
As-weld
Cleaning
LTT
CPP
CEP
田井・三木、土論A1、2015
東京都市大学 81

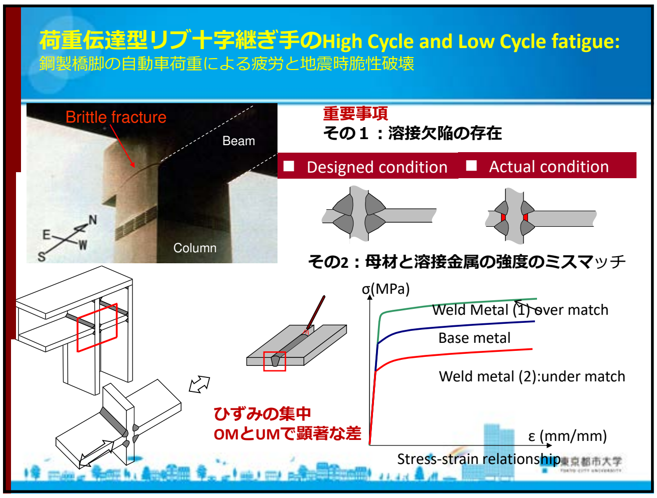
荷重伝達型リブ十字継ぎ手のHigh Cycle and Low Cycle fatigue:
鋼製橋脚の自動車荷重による疲労と地震時脆性破壊
Brittle fracture
Beam
Column
重要事項
その１：溶接欠陥の存在
Designed condition
Actual condition
その2：母材と溶接金属の強度のミスマッチ
σ(MPa)
Weld Metal (1) over match
Base metal
Weld metal (2):under match
ε (mm/mm)
Stress-strain relationship
ひずみの集中
OMとUMで顕著な差
東京都市大学

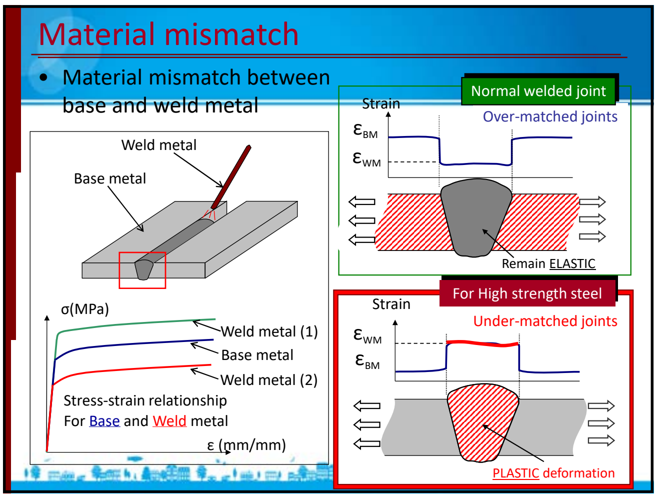
Material mismatch
Material mismatch between base and weld metal
Weld metal
Base metal
σ(MPa)
Weld metal (1)
Base metal
Weld metal (2)
Stress-strain relationship
For Base and Weld metal
ε (mm/mm)
Normal welded joint
Strain
Over-matched joints
Remain ELASTIC
For High strength steel
Strain
Under-matched joints
PLASTIC deformation

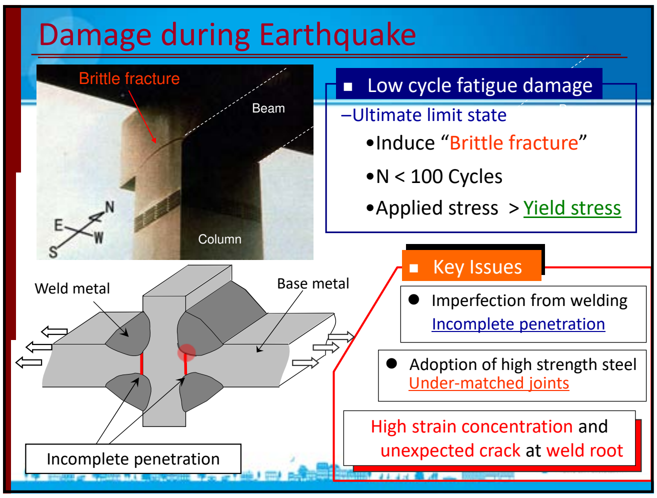
Damage during Earthquake
Brittle fracture
Beam
Column
Low cycle fatigue damage
–Ultimate limit state
•Induce "Brittle fracture"
•N < 100 Cycles
•Applied stress > Yield stress
Weld metal
Base metal
Incomplete penetration
Key Issues
Imperfection from welding
Incomplete penetration
Adoption of high strength steel
Under-matched joints
High strain concentration and unexpected crack at weld root

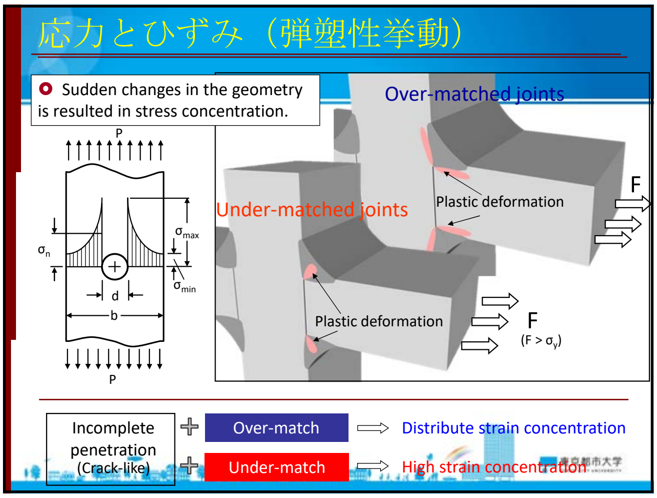
応力とひずみ（弾塑性挙動）
Sudden changes in the geometry is resulted in stress concentration.
Over-matched joints
Under-matched joints
Plastic deformation
Plastic deformation
F
F
(F > σy)
Incomplete penetration (Crack-like)
Over-match
Distribute strain concentration
Under-match
High strain concentration

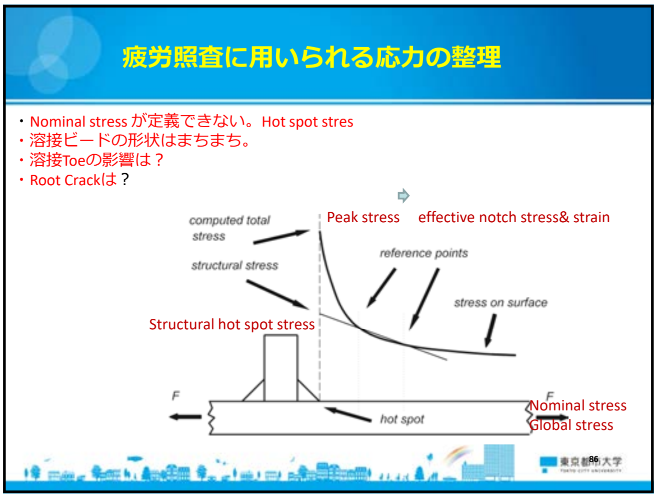
疲労照査に用いられる応力の整理
・Nominal stress が定義できない。Hot spot stres
・溶接ビードの形状はまちまち。
・溶接Toeの影響は？
・Root Crackは？
computed total stress
structural stress
Peak stress
effective notch stress& strain
reference points
stress on surface
Structural hot spot stress
hot spot
Nominal stress
Global stress

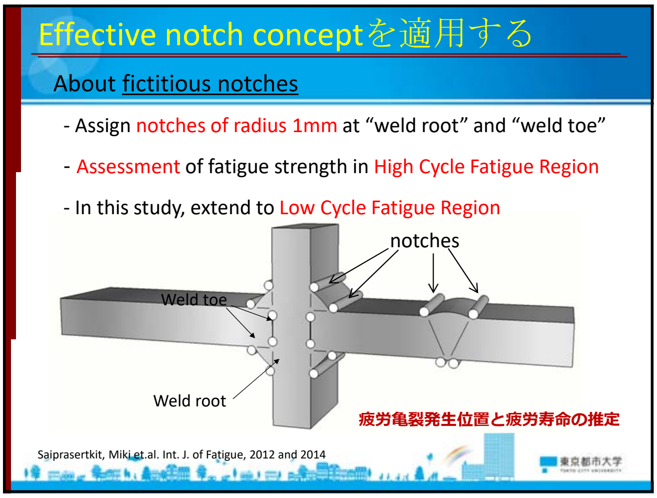
Effective notch conceptを適用する
About fictitious notches
- Assign notches of radius 1mm at "weld root" and "weld toe"
- Assessment of fatigue strength in High Cycle Fatigue Region
- In this study, extend to Low Cycle Fatigue Region
notches
Weld toe
Weld root
疲労亀裂発生位置と疲労寿命の推定
Saiprasertkit, Miki et.al. Int. J. of Fatigue, 2012 and 2014

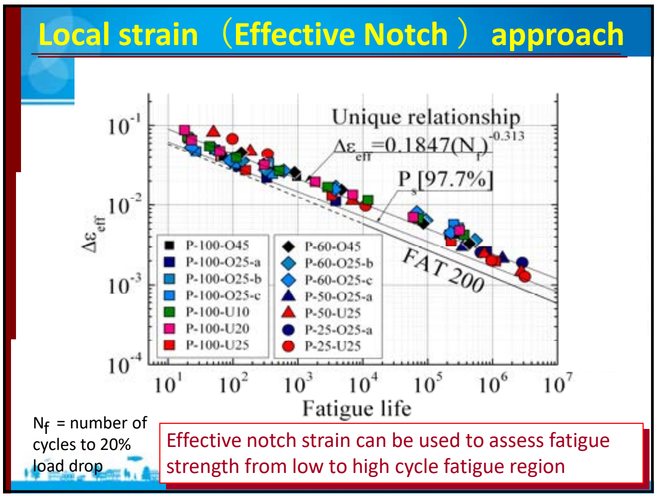
Local strain （Effective Notch ） approach
Unique relationship
Δεeff=0.1847(Nf)-0.313
Ps[97.7%]
FAT 200
Δεeff
Fatigue life
P-100-O45
P-100-O25-a
P-100-O25-b
P-100-O25-c
P-100-U10
P-100-U20
P-100-U25
P-60-O45
P-60-O25-b
P-60-O25-c
P-50-O25-a
P-50-U25
P-25-O25-a
P-25-U25
Nf = number of cycles to 20% load drop
Effective notch strain can be used to assess fatigue strength from low to high cycle fatigue region

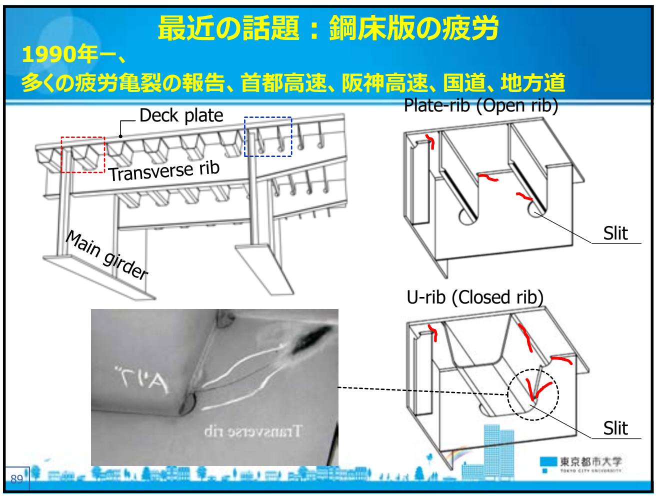
最近の話題：鋼床版の疲労
1990年ー、
多くの疲労亀裂の報告、首都高速、阪神高速、国道、地方道
Deck plate
Transverse rib
Main girder
Plate-rib (Open rib)
Slit
U-rib (Closed rib)
Slit

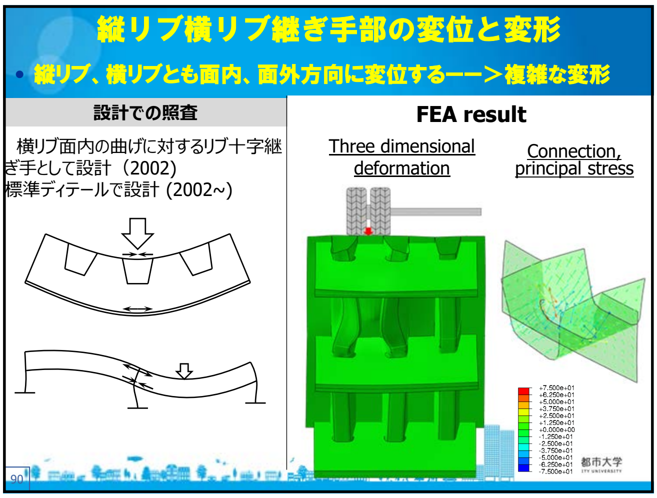
縦リブ横リブ継ぎ手部の変位と変形
縦リブ、横リブとも面内、面外方向に変位する——＞複雑な変形
設計での照査
横リブ面内の曲げに対するリブ十字継ぎ手として設計（2002）
標準ディテールで設計 (2002~)
FEA result
Three dimensional deformation
Connection, principal stress


載荷台での実験：
ディテールを変えた試験パネルを取り付け、トラックを用いて載荷


3連ジャッキ：フェーズを変えての疲労試験
移動荷重の効果を見たい


移動荷重試験機による疲労試験
載荷ライン：狙った疲労亀裂を発生させること
3m
69kN
69kN
Specimen

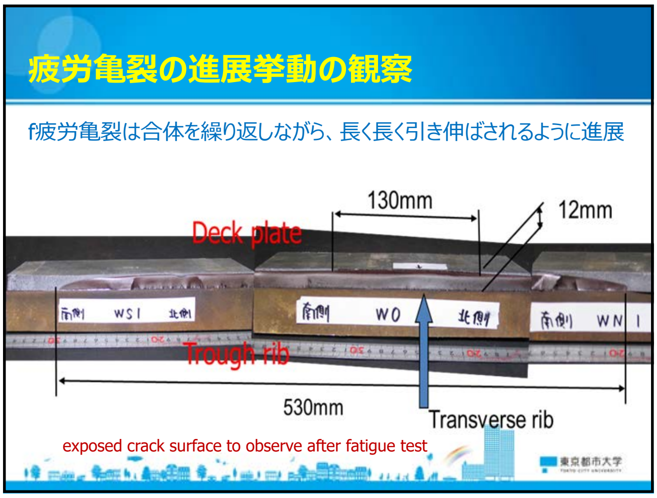
疲労亀裂の進展挙動の観察
f疲労亀裂は合体を繰り返しながら、長く長く引き伸ばされるように進展
130mm
12mm
Deck plate
Trough rib
530mm
Transverse rib
exposed crack surface to observe after fatigue test
東京都市大学

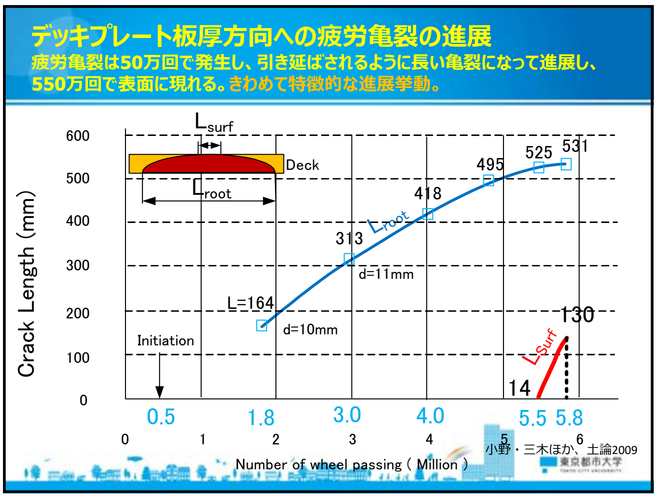
デッキプレート板厚方向への疲労亀裂の進展
疲労亀裂は50万回で発生し、引き延ばされるように長い亀裂になって進展し、
550万回で表面に現れる。きわめて特徴的な進展挙動。
Crack Length (mm)
600
500
400
300
200
100
0
Lsurf
Deck
Lroot
531
525
495
418
313
L=164
d=11mm
d=10mm
Initiation
130
14
0.5
1.8
3.0
4.0
5.5
5.8
0
1
2
3
4
5
6
Number of wheel passing (Million)
小野・三木ほか、土論2009
東京都市大学

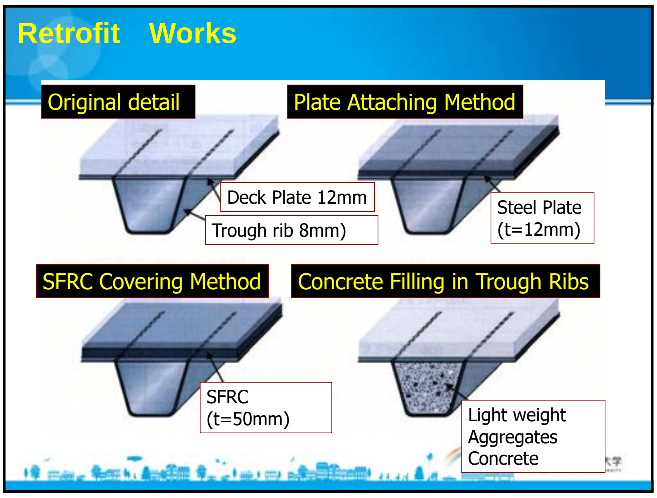
Retrofit Works
Original detail
Plate Attaching Method
Deck Plate 12mm
Trough rib 8mm)
Steel Plate
(t=12mm)
SFRC Covering Method
Concrete Filling in Trough Ribs
SFRC
(t=50mm)
Light weight
Aggregates
Concrete


疲労対策　合成鋼床版化　SFRCの適用
横浜ベイブリッジ下層部（国道357号）、予防保全としての措置
合成鋼床版：名古屋高速の実績、SFRC：湘南大橋でTry
三木、鈴木ほか、土論2006
小野、三木ほか、土論2009
SFRC Pavement
Adhesive
75mm
12mm
デッキプレート周辺
の疲労には有効。
下スリット近傍には？
Deck Plate
Stud


東京ゲートブリッジ（2012年2月12日開通）
設計段階から関与
Total length:760m,
160m+440m+160m
3 span continuous girder bridge,
Truss – Box Hybrid structure
Apply newly developed
High Performance Steel for Bridge
All welded structure
New OSD

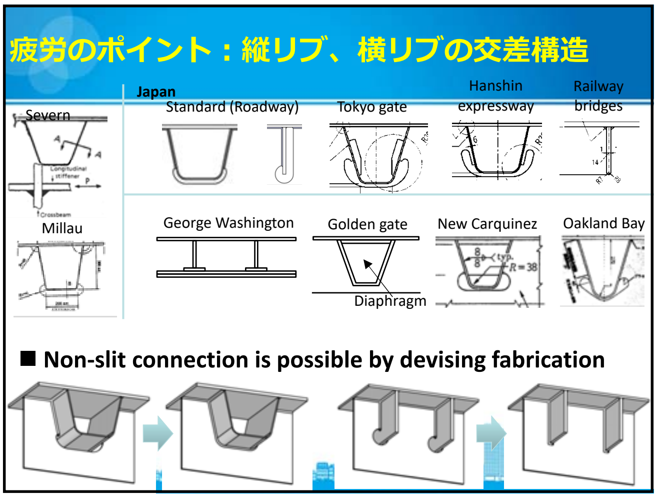
疲労のポイント：縦リブ、横リブの交差構造
Japan
Severn
Standard (Roadway)
Tokyo gate
Hanshin expressway
Railway bridges
Millau
George Washington
Golden gate
New Carquinez
Oakland Bay
Diaphragm
■ Non-slit connection is possible by devising fabrication

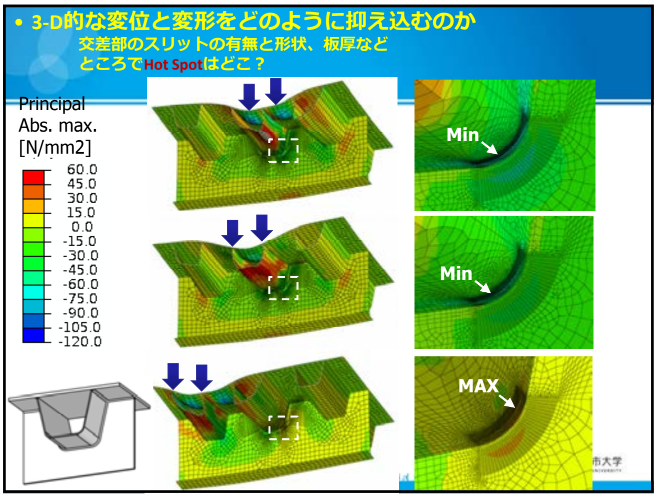
• 3-D的な変位と変形をどのように抑え込むのか
交差部のスリットの有無と形状、板厚など
ところでHot Spotはどこ？
Principal
Abs. max.
[N/mm2]
60.0
45.0
30.0
15.0
0.0
-15.0
-30.0
-45.0
-60.0
-75.0
-90.0
-105.0
-120.0
Min
Min
MAX

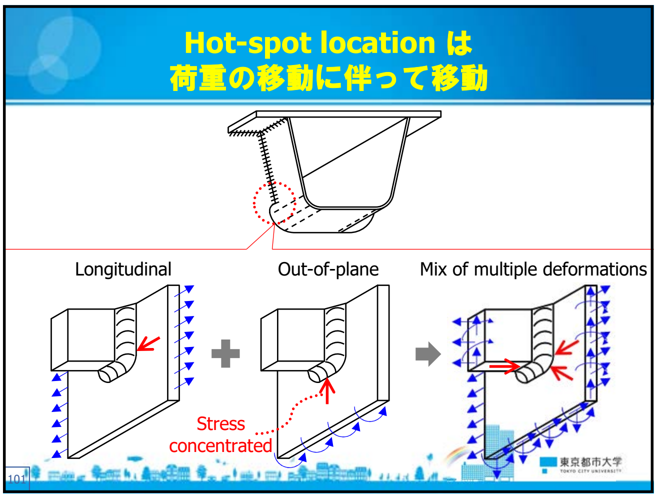
Hot-spot location は
荷重の移動に伴って移動
Longitudinal
Out-of-plane
Mix of multiple deformations
Stress
concentrated

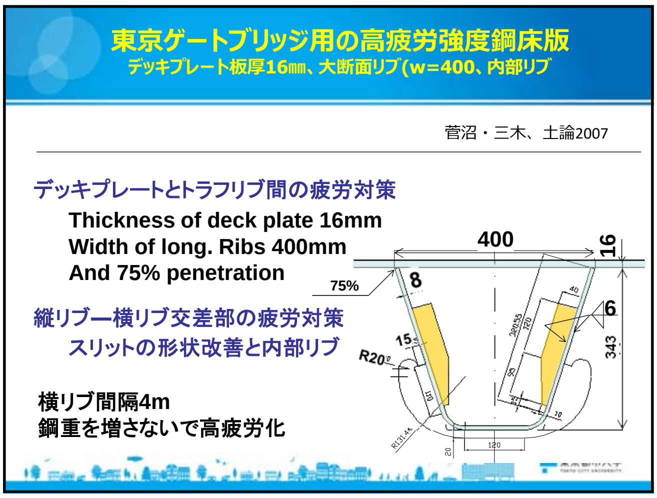
東京ゲートブリッジ用の高疲労強度鋼床版
デッキプレート板厚16㎜、大断面リブ(w=400、内部リブ
菅沼・三木、土論2007
デッキプレートとトラフリブ間の疲労対策
Thickness of deck plate 16mm
Width of long. Ribs 400mm
And 75% penetration
縦リブー横リブ交差部の疲労対策
スリットの形状改善と内部リブ
横リブ間隔4m
鋼重を増さないで高疲労化
400
16
75%
8
6
15
R20
343
120

縦リブー横リブ交差構造の研究

- 無スリットが最も高い構造、
- 平リブが優位、片側溶接によるルート問題から

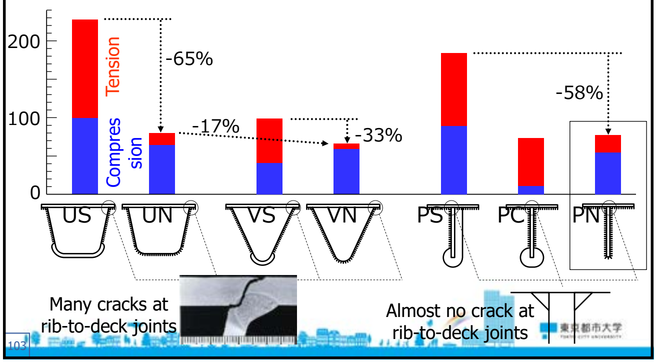

縦リブとデッキプレート間の溶接部ルート部に発生した疲労亀裂

どのように検知？
　３Dフェーズドアレイ

どのように補修？
　レーザーハイブリッド溶接

三木ほか、鋼構造論2016－9

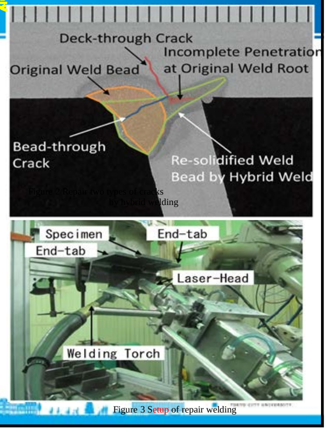

疲労の原因は活荷重と活荷重応力

活荷重の実態
　Weigh　Stationでの実測

WIM（Weigh in Motion)への関心
　BWIMは1980年代　F.Mosesのアイデア、
　米国各州で導入
　1995年（？）東名高速で実施
　Real time 処理とすることによりMonitoring 研究へ

活荷重応答
　実際に生じる応力と設計応力の差：実応力比
　疲労設計への導入（2002年の疲労設計指針）

重たいトラック荷重（B活荷重のレベル）での試験

土論NO.647(2000-4)

スパン中央断面でのG1桁内の応力分布

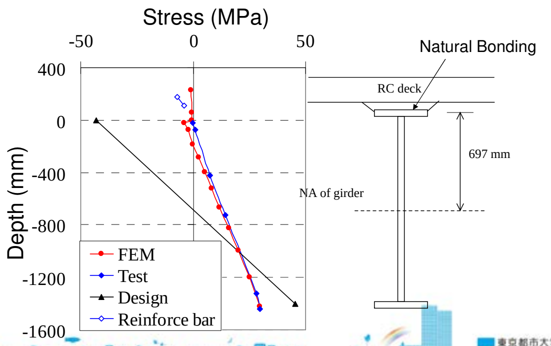

モニタリング研究」ー１
光通信網【情報BOX】を利用した橋梁の健全度長期遠隔モニタリング：2001-

リアルタイム自動測定・自動転送

ひずみ，たわみ，沓変位，
温度，腐食電流

リアルタイムデータ処理

温度寄与分と
荷重寄与分の分離

Weigh-in-Motion
温度変形挙動など

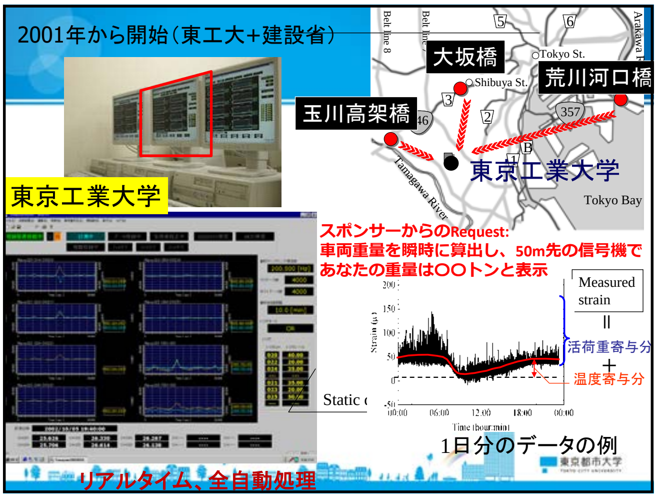
2001年から開始（東工大+建設省）
大坂橋
荒川河口橋
玉川高架橋
東京工業大学
Tokyo St.
Shibuya St.
Tamagawa River
Tokyo Bay
スポンサーからのRequest:
車両重量を瞬時に算出し、50m先の信号機で
あなたの重量は〇〇トンと表示
Measured strain
活荷重寄与分
温度寄与分
Static
Time (hour:min)
1日分のデータの例
リアルタイム、全自動処理
東京都市大学

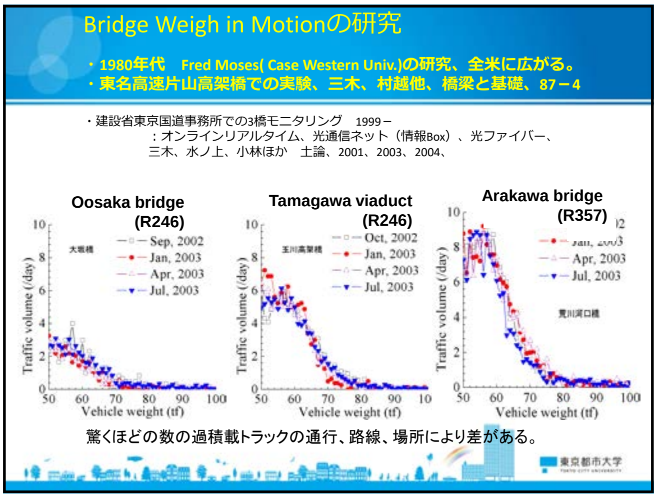
Bridge Weigh in Motionの研究
・1980年代　Fred Moses(Case Western Univ.)の研究、全米に広がる。
・東名高速片山高架橋での実験、三木、村越他、橋梁と基礎、87－4
・建設省東京国道事務所での3橋モニタリング　1999－
：オンラインリアルタイム、光通信ネット（情報Box）、光ファイバー、
三木、水ノ上、小林ほか　土論、2001、2003、2004、
Oosaka bridge (R246)
Tamagawa viaduct (R246)
Arakawa bridge (R357)
Sep, 2002
Jan, 2003
Apr, 2003
Jul, 2003
Oct, 2002
Traffic volume (/day)
Vehicle weight (tf)
驚くほどの数の過積載トラックの通行、路線、場所により差がある。
東京都市大学

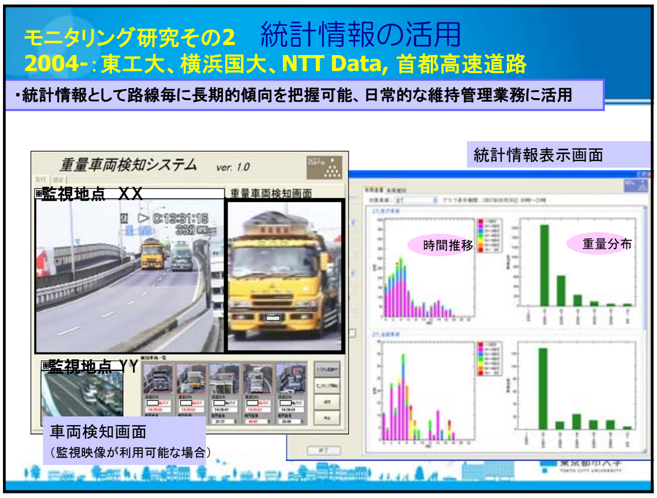
モニタリング研究その2　統計情報の活用
2004-：東工大、横浜国大、NTT Data, 首都高速道路
・統計情報として路線毎に長期的傾向を把握可能、日常的な維持管理業務に活用
重量車両検知システム ver. 1.0
監視地点 XX
監視地点 YY
統計情報表示画面
時間推移
重量分布
車両検知画面
（監視映像が利用可能な場合）

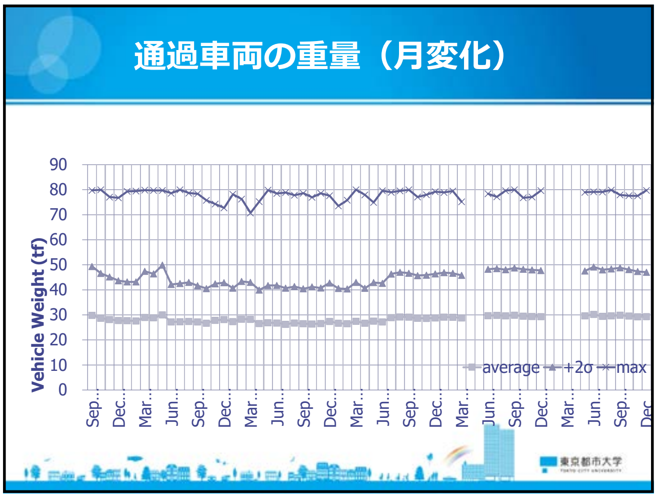
通過車両の重量（月変化）
Vehicle Weight (tf)
average
+2σ
max
東京都市大学


東京ゲートブリッジでのモニタリング
損傷シナリオベース

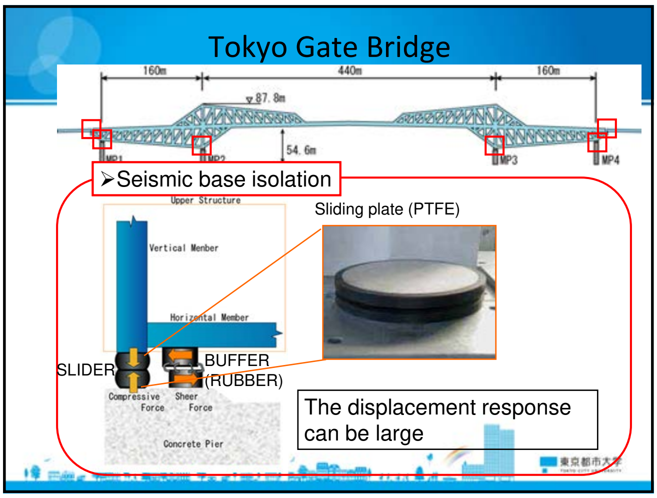
Tokyo Gate Bridge
160m
440m
160m
87.8m
54.6m
MP1
MP2
MP3
MP4
➤Seismic base isolation
Upper Structure
Vertical Member
Horizontal Member
Sliding plate (PTFE)
SLIDER
BUFFER (RUBBER)
Compressive Force
Sheer Force
Concrete Pier
The displacement response can be large
東京都市大学

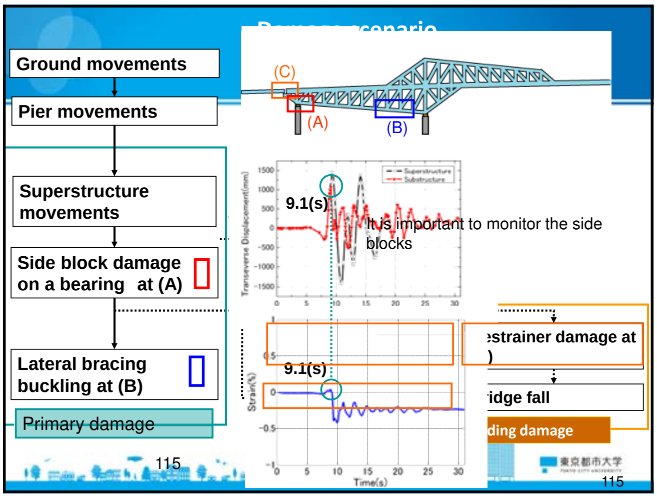

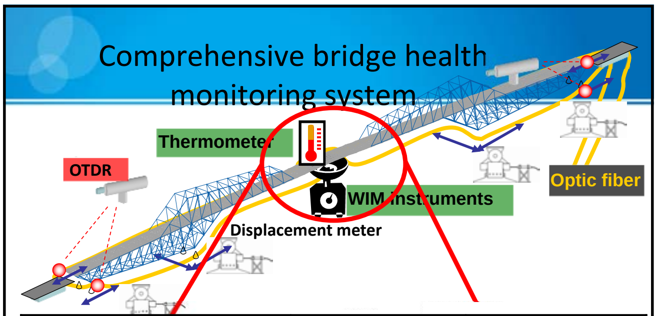

	OTDR (8)	Displ. meter (16)	Optic fiber(whole)
Monitoring item	A side block of the bearing	Displacement of the bearing	Structural failure
Evaluation items	●Bearing failure ●(Lateral bracing) ●Level difference	●Bearing performance	●Large deformation ●Bridge fall

IoTのグループ
MEMSのグループの関心
スマートインフラ
いろいろな団体ができた。

図4　面パターンで異常を捉える
NMEMS技術研究機構は、従来方法では捉えられなかった劣化情報を面パターンでセンシングすることで取得する取り組みを始めた(a)。センサのID情報を送信することで、異常箇所を把握する(b)。(図：NMEMS技術研究機構の資料を基に本誌が作成)

私なら数個のセンサーで十分　NIKKEI ELECTRONICS 2013.8.5

東京都市大学での研究

中村英夫学長の指示
・総合研究所所属で都市インフラのメンテナンス関係の研究をやるように
・都市大教員への科研の指導

疲労試験機などの研究設備なし
何をやろううか

現場がある。首都高速、新幹線など
スマートインフラ
橋に神経と脳を取り付け、傷を受けたら自分で痛いという
中村英夫学長コメント
Self detection, self Diagnosis

橋梁モニタリングの対象

やはりたわみでしょう。
固有振動数や減衰の変化では鋼構造物の損傷は？

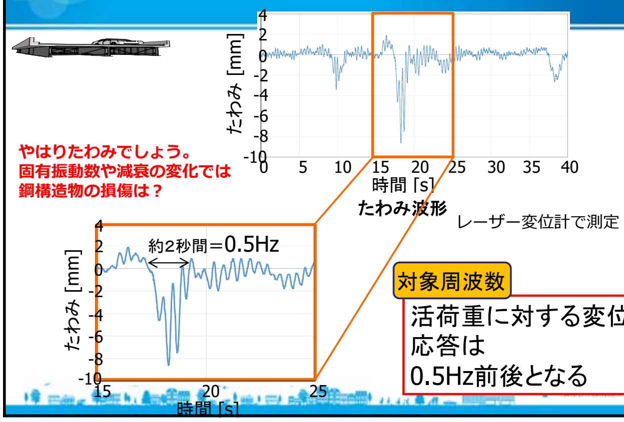

対象周波数
活荷重に対する変位応答は0.5Hz前後となる

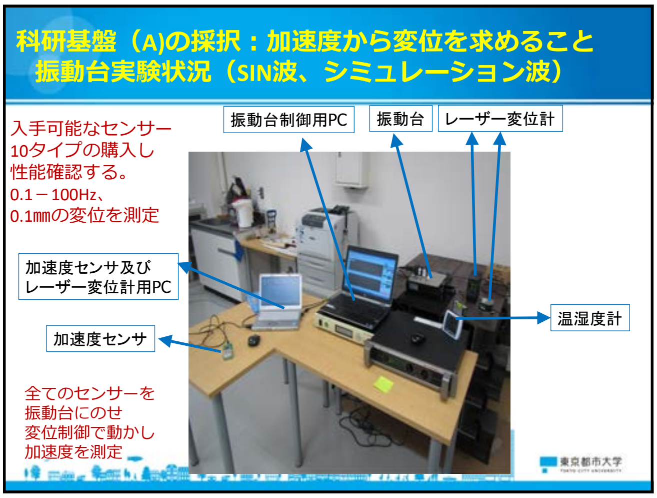
科研基盤（A)の採択：加速度から変位を求めること
振動台実験状況（SIN波、シミュレーション波）
入手可能なセンサー
10タイプの購入し
性能確認する。
0.1－100Hz、
0.1㎜の変位を測定
振動台制御用PC
振動台
レーザー変位計
加速度センサ及び
レーザー変位計用PC
温湿度計
加速度センサ
全てのセンサーを
振動台にのせ
変位制御で動かし
加速度を測定
東京都市大学

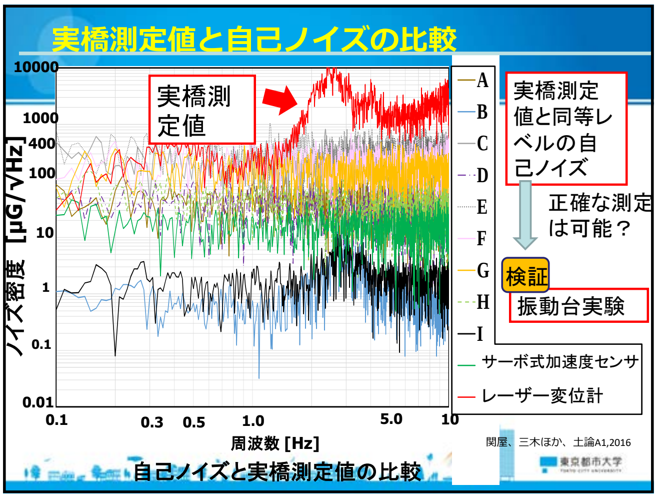
実橋測定値と自己ノイズの比較
実橋測
定値
実橋測定
値と同等レ
ベルの自
己ノイズ
正確な測定
は可能？
検証
振動台実験
ノイズ密度 [μG/√Hz]
周波数 [Hz]
A
B
C
D
E
F
G
H
I
サーボ式加速度センサ
レーザー変位計
関屋、三木ほか、土論A1,2016
自己ノイズと実橋測定値の比較
東京都市大学

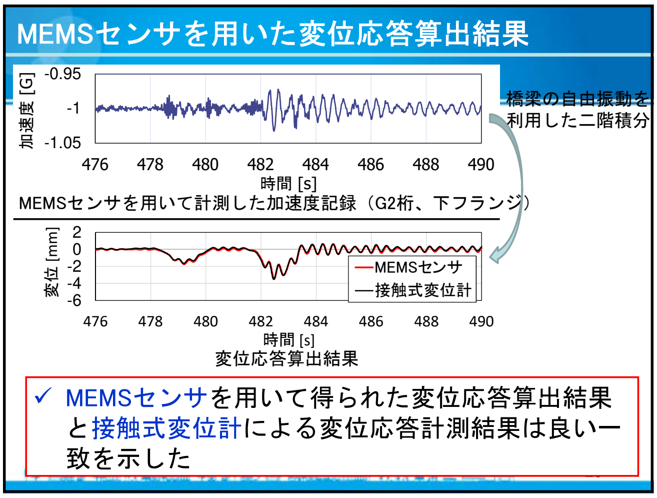
MEMSセンサを用いた変位応答算出結果
加速度 [G]
時間 [s]
橋梁の自由振動を
利用した二階積分
MEMSセンサを用いて計測した加速度記録（G2桁、下フランジ）
変位 [mm]
MEMSセンサ
接触式変位計
時間 [s]
変位応答算出結果
✓ MEMSセンサを用いて得られた変位応答算出結果と接触式変位計による変位応答計測結果は良い一致を示した

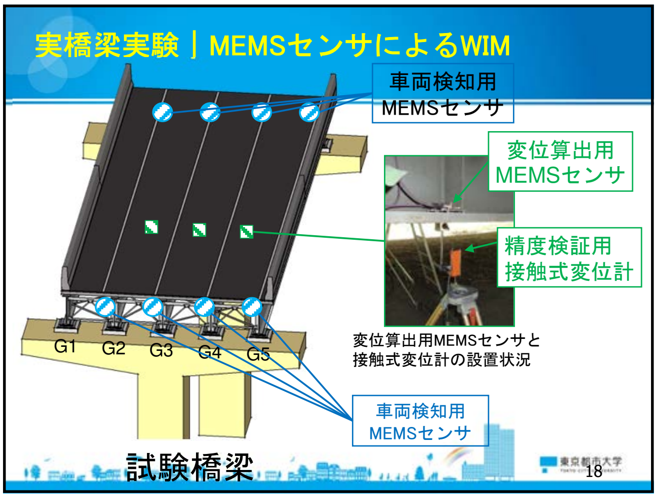
実橋梁実験｜MEMSセンサによるWIM
車両検知用
MEMSセンサ
変位算出用
MEMSセンサ
精度検証用
接触式変位計
G1
G2
G3
G4
G5
変位算出用MEMSセンサと
接触式変位計の設置状況
車両検知用
MEMSセンサ
試験橋梁
東京都市大学
18

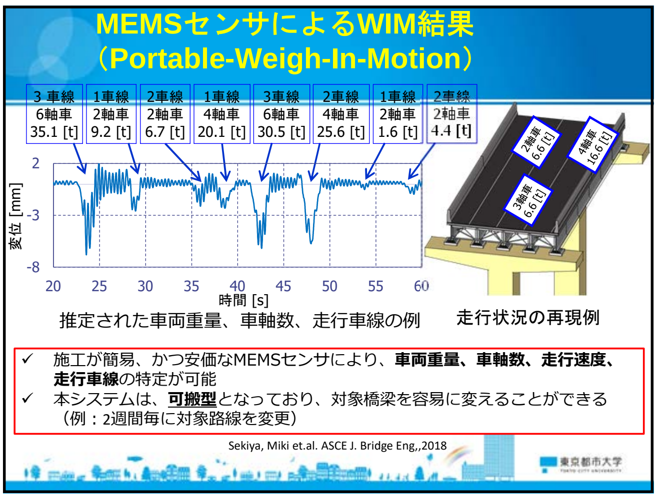
MEMSセンサによるWIM結果
（Portable-Weigh-In-Motion）
3車線 6軸車 35.1 [t]
1車線 2軸車 9.2 [t]
2車線 2軸車 6.7 [t]
1車線 4軸車 20.1 [t]
3車線 6軸車 30.5 [t]
2車線 4軸車 25.6 [t]
1車線 2軸車 1.6 [t]
2車線 2軸車 4.4 [t]
2軸車 6.6 [t]
4軸車 16.6 [t]
3軸車 6.6 [t]
変位 [mm]
時間 [s]
推定された車両重量、車軸数、走行車線の例
走行状況の再現例
✓ 施工が簡易、かつ安価なMEMSセンサにより、車両重量、車軸数、走行速度、走行車線の特定が可能
✓ 本システムは、可搬型となっており、対象橋梁を容易に変えることができる（例：2週間毎に対象路線を変更）
Sekiya, Miki et.al. ASCE J. Bridge Eng,,2018
東京都市大学

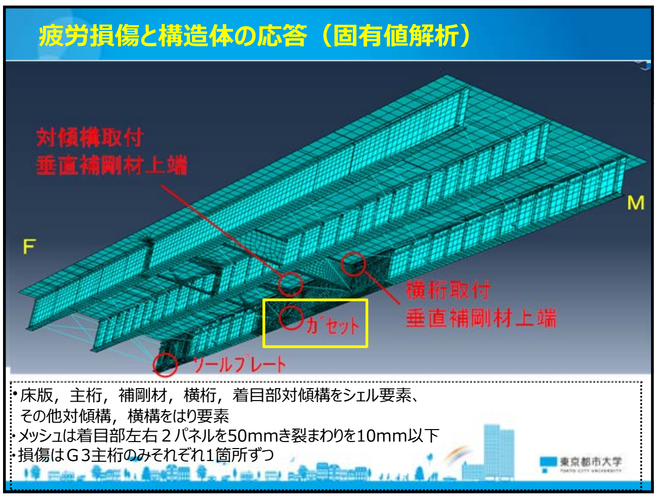
疲労損傷と構造体の応答（固有値解析）
対傾構取付
垂直補剛材上端
F
M
横桁取付
垂直補剛材上端
ガセット
ソールプレート
•床版，主桁，補剛材，横桁，着目部対傾構をシェル要素、
その他対傾構，横構をはり要素
•メッシュは着目部左右２パネルを50mmき裂まわりを10mm以下
•損傷はG３主桁のみそれぞれ1箇所ずつ
東京都市大学

３．固有値解析概要

損傷ケース　横構ガセット付け根に生じるき裂

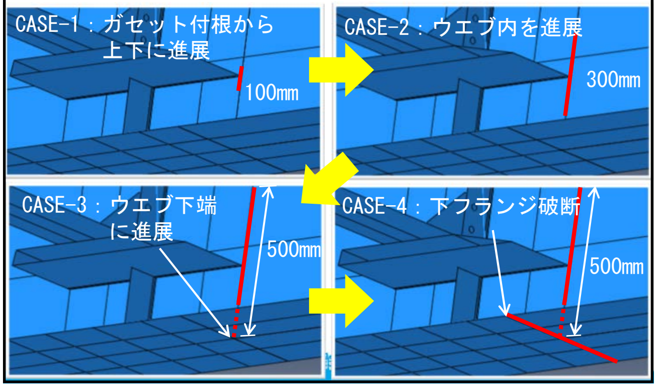

全体モード振動数(Hz)	健全	損傷1			損傷2				損傷3		
		CASE1	CASE2	CASE3	CASE1	CASE2	CASE3	CASE4	CASE1	CASE2	CASE3
		下ﾌﾗﾝｼﾞ 200mm 進展	下ﾌﾗﾝｼﾞ 破断	ｳｴﾌﾞ 進展	ｳｴﾌﾞ 200mm 進展	ｳｴﾌﾞ 400mm 進展	500mm ｳｴﾌﾞ 下端	下ﾌﾗﾝｼﾞ 破断	G3 VS 1箇所 破断	G3 VS全て 破断	橋梁 VS全て 破断
1次：鉛直1次	2.720	2.720	2.719	2.718	2.719	2.719	2.718	2.579	2.720	2.720	2.719
2次：ねじれ1次	4.825	4.820	4.793	4.642	4.825	4.825	4.825	4.768	4.825	4.824	4.819
3次：水平1次	6.962	6.960	6.945	6.878	6.962	6.962	6.962	6.923	6.962	6.955	6.936
4次：鉛直2次	8.534	8.524	8.471	8.229	8.533	8.532	8.532	8.376	8.534	8.533	8.531
5次：ねじれ2次	12.334	12.326	12.275	11.603	12.333	12.330	12.329	11.876	12.334	12.332	12.316
6次：鉛直3次	12.919	12.884	12.729	12.496	12.919	12.918	12.918	12.853	12.917	12.915	12.909
7次：水平2次	13.483	13.476	13.439	13.387	13.482	13.482	13.482	13.492	13.482	13.462	13.424

※着色部は連成モード等モード形状が変化

Sekiya, Miki et.al J. Sound and Vibration 438, 2019

東京都市大学

橋梁の疲労事例についてはData-Baseと2冊の本で公表

http://fatigue.civil.tcu.ac.jp/pukiwiki

206 cases of fatigue failure

多分、世界最大のData-base、
世界中からアクセス
日本からはほとんどなし
関心が低い、それとも英語のため
使ってください！！

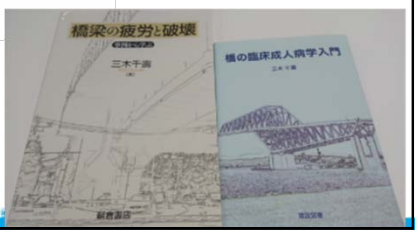

おわりに

研究にお付き合いいただいた
市川教授、助手、卒研生、修士学生、博士学生、研究生、研究員に感謝です

ご清聴、ありがとうございました

東京都市大学

土木学会講堂　　2021年12月16日

第９回 鋼構造技術継承講演会

積雪寒冷地における鋼道路橋の維持管理と耐震性能向上への貢献

北海道大学　名誉教授
工学博士　林川俊郎

略歴（自己紹介）

学 歴

昭和47年3月　北海道大学工学部土木工学科　卒業
昭和49年3月　北海道大学大学院修士課程　修了
昭和59年3月　北海道大学工学博士（論文博士）　取得

職 歴

昭和49年4月　北海道大学工学部　助手
昭和60年3月　プリンストン大学（米国）　客員研究員
昭和63年8月　北海道大学工学部　助教授
平成16年4月　北海道大学大学院工学研究科　教授
平成25年4月　北海道大学　名誉教授
平成25年4月　北海道大学大学院工学研究院　特任教授
平成27年3月　北海道大学大学院工学研究院　退職

研究歴（自己紹介）

昭和49年4月～　北海道大学工学部において
「鋼床版の耐荷力とUリブの規格化」
昭和51年4月～　北海道大学工学部において
「走行荷重による連続桁、吊橋の動的応答」
昭和61年4月～　北海道大学工学部において
「橋梁構造物の固有振動特性と動的応答」
平成 5年4月～　北海道大学工学部において
「歩道橋の動的応答解析と振動使用性」
平成 9年4月～　北海道大学大学院工学研究科において
「橋梁構造物の大地震時非線形挙動」
平成14年4月～　北海道大学大学院工学研究科において
「鋼製斜張橋タワーの大地震時非線形挙動」
平成19年4月～　北海道大学大学院工学研究科において
「免震支承と落橋防止システムの耐震性能」

社会活動（自己紹介）

平成 5年5月　道路管理技術検討委員会委員
平成 5年8月　岩見沢大橋技術検討委員会委員（道）
平成6年10月　白老漁港海岸整備計画調査検討会委員（局）
平成 7年2月　美原大橋及びその周辺高度利用検討委員会委員長
平成8年11月　札幌市地震対策土木技術検討委員会委員
平成 9年9月　道々静内中札内線シビチャリ11号橋検討委員会委員
平成 9年9月　千歳ジャンクションCランプ橋事故対策検討委員会委員
平成13年9月　北郷立体交差技術検討委員会委員（局）
平成13年9月　北海道道路管理技術センター道路防災ドクター
平成14年4月　公物の維持管理更新のあり方検討に係る専門員（道）
平成14年9月　（財）土木研究センター落橋防止構造に関する研究委員会
平成15年7月　追直漁港人工島橋梁景観検討委員会委員長（局）
平成15年9月　平成15年台風10号災害調査委員会委員（道）
平成15年9月　平成15年十勝沖地震検討委員会検討委員会委員

社会活動（自己紹介）

平成16年2月　公共土木施設長寿命化検討委員会委員（道）
平成16年4月　札幌市地震防災検討委員会委員
平成16年6月　北海道土木技術会鋼道路橋研究委員会委員長
平成16年10月　追直漁港施設利用検討委員会委員（局）
平成17年3月　創成橋保存技術検討委員会委員長（札幌市）
平成17年12月　ECCを用いた橋面構造に関する検討委員会委員（局）
平成18年6月　北海道新幹線冬季対策検討委員会委員（鉄道運輸）
平成19年4月　札幌市地震被害想定委員会委員
平成20年3月　溶接学会北海道支部支部長
平成20年8月　札幌市橋梁長寿命化修繕計画策定検討委員会委員
平成21年4月　土木学会北海道支部支部長
平成21年4月　北海道開発局道路防災有識者（局）
平成21年5月　札樽自動車道新川高架橋伸縮装置損傷検討委員会
平成21年8月　橋梁長寿命化修繕計画に関する有識者会議委員（局）
平成24年7月　東日本高速道路北海道支社橋梁長寿命化検討委員会

■道内の国道橋の建設推移

約4,000橋　（H18年時点,側道橋も含む）

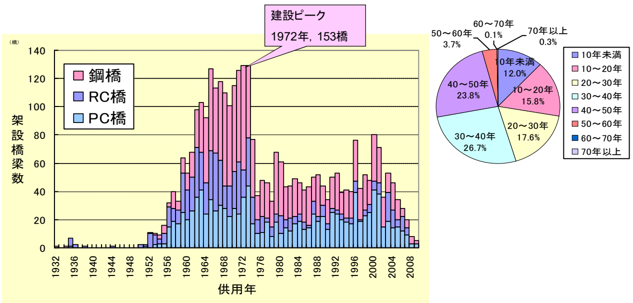

■北海道の損傷の特徴

北海道の国道橋梁の損傷の特徴は？

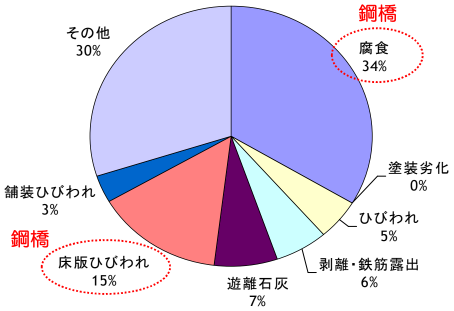

■北海道における鋼橋の損傷について

■鋼橋の損傷

■ 腐 食

第1段階　塗装のはがれ

内部の錆の発生により塗装がはがれる場合もある

第2段階　錆の発生

■ 腐 食

第3段階　鋼材断面の欠損

腐食が進行すると、鋼部材が腐食により欠損する場合もある。

■ 腐 食

北海道での事例

【支承部近傍】

■ 腐 食

北海道での事例

【桁端部】

■ 腐　食

桁端部に腐食・損傷が多い理由として・・・

① 伸縮装置の損傷・劣化
　→ 路面からの土砂・雨水の流れ落ち
　　土砂・雨水の堆積・滞水

② 閉鎖的空間・狭隘（風通しの悪さ）
　→ 堆積物の滞留
　　湿気の滞留
　　メンテナンス性の悪さ

■ 腐食の補修

桁端部の塗装塗り替えによる補修例
（重防食塗装）・（金属溶射）

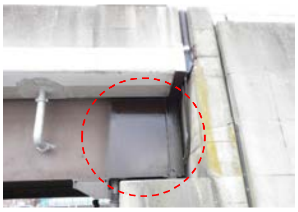

主桁端部塗り替え補修例

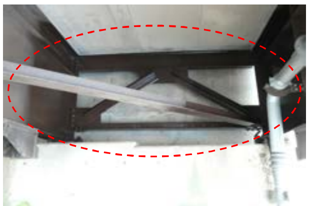

端対傾構塗り替え補修例

■ 腐食の補修

当て板による補修例

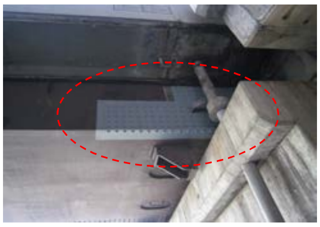

ボルト接合による当て板補修の例

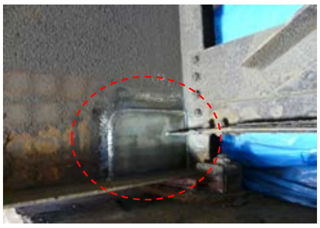

溶接による当て板補修の例

■ 腐食の補修

橋梁洗浄による塗装の延命化対策例

✧ 予防保全の一つの方法として、橋梁部材に付着した汚れや塩分などを取り除き、できるだけ架設初期の状態に近づけて、橋梁全体の腐食寿命を延ばすことを目的とした対策。

第１章　設計条件ＷＧ

■改訂ポイント　その他-1

1.3.2　耐候性鋼材の適用地域

p1-15

【改訂ポイント】
適用地域は，道示（Ⅱ鋼橋編）によることを標準とした。

＜背景＞
従来，道路管理者により適用地域に相違があった。基本方針を統一した。

図-解1.3.4 耐候性鋼橋梁の適用地域

■ 亀　裂

鋼部材は断面が薄いため、少しの亀裂でも、安全性を損なう可能性がある。

■ 亀　裂

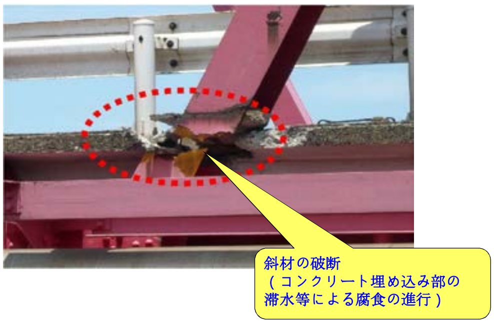

■ 亀　裂

北海道での事例

鋼床版の損傷

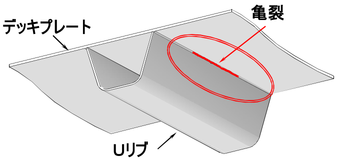

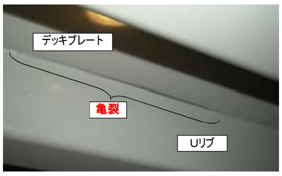

磁粉探傷試験

■ 亀　裂

北海道での事例

Uリブ溶接部の損傷

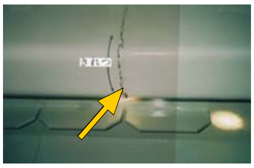

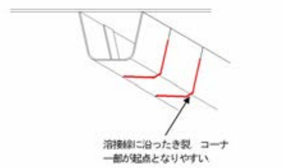

高力ボルトを用いた補修例

■ 亀裂の補修

ストップホールによる補修例（応急対策）

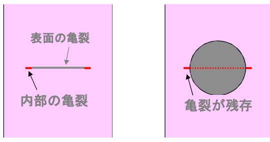

- 確実に先端に孔をあけることが重要
- グラインダーで削りながら非破壊検査により亀裂先端を発見して開孔

■ 亀裂の補修

補強板添加による補修例

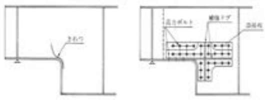

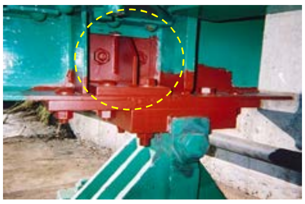

- 下フランジとウェブを一体化させたＬ型補強板が望ましい
- できれば新規支承や大きめのソールプレートへの取り替えが望ましい

■ ボルトの脱落

遅れ破壊による高力ボルトの脱落、または、腐食によるものなど

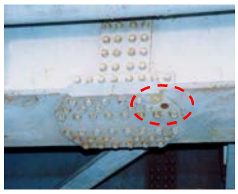

◻遅れ破壊とは？

- 遅れ破壊とは、一定の引張荷重が加えられている状態で、ある時間が経過したのち、突然脆性的に破壊する現象です。
- これまでの調査から、F11T高力ボルトの特に昭和46年～52年頃のものに多く見られます。
- また、腐食環境の厳しい箇所に発生しやすい

■ ボルトの脱落

北海道での事例

遅れ破壊が懸念される橋については、高力ボルトの交換が必要となってくる。

■ 床版の損傷

- 鋼橋において、主にコンクリート床版が用いられる。
- 通行車両が繰り返し通過することで、疲労による損傷が問題となる。
- 疲労破壊とは、小さい力であっても、継続的に繰り返し受け続けると、受けた部材の強度が次第に小さくなり、やがて変形し、破壊に至ることをいう。
- 特に、北海道は凍害による損傷（陥没）が多く発生している。

■ 床版の損傷

床版の損傷プロセス

潜伏期
（一方向ひびわれ）

進展期
（二方向ひびわれ）

■ 床版の損傷

床版の損傷プロセス

加速期
（角落ち、漏水）

劣化期
（局部的な陥没）

■ 床版の損傷

北海道の損傷事例

床版破壊事例 ：2008年6月

床版破壊事例 ：2008年7月

■床版損傷は安全・快適な交通を阻害し、利用者への影響は大きい。そのため、このように事態ならぬよう、日常点検時に十分な配慮が必要である。

■ 床版の損傷

北海道の損傷事例

凍害による損傷

舗装を撤去すると、床版コンクリートのほとんどが砂利化している。また、滞水も確認された。

■ 床版の損傷

北海道の損傷事例

点検時の注意

舗装を撤去してみると、床版上面が砂利化、人力でもザクザクの状態

下面の状況：漏水はあるがひび割れの進展が無い

■ 床版の損傷

北海道の損傷事例

水の影響とは

- 乾燥収縮や交通荷重の繰り返しによりひび割れが発生する
- ひび割れから水の浸入しひび割れ面の摩耗が促進する
- 浸透水によって凍結融解が促進する

　上記現象によって・・・

- ひび割れ面のこすり合わせ現象とひび割れ面内の水が路面に吹き出すポンピング現象が生じる。
- 床版表面のコンクリートはセメントペーストと骨材に分離され骨材化現象が生じる。

■支承の損傷について

■ 支 承

- 支承は、橋台、橋脚上に設置され、上部構造と下部構造をつなぐ役割をもつ。
- 支承(沓)の種類
  - 鋼製
  - ゴム製

- 支承の設置
  - 上部構造とはボルトで直接連結
  - 下部構造ともボルトで連結されるが、下部構造上に、台座コンクリートとモルタル（沓座モルタル）を設け、その上に支承が設置されている。

■ 支承の損傷

- 支承本体
  - 腐食
  - 欠損
- 台座コンクリート
  - 破損
- 沓座部
  - 表面コンクリートの劣化
  - 土砂堆積

第１２章　付属物

■改訂ポイント　【支承】

表－解 12.2.1　支承部の損傷事例（その 1）

写真	損傷状況	主な原因	対策工
	機能障害（回転・水平移動）錆び，腐食，塗装の剥がれ，帯水，モルタル損傷	・伸縮装置からの漏水 ・可動部の防錆・防塵機能不足と維持・管理の不良	①支承交換 ②桁の防錆，防食処理 ③伸縮装置からの止水対策および伸縮装置の改修・交換
	機能障害（回転・水平移動・水平力支持）腐食，アンカーボルトの変形	・伸縮装置からの漏水 ・経年的な腐食 ・可動部の防錆・防塵機能不足と維持・管理の不良	①支承交換 ②桁の防錆，防食処理 ③伸縮装置からの止水対策および伸縮装置の改修・交換
	機能障害（回転・水平移動）錆び，塗装の剥がれ，土砂堆積	・伸縮装置からの漏水 ・凍結防止材の散布 ・可動部の防錆・防塵機能不足と維持・管理の不良	①支承交換 ②桁の防錆，防食処理 ③伸縮装置からの止水対策および伸縮装置の改修・交換 ④支承部の定期的な清掃作業
	沓座モルタルの損傷	・凍害による損傷 ・活荷重等による振動 ・剛構造に伴う偏載荷	①沓座モルタルの打換え ②ジャッキアップにより偏載荷の調整
	桁への損傷誘発 ・上沓の破断 ・損傷原因の判定ならびに補修方法の選定ミスにより主桁の変形と補強上沓が再度損傷	・不測の荷重作用 ・補修方法の選定ミス ・補修箇所・補修部材の選定ミス	①上沓の交換 ②桁の補強，主桁支点部の補強 ③支承交換

表－解 12.2.2　支承部の損傷事例（その 2）

写真	損傷状況	主な原因	対策工
	支承の損壊 ・上沓の破断	・地震による損傷 ・水平力支持機能の不足（耐力不足）	①支承交換 ②耐震設計によりタイプＢの支承に変更
	支承の損壊 ・変位制限装置他全機能への損傷	・地震による損傷 ・水平力支持機能の不足（耐力不足） ・支承本体の及び支承への耐震補強，補修の不徹底	①支承交換 ②耐震設計によりタイプＢの支承に変更ならびに橋梁全体系の改善対策
	支承部材の損壊 アンカーボルトの抜け ・残留変位（移動制限の偏り）	・地震による損傷 ・橋軸及び橋軸直角方向への回転追随性能の不足	①支承交換（橋軸，橋軸直角方向の回転性能が向上した支承構造） ②アンカーボルトの引抜き耐力アップ（アンカーフレーム等）
	支承部取付け部の損傷 ・桁の下フランジの損傷	・地震による損傷 ・橋軸及び橋軸直角方向への回転追随性能の不足 ・主桁の支点補剛材の不足 ・地震前から錆等により回転機能の損傷	①桁の下フランジの補修・補強 ②支承交換（橋軸，橋軸直角方向の回転性能が向上した支承構造）
	支承部取付け部の損傷 ・桁の下フランジの損傷	・地震による損傷 ・橋軸方向への回転追随性能の不足 ・主桁の支点補剛材の不足 ・地震前から錆等により回転機能の損傷	①桁の下フランジの補修・補強 ②支承交換（橋軸，橋軸直角方向の回転性能が向上した支承構造）

第１２章　付属物

■改訂ポイント　【支承】

12.2.4　支承の補修および交換（pp12-8～12-11）

参考)ゴム支承表面クラックの補修の一例

①地震により大きなせん断変位が残ったゴム支承の補修例

写ー解 12.2.1　震災後の支承

写ー解 12.2.2 クラックの拡大

写ー解 12.2.3 補修後

■伸縮装置・防護柵の損傷について

■　伸縮装置・防護柵

- 伸縮装置・防護柵ともに、損傷劣化（腐食等）が多く確認される部位。

- 伸縮装置
  - 橋の端部において、桁の温度による伸び縮みを吸収するために設けられる構造
- 防護柵
  - 車両や歩行者の路外への逸脱を防止するために設けられる柵

■　伸縮装置

■　伸縮装置の損傷

北海道の損傷事例

■錆発生

■止水部材脱落

■除雪機接触損傷

寒冷地特有の損傷状況に対応した伸縮装置の改善提案

第１２章　付属物

■改訂ポイント　【伸縮装置】

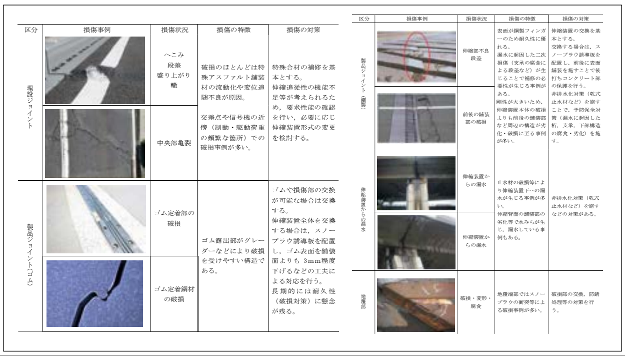

第６章　付属物

■改訂ポイント　【排水設備】

要求性能(pp6-57～58)
(1) 排水性
(2) 耐荷性
(3) 耐腐食性
(4) 維持管理性

■ 防護柵の損傷

- 腐食、亀裂、欠損、破断、凍害

現行基準に則した新規防護柵への取替補修提案

北海道における鋼道路橋の設計及び施工指針の改訂

北海道土木技術会鋼道路橋研究委員会

(平成24年1月　指針の大幅な改訂作業を実施)

初　版：昭和４４年３月
第２版：昭和４７年４月
第３版：昭和５４年４月（P189）
第４版：昭和５８年８月（P215）
第５版：平成元年１１月（P284）
第６版：平成７年１２月（P318）

第７版：平成２４年１月（本改訂）
第1編：設計・施工編（P390）
第2編：維持管理編（P386）
第３編：資料編（P91）

1995年1月17日5時46分　内陸直下型地震

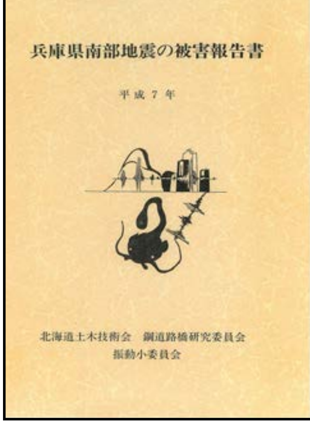

橋梁構造物の地震被害調査派遣

ピルツ橋、神戸大橋、ランプ橋

座屈、塑性ヒンジ

西宮港大橋

鉄道高架橋・ラーメン偶角部

神戸市庁舎・外壁

上部構造・橋脚・建物の壊滅的な崩壊

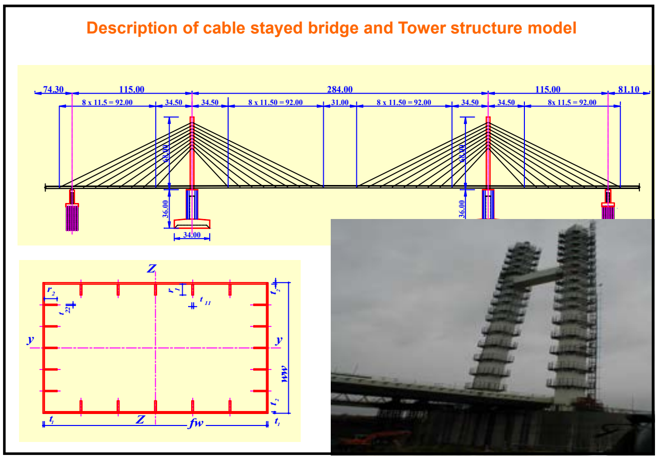
Description of cable stayed bridge and Tower structure model
74.30
115.00
284.00
115.00
81.10
8 x 11.5 = 92.00
34.50
34.50
8 x 11.50 = 92.00
31.00
8 x 11.50 = 92.00
34.50
34.50
8x 11.5 = 92.00
36.00
34.00

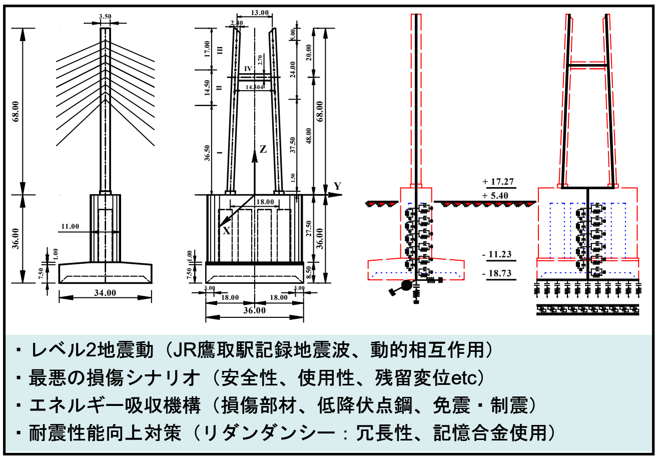
68.00
36.00
34.00
13.00
18.00
36.00
+ 17.27
+ 5.40
- 11.23
- 18.73
・レベル2地震動（JR鷹取駅記録地震波、動的相互作用）
・最悪の損傷シナリオ（安全性、使用性、残留変位etc）
・エネルギー吸収機構（損傷部材、低降伏点鋼、免震・制震）
・耐震性能向上対策（リダンダンシー：冗長性、記憶合金使用）

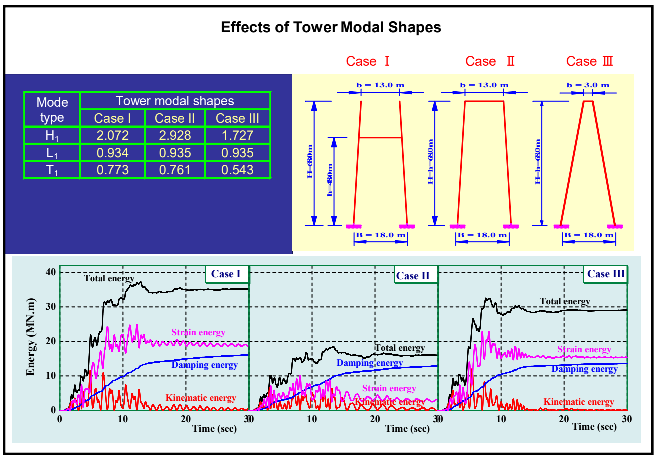
Effects of Tower Modal Shapes
Case Ⅰ
Case Ⅱ
Case Ⅲ
Mode type | Tower modal shapes: Case I | Case II | Case III
H1 | 2.072 | 2.928 | 1.727
L1 | 0.934 | 0.935 | 0.935
T1 | 0.773 | 0.761 | 0.543
b = 13.0 m
b = 13.0 m
b = 3.0 m
B = 18.0 m
B = 18.0 m
B = 18.0 m
Energy (MN.m)
Total energy
Strain energy
Damping energy
Kinematic energy
Time (sec)

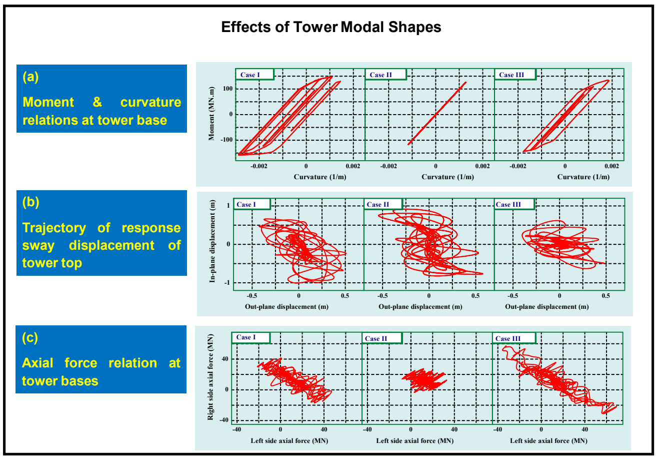
Effects of Tower Modal Shapes
(a)
Moment & curvature relations at tower base
(b)
Trajectory of response sway displacement of tower top
(c)
Axial force relation at tower bases
Case I
Case II
Case III
Curvature (1/m)
Out-plane displacement (m)
Left side axial force (MN)

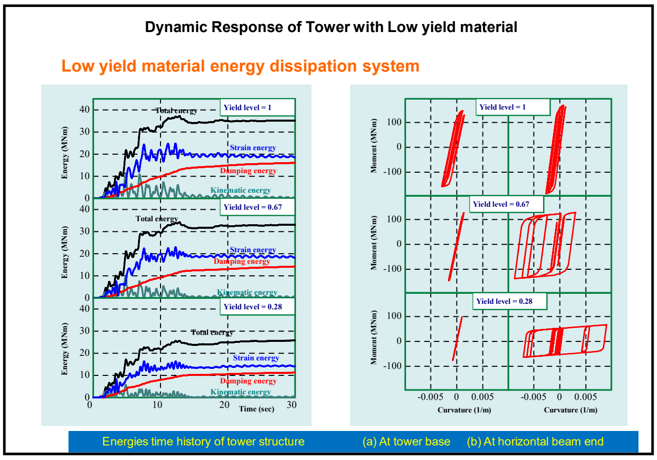
Dynamic Response of Tower with Low yield material
Low yield material energy dissipation system
Yield level = 1
Yield level = 0.67
Yield level = 0.28
Total energy
Strain energy
Damping energy
Kinematic energy
Energy (MNm)
Moment (MNm)
Time (sec)
Curvature (1/m)
Energies time history of tower structure
(a) At tower base
(b) At horizontal beam end


落橋防止システムと機能分散型支承
ライフライン施設として道路橋の大地震時における使用限界状態について
（１）落橋防止システムの正常な状態
（２）落橋防止システムの異常な状態
上部構造の異常な配列
曲線床版の幾何学的な形状
✓複雑な床版の回転
✓橋軸直角方向への変形
上部構造の異常な連続性
伸縮装置の損傷
✓けたかかり長
✓桁間衝突
✓伸縮装置の遊間
上部構造と下部構造間の異常な連結状態
✓支承部の損傷
✓鉛直方向の段差
落橋防止システムの異常な状態
通行止め
部分的な通行開始
・救急車両等の通行障害
・架け替えや補修にかかる直接的なコスト負担
・通行止めによる社会に与える間接的なコスト負担

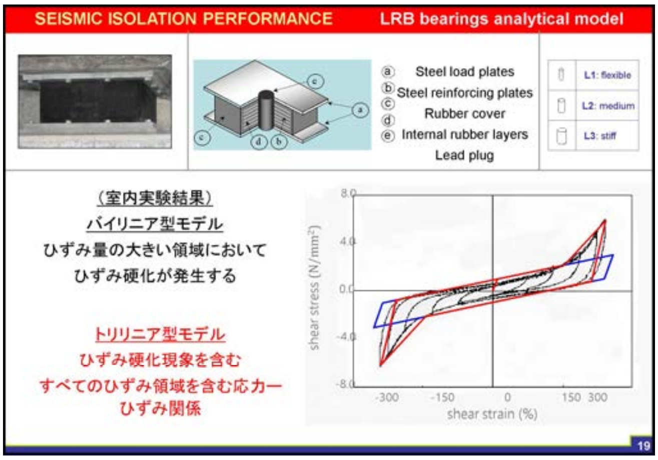

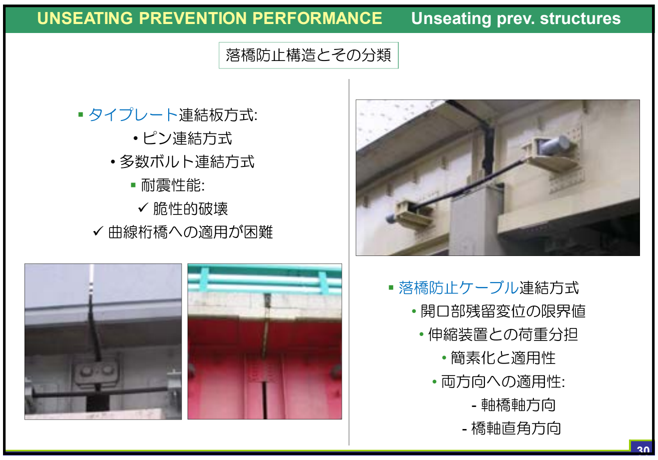

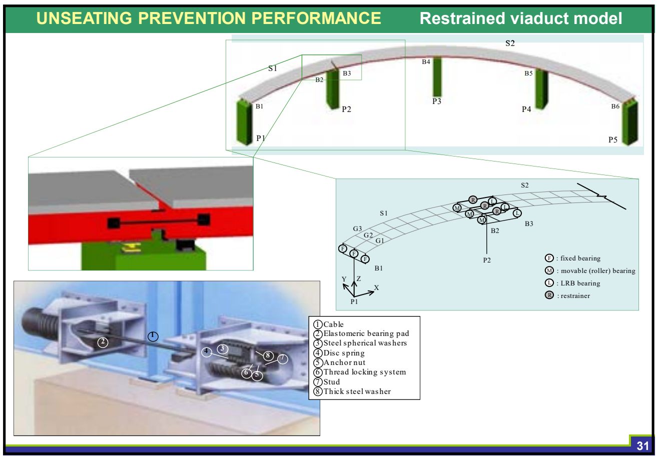

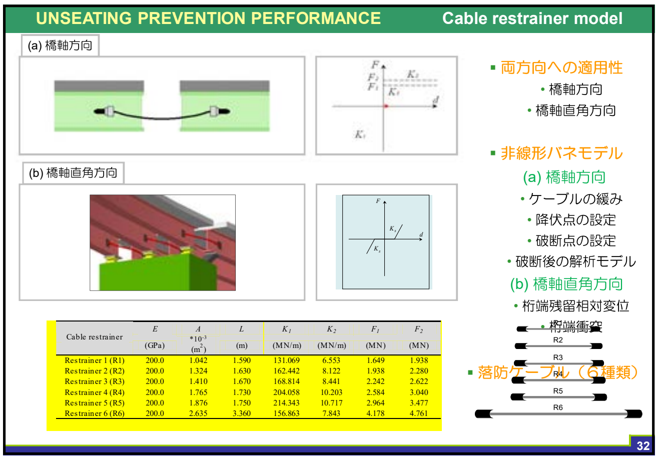

Cable restrainer	E (GPa)	A $*10^{-3}$ (m^2)	L (m)	K_1 (MN/m)	K_2 (MN/m)	F_1 (MN)	F_2 (MN)
Restrainer 1 (R1)	200.0	1.042	1.590	131.069	6.553	1.649	1.938
Restrainer 2 (R2)	200.0	1.324	1.630	162.442	8.122	1.938	2.280
Restrainer 3 (R3)	200.0	1.410	1.670	168.814	8.441	2.242	2.622
Restrainer 4 (R4)	200.0	1.765	1.730	204.058	10.203	2.584	3.040
Restrainer 5 (R5)	200.0	1.876	1.750	214.343	10.717	2.964	3.477
Restrainer 6 (R6)	200.0	2.635	3.360	156.863	7.843	4.178	4.761

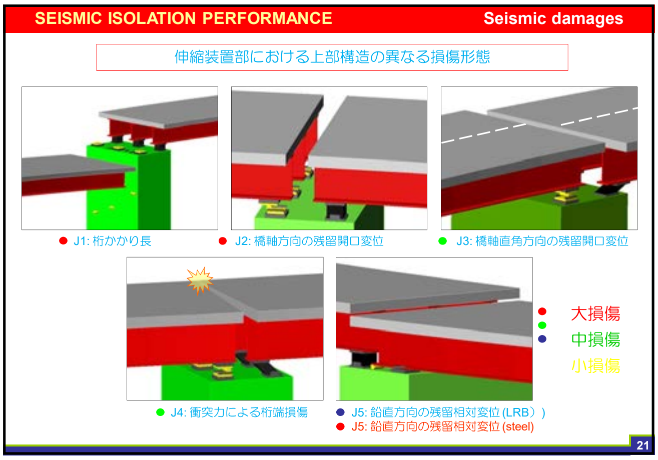

Structural Eng./Earthquake Eng., JSCE, Vol. 20, No. 1, 25s—41s, 2003 April
(J. Struct. Mech. Earthquake Eng., JSCE, No. 731/ I —63)

PARAMETRIC STUDY ON STEEL TOWER SEISMIC RESPONSE OF CABLE-STAYED BRIDGES UNDER GREAT EARTHQUAKE GROUND MOTION

Shehata E. ABDEL RAHEEM [1] and Toshiro HAYASHIKAWA [2]

[1]Graduate Student, Graduate School of Engineering, Hokkaido University
(Nishi 8 Kita 13 Kita-ku, Sapporo 060-8628, Japan)
[2] Fellow of JSCE, Dr. of Eng., Assoc. Prof., Graduate School of Engineering, Hokkaido University
(Nishi 8 Kita 13 Kita-ku, Sapporo 060-8628, Japan)

Analytical parametric study on dynamic characteristics of steel tower of cable-stayed bridges is performed to investigate the individual influence of different design aspects, such as damping mechanism, input ground motion, allowable initial construction imperfections, energy dissipation and tower modal shapes. The results show that the horizontal beam height and length and the low yield energy dissipation system significantly affect tower structural behavior. The initial imperfections within design range have slight detrimental effects on the tower seismic response but these effects grow rapidly beyond the design range. Mass proportional damping leads to overestimate tower axial forces and acceleration response.

Key Words: steel tower, cable-stayed bridge, energy dissipation, seismic design, imperfections

1. INTRODUCTION

In recent decades, long span bridges such as cable-stayed bridges have gained much popularity due to their aesthetic appearance, efficient utilization of structural materials, increase of the horizontal navigation clearances and the economic trade off of span length cost of deep water foundation. The trend nowadays for cable-stayed bridges is to use more shallow or slender stiffening girders combined with increasing span lengths. This structural synthesis provides a valuable environment for the nonlinear behavior due to material nonlinearities and geometrical nonlinearities of the relatively large deflection of the structure on the stresses and forces[1) ~ 3)]. The Hyogoken-Nanbu earthquake of 17th January 1995, led to an increased awareness concerning the response of highway bridges subjected to earthquake ground motions, the ductility design and dynamic analyses have been reconsidered by Japan Road Association[4)]. The necessity has arisen to develop more efficient analysis procedures that can lead to a through understanding and a realistic prediction of the precise three-dimensional nonlinear dynamic response of bridge structural systems to improve the bridges seismic performance, to provide damage control and post-earthquake functionality.

In the analysis and design of earthquake resistant structures, particularly bridge structures, the vertical ground motion tends, in general, to be ignored or underestimated in seismic analysis. The current seismic codes recommend a vertical spectrum with values that vary from half to three quarters of that of the horizontal spectra. This approach seems to be un-conservative in light of ground motion measurements during recent earthquakes, which indicate that the vertical acceleration could reach values even higher than that of the horizontal acceleration. Moreover, in a near field region, the peak of vertical to horizontal spectral ratio is even larger than that of the peak ground acceleration, especially at short periods[5)]. Also field observations proved that many structures experienced significant damage attributable to high vertical forces[6) ~ 8)]. The dynamic analysis of bridge column and pier structures subjected to horizontal and vertical excitations was considered only recently by some researchers[8), 9)], where the results of that analyses with the inelastic plane stress elements, displayed unstable hysteresis loops and little energy dissipation.

The strength and ductility of a thin-walled steel member are particularly sensitive to initial imperfections including geometric imperfection and longitudinal residual stresses. The initial imperfections of these structures that have not been subjected to damage usually result from the fabrication process. Some studies[10) ~ 14)] have been carried out on welded and hot rolled structures, it was reported that the detrimental effects of geometric imperfection and welding residual stresses that led to an appreciable reduction in load carrying capacity. However, a study of the effect of initial imperfections on the dynamic behavior of thin-walled structures is not available in literature. Moreover, the dynamic response of steel tower depends to large extent on tower modal shapes[15], including the horizontal beam position and its elements relative strength. For economical earthquake resistant of steel tower and its protection from the earthquake hazard, the tower structure should be constructed to dissipate a large amount of input seismic energy that could be achieved by proper selection of tower shapes and its elements relative strength. The low strength steels with low yield stresses and large ductility have been introduced for the hysteretic damper concept; the energy dissipation of hysteretic dampers through their materials could be used for structure damage control under large earthquake excitations[16)~18)].

A parametric study on steel tower of cable-stayed bridges is performed for investigation of the individual influence of different design aspects on tower dynamic characteristics. This study aims at clarifying the characteristics of the vertical ground motion and damping mechanism effects on critical seismic response quantities of the steel tower under strong ground motions. A comparison of the response with and without the vertical component is performed for two different cases of spectral damping schemes. It is confirmed from numerical results that the vertical excitation could have a detrimental effect on axial force and overestimated acceleration of tower seismic response for the mass proportional damping scheme, but slightly effects for Rayleigh's damping.

Moreover, this study investigates the steel tower seismic response under initial construction imperfections using finite element method. The amplitude of imperfections in the lowest eigenmodes of vibration is considered to be sufficient to characterize the influential imperfections[19]. As a result, a great deal of insight has been obtained on the dynamic response of steel tower. The results indicate that both the initial geometric imperfection and the welding induced residual stresses within their design range slightly affect on the tower seismic response but beyond the design range, these effects are characterized by rapidly and nonlinearly growth as the initial imperfections approach severe values. The residual stress effects are due to decreasing plastic deformation capability, consequently promoting brittle behavior.

An effective energy . dissipation concept is suggested by a typically concentration of inelastic behavior at tower horizontal beam using low relative strength and stiffness, which can be achieved by inserting low yield material instead of cross section dimensions reduction. Since the horizontal beam is easy to inspect and repair if necessary, the rest of the structure will remain elastic, thus eliminating permanent damage and minimizing the extent of retrofit. The calculated results prove the effectiveness of the proposed energy dissipation system in reducing structural elements forces and control tower maximum displacement, and enable to determine the optimum position of horizontal beam for economical earthquake resistant design.

2. NONLINEAR DYNAMIC ANALYSIS PROCEDURES

The governing nonlinear dynamic equation of the tower response can be derived by the principle of energy that the external work is absorbed by the work of internal, inertial and damping for any small admissible motion that satisfies compatibility and boundary conditions. By assembling the element dynamic equilibrium equation for the time $t+\Delta t$ over all the elements, the incremental FEM dynamic equilibrium equation[1), 20)] can be obtained as:

$$[\mathbf{M}]\{\ddot{u}\}^{t+\Delta t}+[\mathbf{C}]\{\dot{u}\}^{t+\Delta t}+[\mathbf{K}]^{t+\Delta t}\{\Delta u\}^{t+\Delta t} = \{\mathbf{F}\}^{t+\Delta t}-\{\mathbf{F}\} \quad (1)$$

where [M], [C] and $[\mathbf{K}]^{t+\Delta t}$ are the system mass, damping and tangent stiffness matrices at time $t+\Delta t$, the tangent stiffness considers the material nonlinearities through bilinear elastic-plastic constitutive model incorporating a unaxial yield criteria and kinematic strain hardening rule. $\ddot{u}$, $\dot{u}$ and Δu are the accelerations, velocities, and incremental displacements at time $t+\Delta t$, respectively, $\{\mathbf{F}\}^{t+\Delta t}-\{\mathbf{F}\}^{t}$ is the unbalanced force vector. The dynamic equilibrium equation of motion considers both geometrical and material nonlinearities that affect the tangent stiffness and internal forces calculation.

In this study, the Newmark step-by-step integration method is used for the integration of equation of motion, since it has been experienced that the Newmark's β method is the most suitable for nonlinear analysis; it has the lowest period elongation and has no amplitude decay or amplifications. In addition, the stability concern is not a problem with the variable ratio of time increment to natural period. The algorithm is unconditionally stable if $\beta \geq (\gamma + 0.5)^2/4$. In this study, the Newmark's β of constant acceleration scheme for the solution of the differential equation of motion is considered for which β is equal to 0.25, The second numerical parameter γ of Newmark's β method is set as $\gamma = 0.5$ to avoid a superfluous damping in the system. The equation of motion is solved for the incremental displacement using the Newton-Raphson iteration method; the stiffness matrix is updated at each increment to consider the geometrical and material nonlinearities and to speed the convergence rate.

3. FINITE ELEMENT OUTLINE

(1) Finite element model

The steel tower of a three span continuous cable-stayed bridge located in Hokkaido, Japan is considered, in which the main span length is equal to 284m. The steel tower is taken out of the cable-stayed bridge and modeled as three-dimensional frame structure. A fiber flexural element is developed for characterization of the steel tower and that element incorporates both geometric and material nonlinearities. The Hermitian cubic displacement field is employed for the transverse bending displacements of the element and a linear displacement field is employed for the axial and torsional displacements. The stress-strain relationship of the beam element is modeled as bilinear stress strain relation for the beam column element. The yield stress and the modulus of elasticity are equal to 355 MPa (SM490Y) and 200GPa, respectively, the strain hardening in the plastic region is equal to 0.01.

Inelasticity of the fiber flexure element is accounted for by the division of the cross section into a number of fiber zones with uniaxial plasticity defining the normal stress-strain relationship for each zone, the element stress resultants are determined by integration of the fiber zone stresses over the cross section of the element. By tracking the center of the yield region, the evolution of the yield surface is monitored, and a stress update algorithm is implemented to allow accurate integration of the stress-strain constitutive law for strain increments, including full load reversals. To ensure path dependence of the solution, the implementation of the plasticity model for the implicit Newton-Raphson equilibrium iterations employs stress integration, whereby the element stresses are updated from the last fully converged equilibrium state. The transformation between element local and global coordinate systems is accomplished through a vector translation of element forces and displacements based on the direction cosines of the current updated element coordinate system.

The nonlinear behavior of cable elements is idealized by using the equivalent modulus approach, in this approach each cable is replaced by a truss element with equivalent tangential modulus of elasticity E_{eq} that is given by Ernst[21] as:

$$E_{eq} = E \,/\, \{1 + EA\,(wL)^2 \,/\, 12T^3\} \qquad (2)$$

where E is the material modulus of elasticity, L is the horizontal projected length of the cable, w is the cable weight per unit length, A is the cable cross sectional area and T is the cable pretension force. It can be noticed that the nonlinearity of the cable stays originates with an increase in the loading followed by a decrease in the cable sag as a consequence the apparent axial stiffness of the cable increases. The inclined cable is represented by an equivalent straight cable element with relative axial deformation (Δl), the stiffness matrix of the cable element **K** has the value equal to $E_{eq}A/l$ for $\Delta l > 0$, and the cable stiffness vanishes and no element force exist when shortening occurs, i.e. $\Delta l < 0$.

This cable-stayed bridge has nine cables in each tower side. The dead load of the stiffening girder is considered to be equivalent to the vertical component of the pretension force of the cables and acted vertically at their joints. The inertia forces

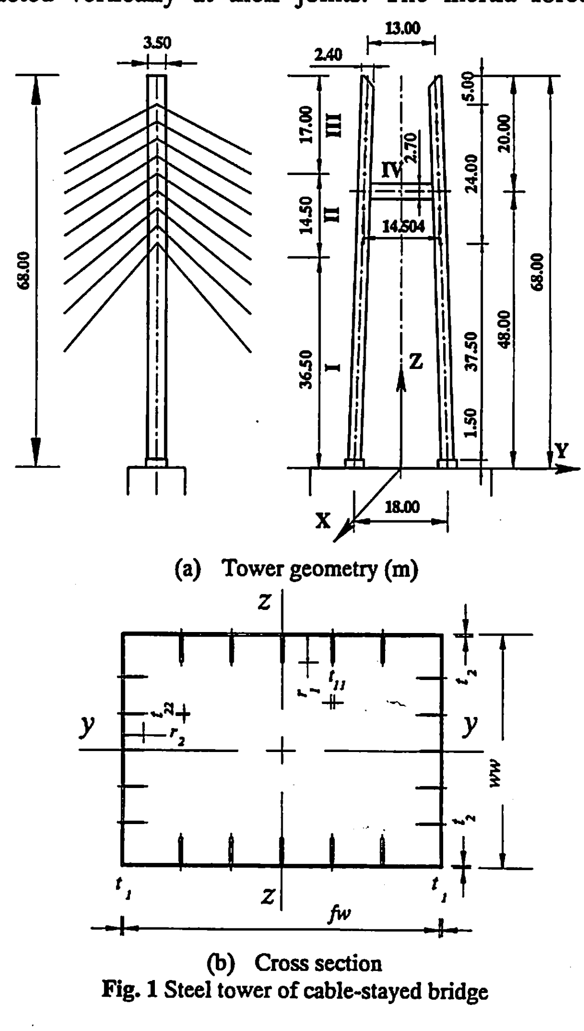

(a) Tower geometry (m)

(b) Cross section

Fig. 1 Steel tower of cable-stayed bridge

Table 1 Cross section dimensions of different tower parts (cm)

Tower parts	Outer dimension				Stiffener dimension			
	fw	ww	t_1	t_2	r_1	r_2	t_{11}	t_{22}
I	240	350	2.2	3.2	25	22	3.6	3.0
II	240	350	2.2	3.2	22	20	3.2	2.8
III	240	350	2.2	2.8	20	20	2.8	2.2
IV	270	350	2.2	2.6	31	22	3.5	2.4

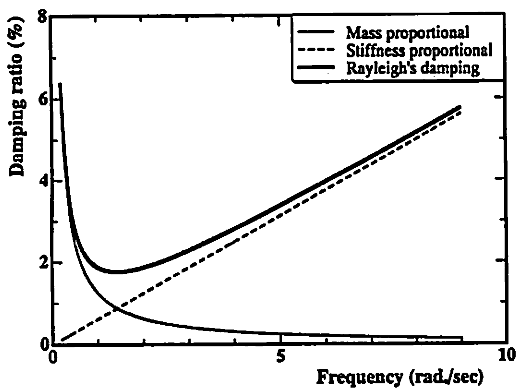

Fig. 2 Damping ratio and frequency relationship

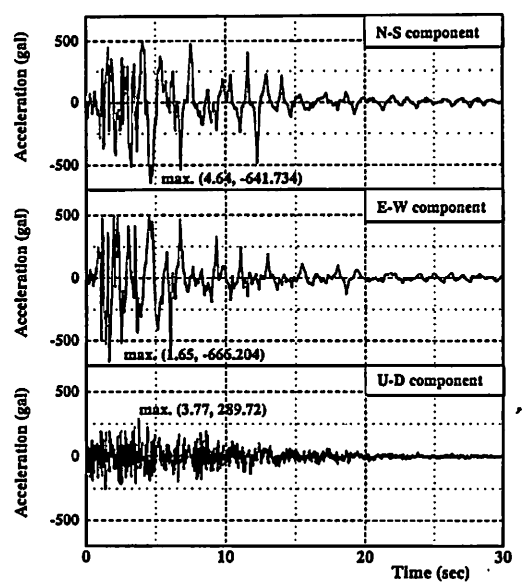

Fig. 3 Strong ground motion recorded at JR Takatori observatory

acting on the steel tower from the stiffening girder is neglected. For the numerical analysis, the geometry and the structural properties of the steel tower is shown in **Fig. 1**, the tower structure has rectangular hollow steel section with internal stiffeners, which has different dimensions along the tower height and its horizontal beam as shown in **Table 1**.

(2) Damping mechanism

The damping mechanism in cable-stayed bridges is not well understood. A correct representation of structural damping cannot be formulated from a practical standpoint. Accordingly, simplified assumptions have to be used. In this analysis, the modal damping is treated in two categories. First, considering physical elastic-plastic hysteresis loss in energy dissipation systems uses a phenomenological damping approach. In the second category, the damping matrix must be explicitly evaluated, where an equivalent viscous damping is introduced in the system in the form of damping matrix [C], as shown in **Fig. 2**.

In this study, two spectral damping schemes are used: The first scheme based on the matrix of simplified damping assumption is used only to clarify vertical ground motion and damping scheme effects on the steel tower dynamic response, where the attenuation of tower structure is adopted the viscous damping of mass proportional type with damping coefficient to the first fundamental natural vibration mode as standard 2%. In the second scheme, Rayleigh's damping is used to form damping matrix as a linear combination of mass and stiffness matrices, which effectively captures the tower structures damping and is also computationally efficient. The damping ratio corresponding to the frequencies of the fundamental in-plane and out-plane modes of tower free vibration is set to 2%, this Rayleigh's damping scheme is adopted for all present parametric study.

(3) Selected input ground motions

In the dynamic response analysis, the seismic motion by an inland direct strike type earthquake that was recorded during Hyogoken-Nanbu earthquake 1995 of high intensity but short duration is used as an input ground motion to assure the seismic safety of bridges. The horizontal and the vertical accelerations recorded at the station of JR Takatori observatory[3), 4)], as presented in **Fig. 3**, are suggested for dynamic response analysis of the steel tower of cable-stayed bridge at type II of soil condition due to its capability of securing the required seismic performance during the bridge service life. The selected ground motion has maximum acceleration of its components (N-S, E-W and U-D) equal to 642, 666 and 290 gal, respectively. From Fourier spectrum analysis, the predominant frequencies for N-S and E-W components are 0.83 and 0.81 Hz, respectively, which are relatively low, and that for the U-D component is 7.96Hz, which includes a high frequency components and indicates the vertical motion time lag to horizontal motions.

(4) Vertical ground motion component

Generally the vertical ground motion attenuates more rapidly than the horizontal motion, and the vertical motion effects are more evident in the near earthquake field. In fact it was observed that the vertical to horizontal peak ground acceleration ratio tends to assume greater values in the near field and to decrease as the epicenter distance increases[22]. Moreover, another aspect is not taken in consideration is the frequency content of the vertical motion, which is noticed to be significantly higher than that of the horizontal motion. Therefore the vertical component may be more dangerous as it is retained, since it may be close to the vertical frequencies of free vibration of many structures. There are a lot of records of instrumented structures, especially from the 1994 Northridge and 1995 Kobe earthquakes, which show a great amplification of the vertical ground motion.

(5) Natural vibration analysis

According to a number of full scale tests conducted for cables-stayed bridges, it is well known that the natural frequencies and natural mode shapes can be predicted with acceptable accuracy by means of linear elastic analyses that assume appropriate mass and stiffness distributions[23]. Depending on the fundamental frequencies of the steel towers of cable-stayed bridge in relation to the dominant frequency content of the seismic input motion, shifting the natural period T of the tower would significantly reduce acceleration responses and tower member forces. The natural vibration analysis is carried out for the previous described steel tower modal. The natural periods, the effective modal mass and the damping coefficient for different vibration modes obtained from the analysis are listed in **Table 2**. The lowest vibration mode, with a 2.072 sec period, involves transverse vibration of the entire tower structure (right angle to the bridge axis). The second mode (0.9335 sec) is the longitudinal vibration (bridge axial direction). The vertical vibration modes have period of 0.5235 sec to 0.1559 sec including modes 4 and 8. It is apparent that the contributions for the first and second modes are not only of larger values. But, there is another mode of vibration with large value of contribution factor showing a very complicated dynamic behavior.

Table 2 Summary of principal vibration modes for tower model

Mode order	Period sec.	Effective mass as a fraction of total mass	Viscous damping percent	Mode type
1	2.0723	33.195	2.00	H_1
2	0.9335	30.330	2.00	L_1
3	0.7726	0.000	2.18	T_1
4	0.5235	0.034	2.81	V_1
5	0.3751	1.735	3.68	L_2
6	0.3625	0.080	3.79	H_2
7	0.3296	0.000	4.12	T_2
8	0.1559	34.079	8.35	V_2
Sum	--	99.423	--	--

H: transverse vibration (in-plane), T: torsional vibration
L: longitudinal vibration (out-plane), V: vertical vibration

4. EFFECTS OF VERTICAL GROUND MOTION AND DAMPING

The principal effect of the vertical motion is the generation of fluctuating axial forces uncoupled from the lateral forces in tower legs. These axial forces are added to the axial forces correlated with the in-plane moments and as a result the compression and tension axial forces in tower legs could reach greater level than that with the horizontal motions alone. The effects of the vertical motion on tower seismic response are studied with the tower model described before. Two cases of analysis for the input ground motion for each spectral damping scheme (mass proportional or Rayleigh's damping) are considered as follows: The first; under the horizontal components only, and the second; under both the horizontal and the vertical components. The vertical excitation main effects can be stated and briefly explained in the following.

(1) Effects on tower axial response

In order to observe directly some of the effects of the vertical motion, the axial force time histories at the tower base are given in **Fig. 4**. For the mass proportional damping, it is evident the superposition of the axial force variations induced by the vertical motion with that due to the horizontal motions and a higher frequency feature. The axial force extreme values could reach great values with the vertical motion, since the maximum compression axial force at the tower base with and without consideration of vertical ground motion becomes, in fact, 4.01 and 3.13 times the initial axial force due to gravity loads, while the maximum tension axial force becomes about 2.46 and 1.36 times the initial axial force, respectively. The contribution of the vertical motion to the total axial force can be comparable to that of the horizontal motions, since that contribution to the extreme compression and tension values of axial forces in the tower base increases and it reaches about 28% and 81% of the total axial force for that case without consideration of vertical ground motion, respectively.

For the Rayleigh's damping scheme, it can be concluded that the vertical motion has slightly effects in axial forces generation, which are uncoupled to that due to lateral forces and have a higher frequency. The axial forces at tower base due to the overturning moments are significant and the vertical motion has small contribution to the total axial force compared to that of the horizontal motion, since the extreme compression and tension values of axial forces in the tower base indicate that the contribution of the vertical motion reaches about 10% and 6% of the total axial force for that case without vertical ground motion, respectively. For the case of horizontal input ground motions only, the tower dynamic response is slightly affected by the damping scheme. Moreover, it can be concluded that the damping scheme in the dynamic analysis essentially affects structure seismic response.

(2) Effects on tower flexural response

The moment-curvature diagram of the tower base, obtained with and without vertical motion, as shown in **Fig. 5**, presents the characteristics of the column behavior under coupled axial and lateral force variations. For the mass proportional damping, it can be observed that the asymmetry strength and moment curvature diagram shift due to fluctuating axial force effect. The diagram obtained with the vertical motion reveals an unusual and irregular shape with significant fluctuations in strength and stiffness due to the axial force-moment interaction. The contribution of vertical motion in maximum curvatures reaches about 31% of that case without vertical motion, and this indicates the lower dissipation capacity considered with the vertical excitation. However this is not only reason of the lower dissipated energy, since the tower hysteresis energy decreases as the curvature experiences greater values, moreover another cause is the irregular shape of the hysteresis loops. It can be seen also the growth of the inelastic behavior with the vertical ground motion, since the axial force fluctuation has the ability of generation of new plastic zones through the tower elements.

For the Rayleigh's damping scheme, the tower response with vertical ground motion shows very slightly effects in the tower flexural behavior. Moreover, The damage caused by the horizontal motions is similar to that caused by the vertical and horizontal motions. Since tower overall flexural response is not significantly altered by the fluctuation in the axial force associated to the vertical excitation. It can be observed that the analysis using Rayleigh's damping scheme displays more growth of tower inelastic behavior that can be attributed to greater input energy of ground motion leading to cause more damage and ductility demand.

(3) Effects on tower acceleration response

The vertical motion detrimental influence on tower acceleration response can be clarified through acceleration time history study. For the first damping scheme, as shown in **Fig. 6**(a), the tower top horizontal acceleration is resulted to increase of a non-negligible amount with the vertical motion. The extreme in-plane acceleration values are seen that the contribution of the vertical motion increases and it reaches about 81% of that for case without consideration of vertical ground motion, the in-plane acceleration for the cases with and without considering the vertical motion could reach 5.94 and 3.28 times that of the input ground motion, respectively. For the second damping scheme, it can be concluded that the vertical motion has no significant effect on the acceleration tower response, but it is characterized by effectiveness response and greater energy that causes more damage for tower

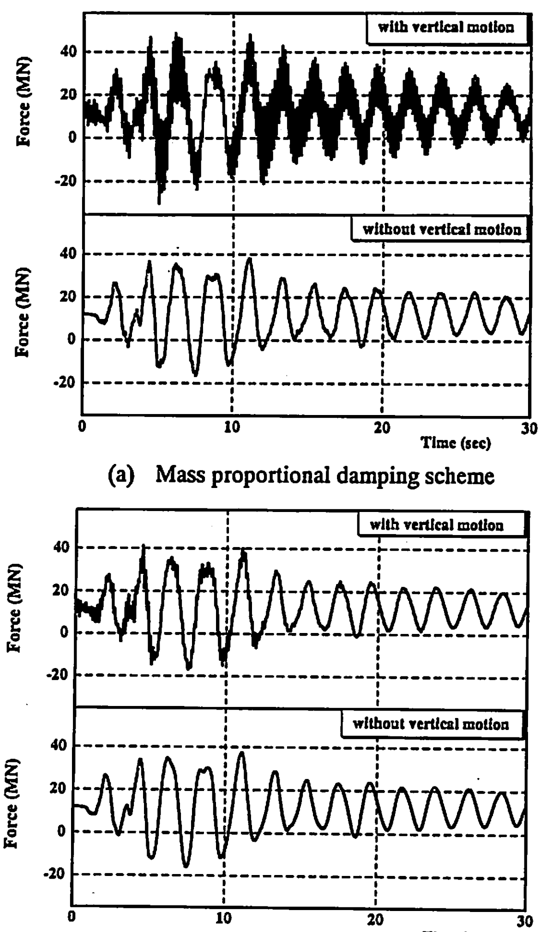

(a) Mass proportional damping scheme

(b) Rayleigh's damping scheme

Fig. 4 Vertical force time history at tower base

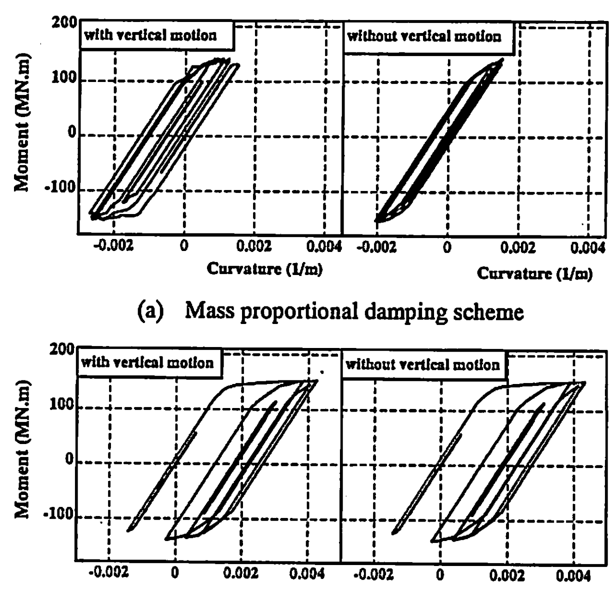

(a) Mass proportional damping scheme

(b) Rayleigh's damping scheme

Fig. 5 Moment-curvature diagrams at tower base

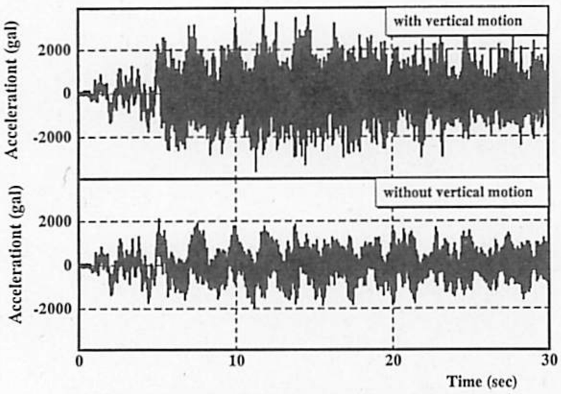

(a) Mass proportional damping scheme

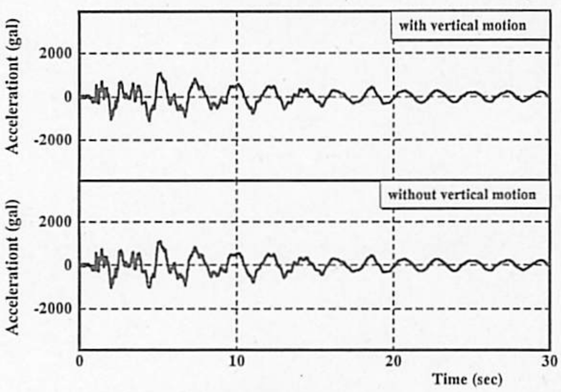

(b) Rayleigh's damping scheme

Fig. 6 In-plane acceleration time history of the tower top

structure, as shown in **Fig. 6**(b). The vertical ground motion effect on seismic response depends totally on the spectral damping scheme considered for nonlinear dynamic analysis. For the mass proportional damping scheme, the vertical motion displays significantly effect on tower seismic response, which may be attributed to the amplification of high frequencies mode of tower vibration included in the frequency content of the vertical motion, in terms lead to overestimation of the tower response. For the Rayleigh's damping scheme, it is appeared that the vertical motion has slightly effect on tower dynamic behavior due to high damping ratio for high frequency modes, which is pronouncedly affected by the vertical ground motion that has high frequency content compared with that of horizontal ground motions. The Rayleigh's damping could be recommended for conservative nonlinear seismic response of high-rise tower structures.

5. EFFECTS OF CONSTRUCTION INITIAL IMPERFECTIONS

(1) Initial geometric imperfections

Initial imperfections in structures that have not been subjected to damage usually result from the fabrication process and the strength of a thin-walled steel member is particularly sensitive to imperfections in the shape of its natural vibration modes. The amplitude of imperfections in the lowest eigenmodes of vibration is often sufficient to characterize the influential imperfections[19]. The initial geometric imperfection is applied by modifying the nodal coordinates using a field created by scaling the appropriate vibration eigenvector obtained from an elastic natural vibration analysis of tower model.

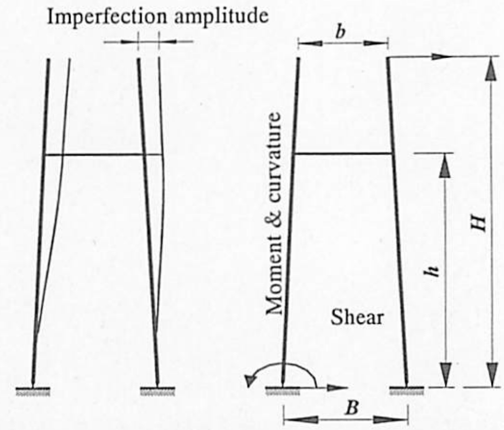

Fig. 7 Initial geometric imperfection pattern and different measured aspects of tower response

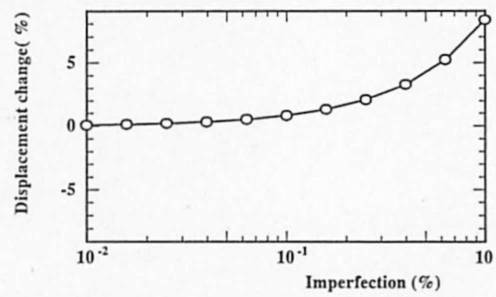

Fig. 8 Displacement &imperfection amplitude relationship

The dynamic response of the steel tower with consideration of initial geometric imperfection is investigated for different imperfection amplitudes of range from 0.01 up to 1% of tower height. The initial geometric imperfection is taken to be the first fundamental vibration mode pattern. **Fig. 7** describes the mode shape of the steel tower obtained from eigenvalue analysis. The mode is normalized so that the modal displacement at tower top is adjusted to the imperfection amplitude. The effects of the magnitude of initial geometric on the extreme values of in-plane displacement of tower top, shear force, in-plane moment and curvature at tower base are presented.

It can be concluded that the initial geometric imperfection within its design range of upper limit equal to 0.1% slightly affect on the tower seismic response but beyond this range, these effects are characterized by rapidly and nonlinearly increase and become significant as the initial imperfection approach severe values (1%). The extreme values of

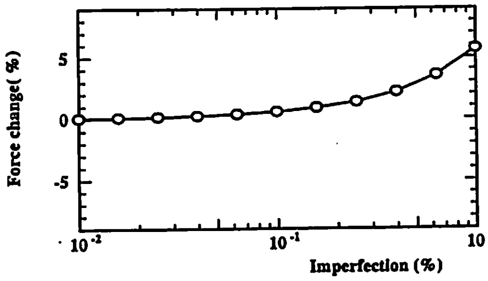

Fig. 9 Shear force & imperfection amplitude relationship

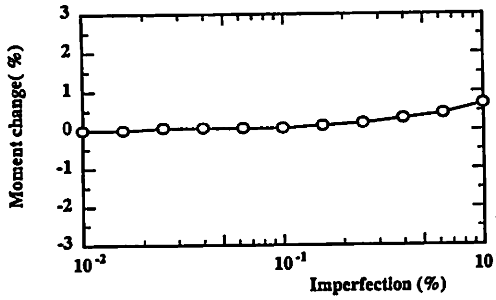

Fig. 10 Moment & imperfection amplitude relationship

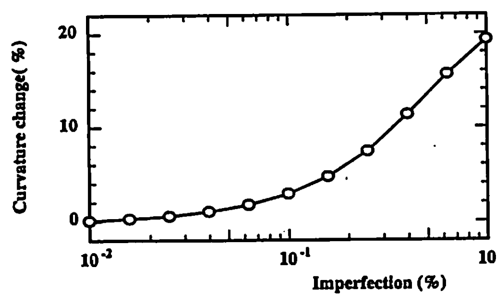

Fig. 11 Curvature & imperfection amplitude relationship

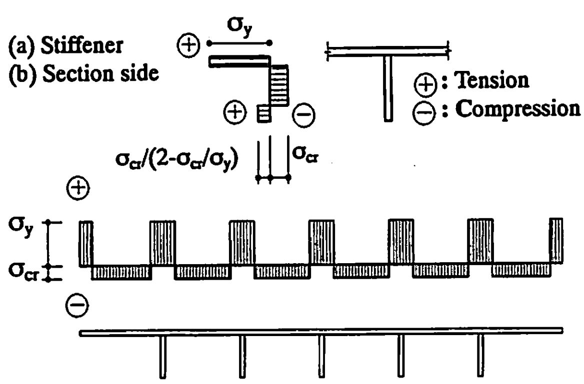

Fig. 12 Residual stresses in each side tower cross section

in-displacement at tower top and shear at tower base increase as imperfection amplitude increase under the same loading and have values 8% and 6% of that of perfect tower at maximum imperfection 1% of tower height as given in **Figs. 8** and **9**, respectively. But the extreme values of bending moment at tower base slightly increase up to 1.5% of that of perfect tower as a result of tower inelastic response that is characterized by large deformation corresponding to small force response, as illustrated in **Fig. 10**. Moreover, the imperfection amplitude has pronounced effects on curvature at tower base and

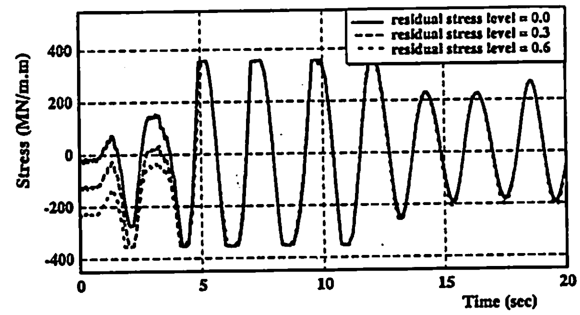

(a) Stress of compression residual stress fiber at tower base

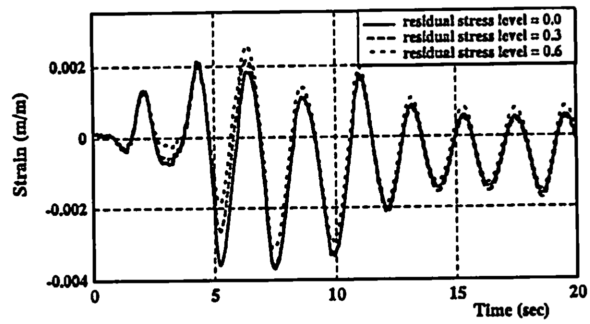

(b) Stain of compression residual stress fiber at tower base

Fig. 13 Stress and stain time histories

as a consequence the tower structure response, since the curvature increases up to 20% of that of perfect tower as shown in **Fig. 11**.

(2) Residual stresses

The presence of longitudinal residual stresses in stiffened rectangular hollow cross section is mainly attributed to the welding of stiffening members in addition to hot rolling of the hollow cross section. The residual stresses in the weld, stiffener and hollow section material in the vicinity of the weld are close to the yield as a result of the contraction of the welds. The magnitude and distribution of the residual stress are governed by welding parameters such as heat input and cooling rate of the welding process adopted for fabrication processes. To model the distribution of longitudinal membrane residual stresses in the cross section and the plasticity spread, the integration through the division of fiber model is considered to be sufficient. **Fig. 12** illustrates a typical residual stress pattern[24)] of tower cross section that is used in the computational model. It has been presented that the magnitude of the compressive residual stresses increases as the component plates of hollow section slenderness becomes smaller, values of stress up to 75% of the yield strength have been measured[25)].

The formation of residual stresses is inevitable in any welding and hot rolled operations, when they are superimposed on the externally applied stress fields, the residual stresses can result in significant differences in the performance of welded structures. The effects of residual stresses on the dynamic response of the steel tower is studied by varying residual stress level, where the compressive residual stresses range from 0.0 up to 0.60 times with interval of 0.1 of the yield stress are used to represent the condition of stress relieved, from lightly welded to heavily welded stiffener to the cross section. It can be observed that residual stresses have a more pronounced effect on the tower dynamic response, which will yield at a lower load stress due to the presence of compressive residual stresses. It can be seen how the applied membrane stresses is used to reflect the removal of residual stresses through the first cycle of the stress response in **Fig. 13** (a). But the residual effects extent over most of time history of strain response, and could be presented as peak time lag and decreasing plastic deformation capability as illustrated in **Fig. 13**(b). The tower top displacement decreases as the residual stress level increases, due to plastic deformation decrease as shown in **Fig. 14**.

In addition, the tower strength and stiffness are reduced by the presence of residual stresses and decrease with residual stress level increase as seen in **Figs. 15 and 16**. The tower flexural response is slightly affected by the presence of residual stress up residual stress level about 0.4, behind this level, the tower base curvature abruptly increases up to 20% of that of the original tower, as illustrated in **Fig. 17**(a), this behavior could be attributed to the peak time lag in curvature time history response as indicated in **Fig. 17**(b). From the total, damping and strain energies of the whole tower study, it is appeared the energies decrease in gradually as the compression residual stress increases and much effect on strain energy. This reduction can be attributed to decreasing of tower plastic deformation capability and gradual decreasing of tower stiffness due to presence of compression residual stresses, as given in **Fig. 18.**

In general, it can be concluded that the residual stress effects on the tower seismic response are sensitive to its stiffness in the longitudinal and transverse directions. Since the tower deformations response in the out-plane direction are more sensitive to the existence of residual stresses, which can be attributed to the long period of vibration and more flexibility of tower in-plane direction compared

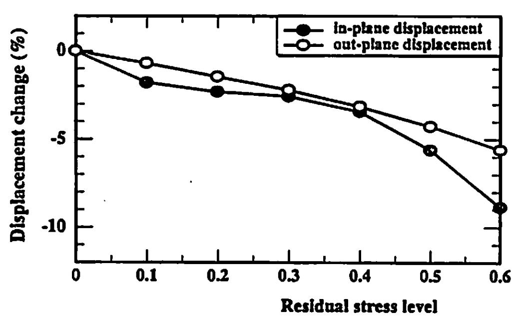

Fig.14 Displacement & residual stress level at tower top

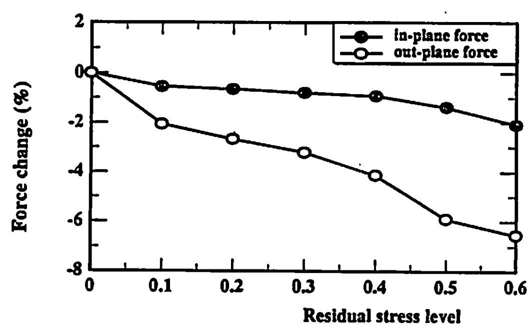

Fig. 15 Shear force & residual stress level at tower base

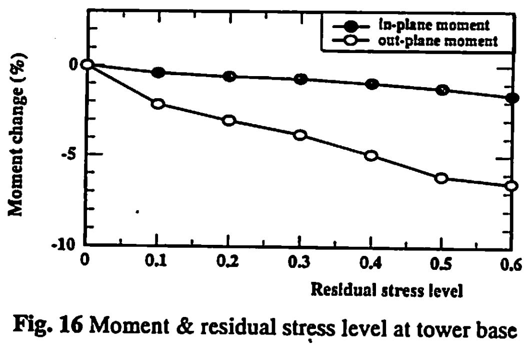

Fig. 16 Moment & residual stress level at tower base

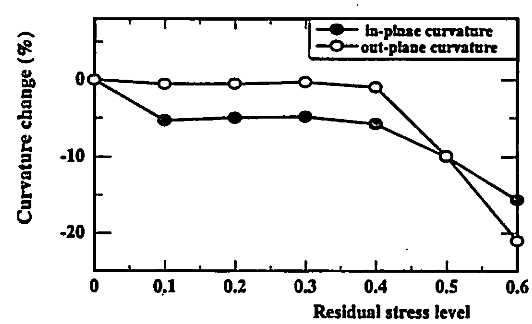

(a) Curvature & residual stress level at tower base

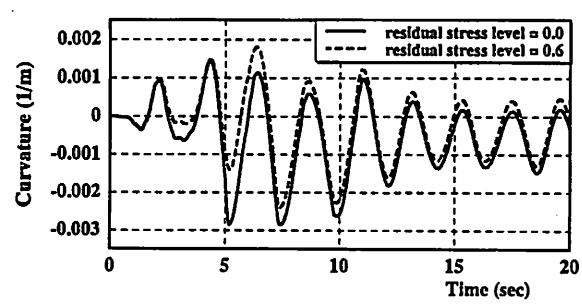

(b) Time history

Fig. 17 Curvature at tower base

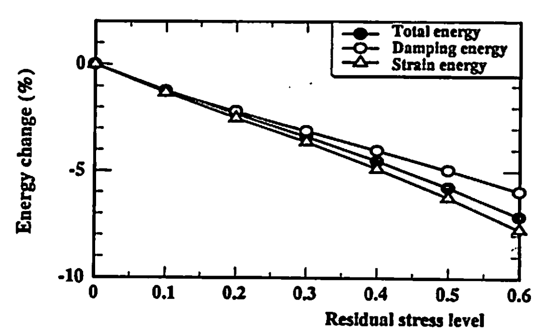

Fig. 18 Total, damping and strain energies of the whole tower & residual stress level relationship

to that of the out-plane direction. The residual stresses within the design range of upper limit equal to 0.3 affect the tower seismic response not more than 3% and 5% for displacement and in-plane curvature demand, respectively. Also, these effects are not more 4% for both out plane shear and flexural capacity. The other aspects of tower seismic response are slightly affected by residual stresses values up to the design range upper limit. The residual stresses have the time lag effect on tower peak response, which can be noted form curvature rate of change at residual stress level of 0.4.

6. LOW YIELD MATERIAL ENERGY DISSIPATION SYSTEM

The design of a passive energy dissipation system depends on many factors, including the period of original tower configuration, the input ground motion response spectrum, force deformation relationship, and so on. The design of isolation system should be able to provide supplemental damping to significantly reduce tower response to ground motion and dissipation a large portion of earthquake input energy through inelastic deformations in certain positions, which could be easily retrofit after damage. Thus the spectral acceleration and structural element forces could be significantly reduced when they are compared to that of original tower. The nonlinear dynamic behavior and seismic performance of the steel tower under three dimensional great earthquake motion are studied for three different cases, a case of original tower and other two cases of proposed energy dissipation system. In these two cases, the concentration of inelastic behavior along the tower horizontal beam by reduction of its strength is considered, this reduction is done by using low yield steel material instead of cross section dimensions reduction. Two yield stresses are used that equal to 235 MPa and 100 MPa corresponding to medium and low yield level equal to 0.67 and 0.28 relative to that of original tower, respectively.

The performance of the proposed energy dissipation system is analyzed by comparing the energies time history, where the input energy is defined as the total energy related to inertia forces induced by the ground motion. It is appeared that the proposed energy dissipation system has two effects on the tower response: The first is to increase the tower structural system ability to reflect a portion of earthquake input energy, since as the horizontal beam yield early attains, the tower becomes more flexible. In effect, the increased flexibility acts as a filter. Secondly, it increases the amount of damping and dissipation energies through inelastic deformation hysteresis. The calculated results of different yield levels show effective energy dissipation through the horizontal beam. As the yield level decreases, the energy dissipation system becomes more effective in energy absorption and damage control, as seen in **Fig. 19**.

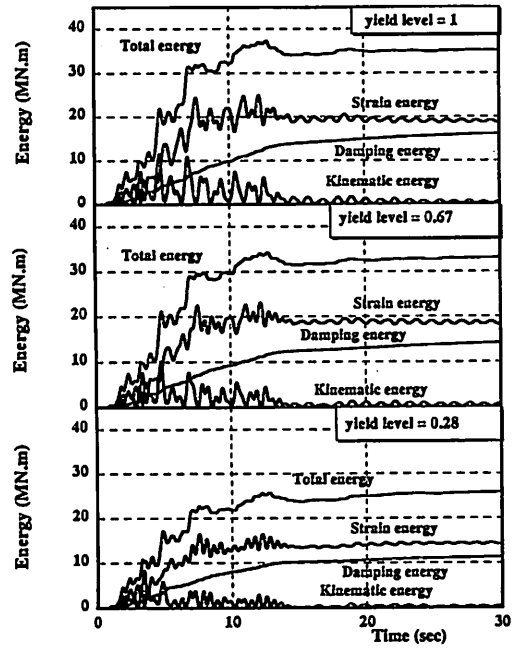

Fig. 19 Different energies time history of the whole tower

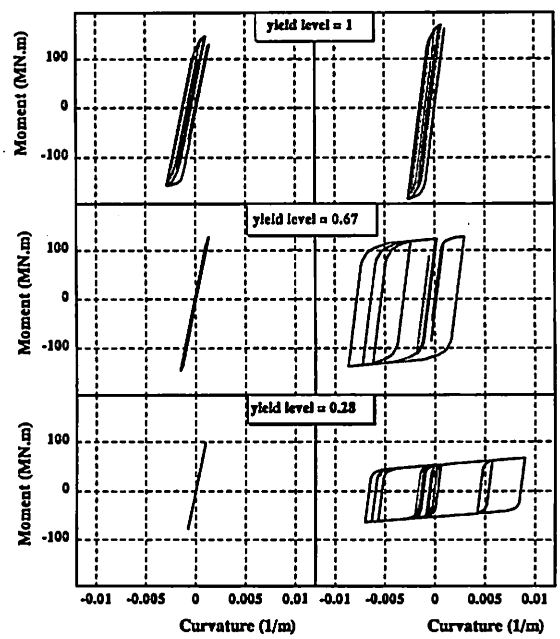

(a) At tower base (b) At horizontal beam end

Fig. 20 Moment & curvature relationship

As the yield level of horizontal beam material decreases, thus the load capacity of tower horizontal beam decreases and forces redistribution in tower structural elements occurs. It can be seen from **Fig. 20(b)** that more concentration of inelastic behavior and ductility at tower horizontal beam is attained as yield level change for low values, which is easy to inspect and repair if necessary. The rest of the structure approaches elastic behavior as yield level decreases, thus there is a possibility of eliminating permanent damage and minimizing the extent of retrofit. The main tower parts attain almost elastic behavior at study case of yield level equal to 0.28, as seen in **Fig. 20**(a).

In general, the isolated tower exhibits elastic response due to the redistribution of the seismic forces to the tower elements in accordance to their strength. It can be concluded that the proposed energy dissipation system is effective in controlling the maximum tower displacement, since the displacement tower response decreases as the horizontal beam capacity decrease, as illustrated in **Fig. 21**. The better performance of the isolation proposed energy dissipation system is indicated by comparing the reaction force time history at the tower base for different levels of yield strength of the horizontal beam. It is illustrated from **Figs. 22** and **23** that the isolated tower provides pronounced reduction in the reaction forces response compared to the original tower response, this reduction becomes more pronounced as the yield level decreases, due to seismic forces redistribution to tower elements according to their strength and stiffness. The proposed energy dissipation system effect can be understood from the in-plane shear and vertical force time histories at tower base. The tower main structures approach elastic behavior as yield capacity of horizontal beam decreases. Since for yield level equal to 0.67, tower flexural response represented in the moment ratio relative to yield moment capacity (M_y that equal to 130 MN·m) time history at tower base, enters the plastic response four times compared with the original tower enters the plastic response seventh times, while for low yield level equal to 0.28, the elastic behavior is displayed along the time history, as seen in **Fig. 24**.

The hysteretic dampers of low yield steel material can provide relatively large energy dissipation through their materials that are strained beyond their yield limits, thus can be cost effective. The hysteretic dampers cannot be activated as dampers unless their materials receive inelastic excursions, so the hysteretic dampers are effective only for larger earthquake excitation that can be understood from this study, but fail in providing the required damping for smaller vibrations. Another aspects of post-yield buckling capacity should be considered in the design. In this case of study, as horizontal beam receive inelastic excursions; the buckling effective length could get larger, as a result, the load carrying capacity decreases.

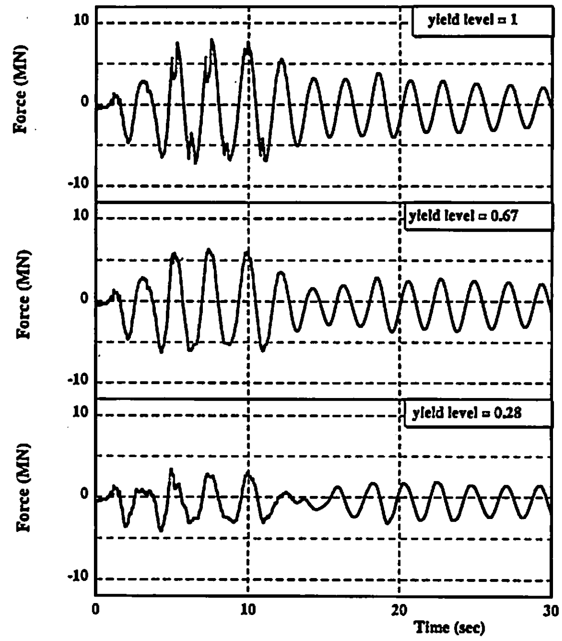

Fig. 22 In-plane shear force time history at tower base

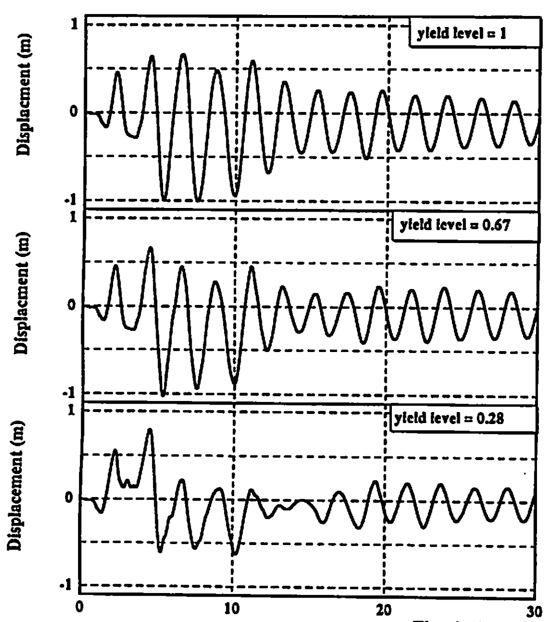

Fig. 21 In-plane displacement time history at tower top

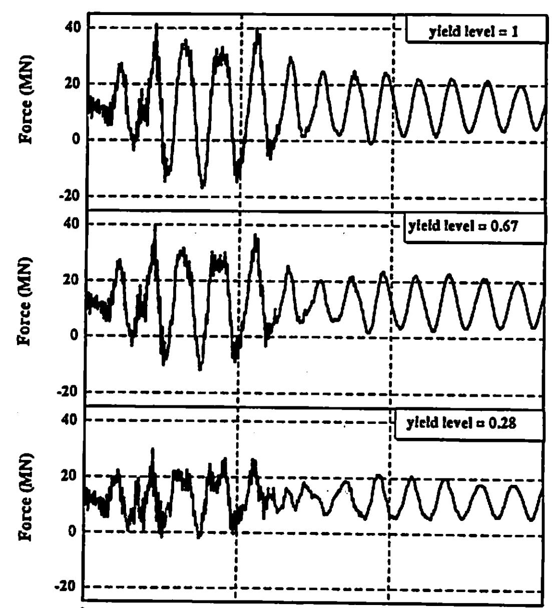

Fig. 23 Vertical force time history at tower base

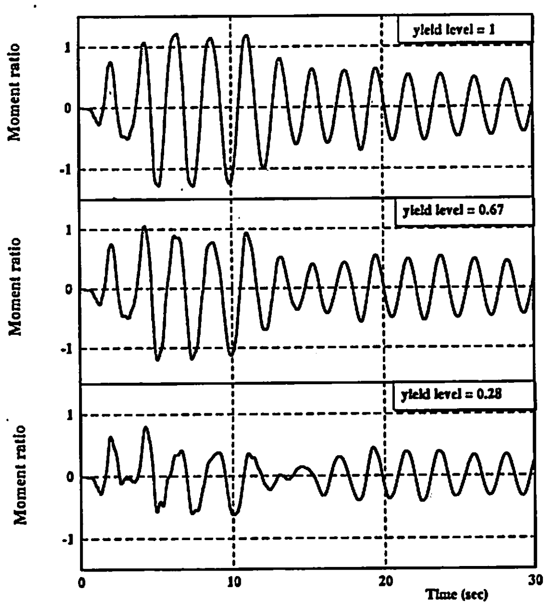

Fig. 24 Moment ratio time history at tower base

The buckling load carrying capacity is calculated for the worst case of no contribution of horizontal beam to the tower legs stiffening, it is found to be equal to 49.5 MN, which is much greater than the corresponding tower response. Moreover, the proposed low yield hysteretic dampers lead to effective reduction of vertical force response as yield level decreases, as a result buckling demand decreases, as shown in **Fig. 23**.

7. EFFECTS OF TOWER MODAL SHAPES

The natural vibration periods of the in-plane, out-plane and torsion fundamental modes of the steel tower with different modal shapes have been studied for different height and length of the horizontal beam. A detailed natural vibration characteristic is provided for horizontal beam different height relative to the total tower height (height ratio, h/H = 39/68 – 68/68) and different width at tower top relative to that at tower base (length ratio, b/B = 13/18 – 3/18). **Fig. 25** presents the natural period of these three modes of vibration and height and length ratios relationship.

The effectiveness of the tower modal shapes can be measured by their capabilities in the energy dissipation through shifting natural period of the fundamental mode and increasing structural damping. The natural vibration analysis indicates that the height and length of tower horizontal beam have effective role in shifting the primary period of the tower free vibration, and slightly affect the higher mode of vibration. Longer natural period can be attained by either horizontal beam height (h/H) relative to tower height or tower top to base width ratio (b/B) increase. For the original steel tower of cable-stayed

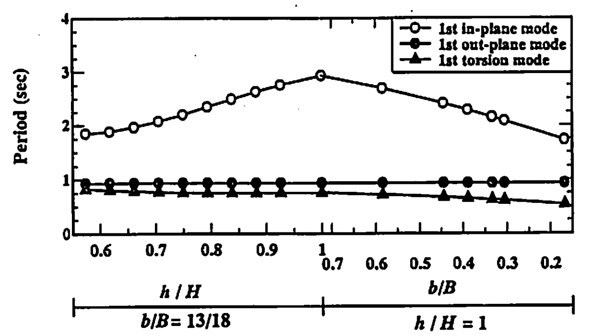

Fig. 25 Natural period & horizontal beam height/length relation

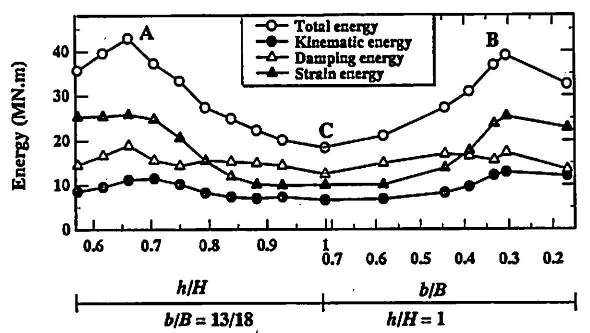

Fig. 26 Total, damping and strain energies of the whole tower & horizontal beam height/length relationship

bridge, the better performance could be attained by moving the horizontal beam from its currant designed at h/H = 48/68 toward tower top. This modification in tower design could lead to natural period about 1.5 times longer, hence reduces the seismic demand required for earthquake mitigation.

It is indicated from **Fig. 26** through the energies extreme values study that the horizontal beam has two critical positions corresponding to point A (h/H=45/68, b/B=13/18) and point B (h/H=68/68, b/B=5.5/18), where the maximum total energy occurs, as a result the seismic demands are increased. The kinematic and damping energies is slightly affected by the horizontal beam position of tower, while the total and strain energies along the range between critical points A and B decrease highly nonlinear as either the height ratio or the length ratio increase up to optimum position of horizontal beam corresponding to point C. The tower base shear and vertical force variations with different horizontal beam height and length ratios are described in **Figs. 27** and **28**, respectively, which confirm the optimum position of horizontal beam at tower top as detected from the energetic study. The height of horizontal beam has effective role in the dynamic response of steel tower depends to large extent to tower shapes[15], including the horizontal beam position and strength represented in material yield level. The effects of height and length of the horizontal beam on tower dynamic response are discussed through time history analysis to examine the tower shapes effects. For this purpose, three different cases of tower modal shape, as illustrated in **Fig. 29**, are considered as follow:

Case I: The original tower of cable-stayed bridge.
Case II: Portal frame-type where the horizontal beam in case I is raised to tower top.
Case III: Inverted V-type where the tower top length decreases from case II up to 3 m.

The natural period of the predominant modes of free vibration for studied cases of tower model shapes is given in **Table 3**, where the symbols H_1, L_1 and T_1 are the first natural mode in the direction of the right angle to bridge axis (in-plane), of bridge axis (out-plane) and torsion, respectively. The first natural periods of out-plane and torsion modes are smaller than that of in-plane mode due to the stiffening of cables. It is seen that the natural period of the portal frame-type tower has tendency to be getting longer in compared with the inverted V-type and original tower (H-type) because of more flexibility of tower frame structure due to its height increases and also there is a massive horizontal beam situated on the tower top.

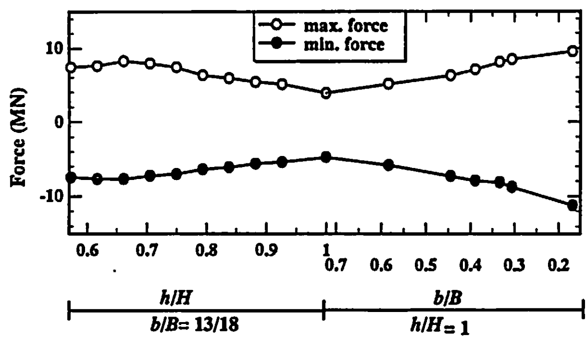

Fig. 27 In-plane shear at tower base & horizontal beam height/length relationship

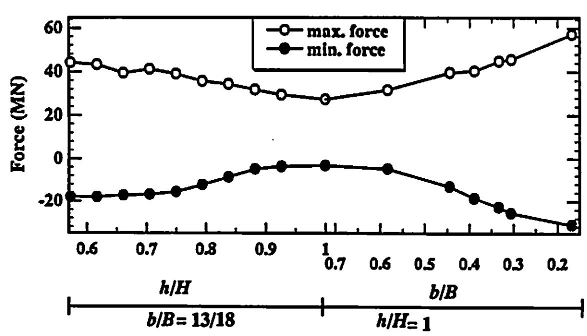

Fig. 28 Vertical force at tower base & horizontal beam height/length relationship

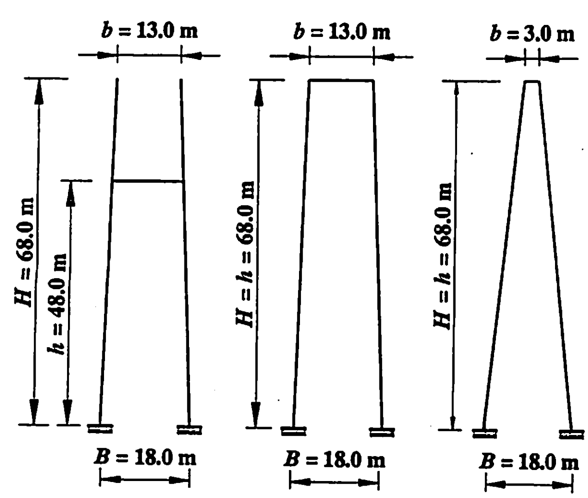

Fig. 29 Tower modal shapes

Fig. 30 displays the energy time history for different cases of tower modal shape. The portal frame-type tower has enough flexibility to reflect most of the absolute input energy by flexibility filtering; the damping energy becomes larger and reaches about 80% relative to input energy. Moreover, the strain energy dissipated through tower inelastic hysteretic deformation decreases, since the tower still keeps elastic behavior as illustrated in **Fig. 31**. The hysteresis of the other types of tower modal shape (cases I and III) becomes larger and pronouncedly displays inelastic behavior especially for H-type. The largest inelastic deformation damage has been attained, leading to high strain energy dissipated through tower hysteric behavior. Moreover, the total input energy is getting higher, which requires greater seismic demand for mitigation of earthquake hazards. **Fig. 32** indicates the trajectory of tower top displacement response in the two horizontal directions. The right tower top

Table 3 Natural period for tower different modal shapes (sec)

Mode type	Cases of tower modal shapes		
	Case I	Case II	Case III
H_1	2.072	2.928	1.727
L_1	0.934	0.935	0.935
T_1	0.773	0.761	0.543

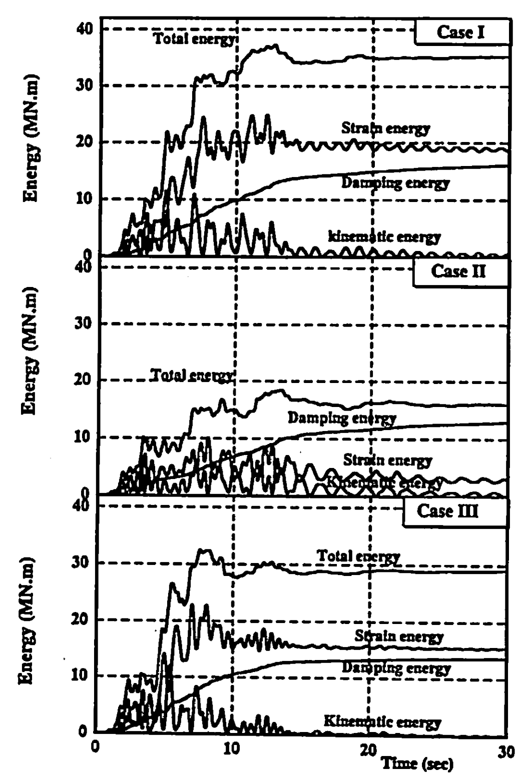

Fig. 30 Different energies time history of the whole tower

displacement response is considered. The vertical axis is the in-plane displacement (right angle to bridge axis direction) and the horizontal axis is the out-plane displacement (bridge axis direction). The results indicate that all studied three cases are characterized by in-plane larger displacement than that of the out-plane response, which is related to long period of the in plane free vibration compared with the out-plane vibration. In addition, the existence of cables reduces tower shape effects on the out plane tower displacement response. The H-type (case I) tower has the largest in-plane displacement response among three considered tower shapes due to the absence of frame action at tower top. The tower part above the horizontal beam approaches to a cantilever behavior, also it is noted the asymmetric in-plane displacement that related to torsional vibration effects. The portal frame-type (case II) tower displays reasonably large displacement, since it has the longest period of vibration and massive effect of the horizontal beam at tower top. The inverted V-type (case III) tower model displays the smallest top displacement response in both directions due to stiff frame action of this shape and short period of in-plane and torsional vibrations. The dynamic response of each tower model is examined on axial force at tower basement as illustrated in **Fig. 33**, which shows the orbits of axial force response that occurs at both sides of the tower basement.

The vertical and horizontal axes are the axial force response at right and left sides of tower basement, respectively. A dead load equivalent to the stiffening girder weight is equal to 12.15 MN and it acts on both sides of the tower basement through cables. It is noted that tower modals have symmetrical form of axial force dynamic response around the dead load. The inverted V-type has the largest axial force response, where the maximum compressive and tension axial forces are about 4.70 and 2.55 times of the gravity loads, the large negative reaction makes the problem that the anchor

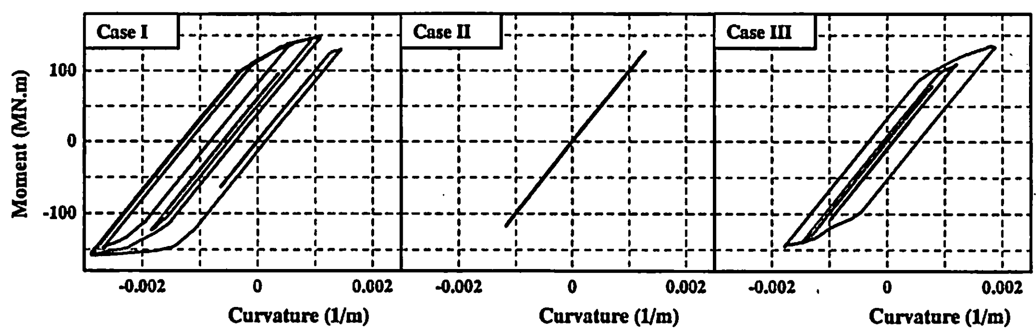

Fig. 31 Moment curvature relations at tower base

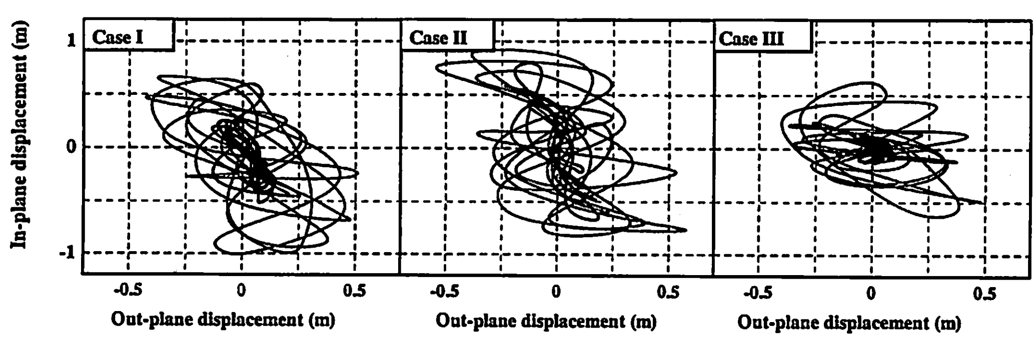

Fig. 32 Trajectory of response sway displacement of tower top

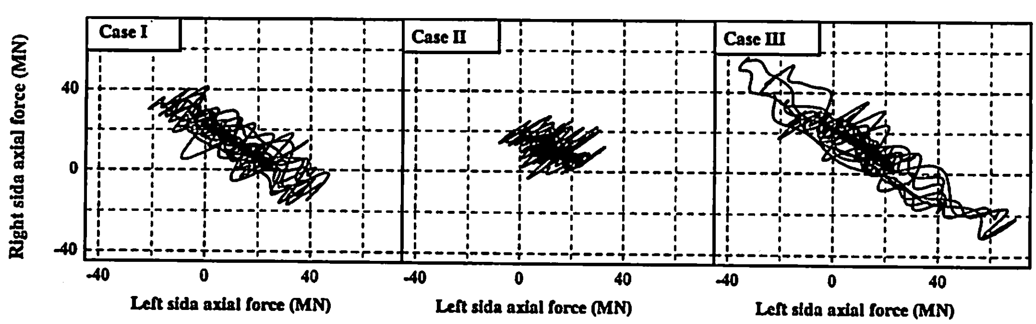

Fig. 33 Axial force relation at tower bases

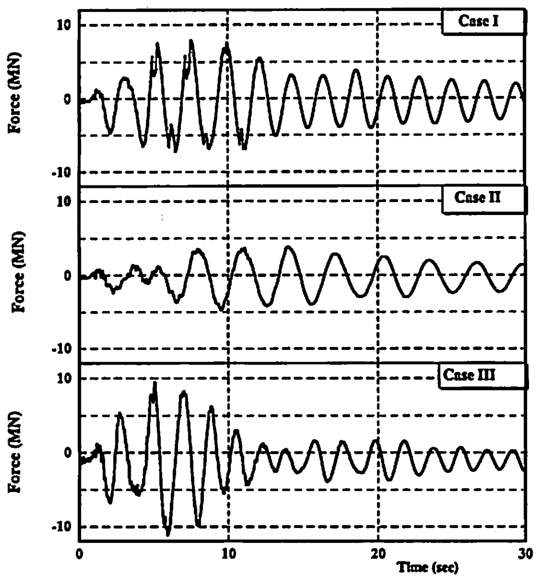

Fig. 34 In-plane force time history at tower base

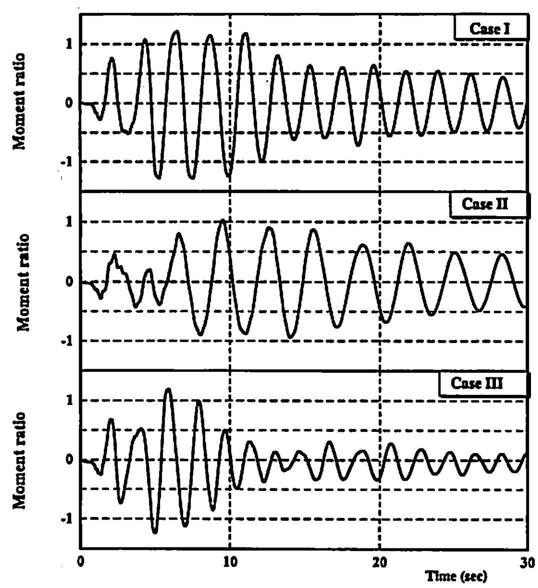

Fig. 35 In-plane moment time history at tower base

bolts may fail in the lift up and the safety of the tower should be considered. The same behavior but slightly less severe can be seen for the H-type (original tower), where the maximum compressive and tension axial forces are about 3.39 and 1.39 times of the gravity loads. On the other side, the portal frame-type (case II) model displays reasonable axial force response with small amplitude, since the maximum compressive and tension axial forces are about 2.26 and 0.27 times of gravity loads. The current results prove again the effectiveness of the horizontal beam position on tower axial force dynamic response. The change of horizontal beam height from that of the original tower (h/H=48/68 m) toward tower top (h/H=68/68) will reduce the compressive and tensile axial forces at tower base about 34% and 81% of that of original tower, respectively, and almost the uplift problem disappears that secure the tower seismic response

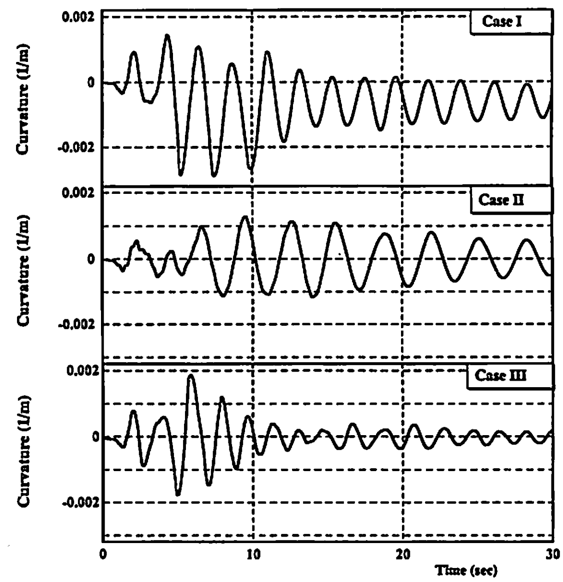

Fig. 36 In-plane curvature time history at tower base

against anchor bolts lift up failure. The severe axial force response of the inverted V-type could be attributed to inclination of the tower legs that leads to significant flexural-axial interaction and increases the flexural contribution in the tower vertical force response under external seismic excitation.

The reaction force time history at the tower base for different tower shapes could indicate the better performance of the tower modal shapes, as indicated in **Fig. 34.** It is found that the portal frame-type tower (case II) provides pronounced reduction in the reaction force response compared to the original tower response (case I), and its response is characterized by long period of vibration and elastic behavior, while the inverted V-type displays larger shear as well as axial response. From the moment ratio relative to the yield moment capacity (M_y) at the tower base, which is equal to 130 MN·m, the original tower enters the inelastic response many times within the first twelve seconds, which explains the large damage occur.

The inverted V-type tower enters the inelastic response three times within the first ten seconds leading to less damage compared to case I, while the portal frame-type tower still has elastic response along the time history, as shown in **Fig. 35**. The curvature time history at tower base displays residual deformation and damage for original tower, however, the residual deformations disappear for both portal frame and inverted V-type models due to elastic behavior of portal frame-type and ability of inverted V-type to restore symmetric behavior with no residual deformation even it has inelastic deformation at early stage of response, as illustrated in **Fig. 36.**

8. CONCLUSIONS

Analytical parametric study on steel tower of cable-stayed bridges is performed for investigation the individual influence of different design aspects on its dynamic characteristics, such as damping scheme, input ground motion, allowable initial imperfections, energy dissipation and tower modal shapes. A finite element procedure based on total Lagrangian formulation for the nonlinear dynamic analysis of steel tower of cable-stayed bridge under three dimensional great earthquake ground motion is carried out. From the performed investigations and discussions, the following conclusions can be summarized:

(1) The effect of vertical ground motion has highly dependence on damping scheme. The Rayleigh's damping is more effective in high frequency range, which leads to slightly effects of the vertical ground motion on tower dynamic response. The Rayleigh's damping could be recommended for conservative nonlinear seismic response of high-rise towers.

(2) For mass proportional damping scheme, a significant axial force fluctuations due to vertical motion inertia forces affects the tower behavior and as a consequence the global structural response. The contribution of the vertical motion to extreme compression and tension axial forces at tower base reaches about 28% and 81% of that of horizontal motions only, respectively. Moreover the tower axial forces response is characterized by high frequency. The consideration of horizontal excitations only could underestimate the curvature ductility demand.

(3) For Rayleigh's damping scheme, the tower response with vertical motion shows slightly effects on its flexural behavior, but more growth of inelastic behavior arises due to greater input energy. The contribution of the vertical motion to extreme compression and tension axial forces at tower base reaches about 6% and 10% of that case of horizontal motions only, respectively.

(4) The initial geometric imperfections of tower fundamental vibration mode pattern, within its design range of upper limit equal to 0.1%, slightly affect the tower seismic response. But beyond this range, these effects are characterized by rapidly and nonlinearly increase and become significant as the initial imperfections approach severe value (1%).

(5) The normal stress distribution is affected by the residual stress; as a result, the tower load carrying capacities and stiffness decease as the residual stress level increases. Moreover, the residual stress has detrimental effects on tower structural performance, which can be characterized by decreasing plastic deformation capability.

(6) The residual stress effects on the tower seismic response are sensitive to its stiffness in the longitudinal and transverse directions. These effects within the design range of upper limit equal to 0.3 on the tower seismic response are not more than 5% that of perfect tower response.

(7) The proposed energy dissipation system demonstrates its capability and effectiveness in reducing structural elements forces and controlling tower maximum displacement through its capability achieving the concentration of inelastic behavior at tower horizontal beam and keeping the rest of the structure elastic behavior as yield level decreases. The post-yield buckling capacity should be considered in the design of tower structures.

(8) This technique could add damping primarily by material hysteresis and increase tower flexibility as the horizontal beam yield early attains, in terms tower structural system ability to reflect a portion of earthquake input energy increases. The energy dissipation system becomes more effective in energy absorption through the horizontal beam.

(9) The portal frame-type tower has the longest natural period and enough flexibility to reflect most of the absolute earthquake input energy by flexibility filtering. The damping energy could reach larger values relative to input energy about 80% and minimum strain energy is dissipated through inelastic hysteric deformations of the tower.

(10) The inverted V-type has the largest axial force response, where the maximum compressive and tension axial forces are about 4.70 and 2.55 times of the gravity loads, respectively. The large negative reaction makes the problem that the anchor bolts may fail in the lift up and the safety of the tower should be considered.

(11) The effectiveness of the horizontal beam position on tower axial force dynamic response is assured. The change of horizontal beam height from that of the original tower (h/H=48/68) toward tower top (h/H=68/68) reduces the compressive and tensile axial forces at tower base about 34% and 81% of that of original tower and almost the uplift disappears.

REFERENCES

1) Ali, H. M. and Abdel-Ghaffar, A. M.: Modeling the nonlinear seismic behavior of cable-stayed bridges with passive control bearings, *Computers & Structures*, Vol. 54, No. 3, pp. 461-492, 1995.
2) Hayashikawa, T. and Abdel Raheem, S. E.: Nonlinear dynamic behavior of steel tower of cable-stayed bridges with passive energy dissipation system, *Journal of Structural Engineering, JSCE*, Vol. 48A, pp. 863-874, 2002.
3) Committee of Earthquake Engineering: *The 1995 Hyogoken-Nanbu Earthquake, Investigation into Damage to Civil Engineering Structures, JSCE*, 1996.

4) Japan Road Association: *Specification for Highway Bridges-Part V Seismic Design*, Maruzen, Tokyo, 1996.
5) Bozorgnia, Y., Niazi, M. and Cambell, K. W.: Characteristics of free-field vertical ground motion during the Northridge earthquake, *Journal of Earthquake Spectra*, Vol.11, No. 4, pp. 515-525, 1995.
6) Papazoglou, A. J. and Elnashai, A. S.: Analytical and field evidence of the damaging effect of vertical earthquake ground motion, *Earthquake Engineering and Structural Dynamics*, Vol. 25, pp. 1109-1137, 1996.
7) Diotallevi, P. P. and Landi, L.: Effect of the axial force and of the vertical ground motion component on the seismic response of R/C frames, *Proceedings of 12th. World Conference on Earthquake Engineering*, Paper No. 1026, 2000.
8) Saadeghvaziri, M. A. and Foutch, D. A.: Behavior of RC columns under non-proportionally varying axial loads, *Journal of Structural Engineering, ASCE*, Vol. 116, No. 7, pp. 1835-1856, 1990.
9) Hayashikawa, T., Aly, G. A., Abdel Raheem, S. E.: Effect of vertical ground motion on seismic response of steel tower of cable-stayed bridges, *Proceedings of Hokkaido chapter of the Japan Society of Civil Engineers, JSCE*, No. 58(A), pp. 112-115, 2001.
10) Usami, T. and Fukumoto, Y.: Local and overall buckling of welded box columns, *Journal of Structural Division, ASCE*, Vol. 108, No. 3, pp. 525-542, 1982.
11) Zhang, J. and Dong, P.: Residual stresses in welded moment frames and implications for structural performance, *Journal of Structural Engineering, ASCE*, Vol. 126, No. 3, pp. 306-315, 2000.
12) Grondin, G. Y., Elwi, A. E. and Cheng, J. J. R.: Buckling of stiffened plates – a parametric study, *Journal of Constructional Steel Research*, Vol. 50, pp. 151-175, 1999.
13) Fujikubo, M. and Yao, T.: Elastic local buckling strength of stiffened plate considering plate/stiffener interaction and welding residual stress, *Marine Structures*, Vol. 12, pp. 543-564, 1999.
14) Banno, S., Usami, T. and Mizuno, E.: Cyclic elasto-plastic finite displacement analysis of plates with modified two-surface model, *Proceedings of the Japan Society of Civil Engineers, JSCE*, No. 525/I-33, pp. 1-15, 1995.
15) Hayashikawa, T., Matsui, Y. and Kaneko, T.: Nonlinear dynamic behavior and seismic isolation of steel towers of cable-stayed bridges under great earthquake ground motion, *Proceedings of 12th. World Conference on Earthquake Engineering*, Paper No. 0469, 2000.
16) Nakashima, M.: Strain-hardening behavior of shear panels made of low yield steel. I: test, *Journal of Structural Engineering, ASCE*, Vol. 121, No. 12, pp. 1742-1749, 1995.
17) Nakashima, M., Akazawa, T. and Tsuji, B.: Strain-hardening behavior of shear panels made of low yield steel. II: model, *Journal of Structural Engineering, ASCE*, Vol. 121, No. 12, pp. 1750-1757, 1995.
18) Nakashima, M., Iwai, S., Iwata, M., Takeuchi, T., Konomi, S., Akazawa, T. and Saburi, K.: Energy dissipation behavior of shear panels made of low yield steel, *Earthquake Engineering and Structural Dynamics*, Vol. 23, pp. 1299-1313, 1994.
19) Schafer, B. W. and Peköz, T.: Computational modeling of cold-formed steel: characterizing geometric imperfections and residual stresses, *Journal of Constructional Steel Research*, Vol. 47, pp. 193-210, 1998.
20) Chen, C. N.: Efficient and reliable solutions of static and dynamic nonlinear structural mechanics problems by an integrated numerical approach using DQFEM and direct time integration with accelerated equilibrium iteration schemes, *Applied Mathematical Modelling*, Vol. 24, pp. 637-655, 2000.
21) Ernst, J. H.: Der E-modul von seilen unter berucksichtigung des durchhanges, *Der Bauingenieur*, Berlin, Vol. 40, No. 2, 52-55, 1965 (in German).
22) Kikuchi, M., Dan, K. and Yoshiro, K.: Seismic behavior of a reinforced concrete building due to large vertical ground motion in near source regions, *Proceedings of 12th. World Conference on Earthquake Engineering*, Paper No. 1867, 2000.
23) Wilson, J. C. and Liu, T.: Ambient vibration measurements on a cable-stayed bridge, *Earthquake Engineering and Structural Dynamics*, Vol. 20, pp. 723-747, 1991.
24) Usami, T. and Ge, H. B.: Cyclic behavior of thin-walled steel structures – numerical analysis, *Thin-Walled Structures*, Vol. 32, pp. 41-80, 1998.
25) Grondin, G. Y., Elwi, A. E. and Cheng, J.J.R.: Buckling of stiffened steel plates - a parametric study, *Journal of Steel Constructional Steel Research*, Vol. 50, pp. 151-175, 1999.

(Received March 27, 2002)

斜張橋鋼製タワーの大地震時動的応答に関するパラメトリックスタディー

Shehata E. ABDEL RAHEEM・林川　俊郎

斜張橋鋼製タワーの動的応答性状に与える減衰特性，入力地震動，初期不整，エネルギー吸収機構およびタワーの骨組形状などの諸因子の影響を調べるためにパラメトリックスタディーが実施される．大地震動による斜張橋鋼製タワーの非線形動的応答解析には有限要素法が用いられる．タワー形状により水平梁の位置や長さによっては動的応答に好ましくない影響を与えることが数値計算で示される.また，建設時における初期不整の影響が明らかにされる．質量比例型減衰は鋼製タワー基部に発生する軸力および加速度応答を過大評価することが判明した．